A SOURCE-TO-SINK HISTORY OF THE SUPRADETACHMENT GEDIZ GRABEN (W TURKEY): FROM EXHUMATION OF THE CENTRAL MENDERES MASSIF THROUGH THE GEDIZ DETACHMENT FAULT TO SEDIMENTATION IN THE BASIN

A PhD Thesis

By

Riccardo Asti

Scuola Dottorale in Geologia dell'Ambiente e delle Risorse (SDiGAR)

XXVIII Cycle

Department of Sciences

Università degli Studi Roma Tre

Rome, Italy

Advisor:

Prof. **Claudio Faccenna**[1]

Co-advisors:

Prof. **Marco Giovanni Malusà**[2]

Prof. **Federico Rossetti**[1]

Prof. **Domenico Cosentino**[1]

1) Università degli Studi Roma Tre, Department of Sciences, Rome, Italy

2) University of Milano-Bicocca, Department of Earth and Environmental Sciences, Milan, Italy

TABLE OF CONTENTS

CHAPTER 1 - INTRODUCTION 5

REFERENCES 7

CHAPTER 2 - UNRAVELING THE TECTONO-SEDIMENTARY EVOLUTION OF A SUPRADETACHMENT BASIN BY DETRITAL APATITE FISSION TRACK THERMOCHRONOLOGY – THE GEDIZ GRABEN, MENDERES MASSIF, WESTERN TURKEY 10

Abstract 10

1. INTRODUCTION 11

2. GEOLOGICAL SETTING 12

2.2. The Gediz Graben 14

3. METHODS 15

3.1. Sampling strategy 16

3.2. Samples preparation and analysis 19

4. RESULTS 21

4.1. Modern rivers 21

4.2. Neogene-to-Quaternary basin fill 25

5. DISCUSSION 27

5.1. Detrital AFT age evolution of the Neogene-to-Quaternary sedimentary sequence 27

5.2. Information from main river's tributaries detrital AFT ages and along-strike variations of the cooling pattern of the southern margin of the basin 30

5.3. Considerations on apatite fertility and short-term erosion pattern 33

5.4. Schematic evolution of the Gediz Graben 36

6. CONCLUSION 39

REFERENCES 40

CHAPTER 3 - MAGMATISM EMPLACEMENT AND CRUSTAL EXTENSION: CONSTRAINING THE ACTIVATION OF DUCTILE SHEARING ALONG THE GEDIZ DETACHMENT, MENDERES MASSIF (WESTERN TURKEY) 47

Abstract 47

1. INTRODUCTION 48

2. GEOLOGICAL BACKGROUND 49
3. METHODS 52
4. RESULTS 53
4.1. Structures, textures and petrography 53
4.2. Titanite crystallisation 56
4.3. Titanite U-Pb geochronology 57
5. DISCUSSION 59
5.1. Cooling history of the Salihli granodiorite: linking exhumation to extensional shearing 60
6. CONCLUDING REMARKS 62
REFERENCES 63
CHAPTER 4 - TECTONO-STRATIGRAPHIC EVOLUTION OF THE GEDIZ SUPRADETACHMENT BASIN (MENDERES MASSIF, W TURKEY) 73
Abstract 73
1. INTRODUCTION 75
2. GEOLOGICAL SETTING 75
3. METHODS 79
3.1. Field data collection 79
3.2. Sampling strategy and samples preparation for micropaleontological analyses 80
4. RESULTS 81
4.1. Stratigraphic setting 81
4.1.1. Alaşehir Formation 81
4.1.2. Çaltilik Formation 83
4.1.3. Gediz Formation 87
4.1.4. Kaletepe Formation 88
4.2. Micropaleontological analyses 90
4.3. Structural analysis 94
4.3.1. Structure of the basin margin in the Salihli area – The Gediz Detachment 94
4.3.2. Structure of the basin margin in the Alaşehir area 97
4.3.3. High-angle brittle faulting and syn-sedimentary faults 98
5. DISCUSSION 102

5.1. Insights from micropaleontological data 102
5.2. Considerations on the Neogene-to-Quaternary basin fill 103
5.3. Considerations on the structural pattern 104
5.4. Evolution of Neogene-to-Present extensional process revealed by schematic 2D across-strike reconstruction of the activity of the Gediz Detachment 105
5.5. Evolutionary model 108
5.6. Implications for the exhumation of the Central Menderes Massif 111
6. CONCLUSION 112
REFERENCES 114

CHAPTER 1

INTRODUCTION

Continental metamorphic core complexes are generally considered the result of large-scale crustal stretching in orogenic belts following the contractional phase; here, mid-crustal metamorphic rocks are exhumed to the surface at the footwall of gently dipping ductile-to-brittle shear zones, commonly referred to as detachment faults (e.g. Coney, 1974, 1980; Crittenden et al., 1980; Davis et al. 1980, 2004; Wernike, 1985; Lister and Davis, 1989; Whitney et al., 2013; Platt et al., 2015). At the footwall of detachment faults it is common the occurrence of pre- or syn-deformational magmatic intrusions (e.g. Lister and Baldwin, 1993; Parsons and Thompson, 1993), whereas at the hanging wall supradetachment sedimentary basins may record major tectonic and exhumation events (e.g. Friedmann & Burbank, 1995). Understanding the dynamic of detachment faulting and the tectonostratigraphic evolution of supradetachment basins can thus give a complete framework of the extensional and exhumation processes that lead to the formation of metamorphic core complexes.

The Menderes Massif of western Turkey constitutes the eastern termination of the Aegean Extensional Province, a portion of the Alpine-Himalayan belt related to the north-dipping Hellenic subduction (e.g. Jolivet and Brun, 2010 and references therein). This region is undergoing ~N-S oriented extension in a back-arc tectonic setting since Eocene times (Dinter and Royden, 1993; Brun and Facenna, 2008; Brun and Sokoutis, 2012); this tectonic regime led to the formation and exhumation of a series of Cenozoic metamorphic core complexes (e.g. Jolivet and Brun, 2010; Ersoy et al., 2014 and references therein), among which the Menderes Massif (e.g. Şengör & Yilmaz, 1981; Şengör et al., 1984; Bozkurt and Park, 1994).

The aim of this PhD study is the reconstruction of the whole source-to-sink evolution of the supradetachment Gediz Graben, from the intrusion of the Salihli Granodiorite in the upper crust presently outcropping at its southern margin, to the activation and evolution of the ductile-to-brittle Gediz Detachment Fault, to the tectono-stratigraphic evolution of the basin itself and of its margins. The main purposes are the understanding of the exhumation process of the Central Menderes Massif at the footwall of the detachment (and in general the exhumation pattern), the quantification of the amount of extension accommodated during the

extensional process and in general the identification of key chronological constrains to reconstruct the Neogene tectonic history of this portion of the Menderes Massif.

This PhD thesis is built up as a collection of three scientific papers ready to be submitted for publication, presented in the next chapters, that are the result of the work done in the last three years. These complementary papers form a coherent work on the Neogene evolution of the Gediz Graben and of the Gediz Detachment, with relevant implications for the tectonic and exhumation history of the Central Menderes Massif and for the evolution of detachment fault systems in general.

In the first of these papers (Chapter 2: "*Unraveling the tectono-sedimentary evolution of a supradetachment basin by detrital apatite fission track thermochronology – The Gediz Graben, Menderes Massif, Western Turkey"*) the results of a detrital apatite fission track thermochronology study of the Gediz Graben are presented. By integrating detrital apatite fission track ages from modern rivers' sediments and from the Neogene-to-Quaternary sedimentary fill of the basin, the exhumation history of the northern margin of the Central Menderes Massif, the Neogene-to-Present evolution of the Gediz Graben and the modern erosion pattern of the surrounding bedrock have been reconstructed. This allowed to identify the major bedrock erosion events recorded in the basin sedimentary fill and to reveal that major along-strike variations in the recent cooling and short term erosion pattern exist at the southern margin of the basin; these variations have been attributed to the extremely localized nature of the last exhumation event that occurred in this area.

In the second paper (Chapter 3: *"Magmatism emplacement and crustal extension: constraining the activation of ductile shearing along Gediz Detachment, Menderes Massif (western Turkey)")* the relationship between the intrusion of the Miocene Salihli Granodiorite and the onset of ductile extensional deformation on the Gediz Detachment has been investigated. Textural analysis and in situ U-Th-Pb titanite dating have been carried out from selected samples collected in the transition from the undeformed to the mylonitized zones of the Salihli granodiorite at the footwall of the Gediz detachment fault. This study highlighted a bimodal distribution of the $^{206}Pb/^{238}U$ titanite ages that likely recorded the transition from magma crystallization and emplacement to the syn-tectonic, solid-state recrystallization, thus pointing to a major role of the magmatic intrusion in triggering the ductile extensional

detachment tectonics. This new dataset, integrated with previously published thermochronological data, allowed to produce a complete reconstruction of the cooling history of the Salihli Granodiorite, since its uppermost Early Miocene intrusion at shallow crustal depths until its Quaternary exhumation at the surface.

In the third and last paper (Chapter 4: *"Tectono-stratigraphic evolution of the Gediz supradetachment basin (Menderes Massif, W Turkey)"*) field data collected during the 1:25.000 scale geological mapping of the study area are presented together with new micropaleontological constrains. This work allowed to identify major differences in both the structural and stratigraphic patterns between the western and eastern sector of the study area. Moreover, new paleontological data allowed to refine the poorly constrained age of formation of the basin and revealed the presence of a Late Miocene short-lived marine episode in the stratigraphic record. At the end of this chapter an evolutionary model for the Gediz Graben is proposed to reconcile all the evidences presented in this thesis. This reconstruction show that this supradetachment basin displayed many different structural styles during its extensional evolution, from ramp-basin, to half-graben, to symmetric graben. In general, the aim of this work is to quantify the amount of extension accommodated since the formation of the basin to exhume the ductile-to-brittle Gediz Detachment and its footwall and to unravel the contribution of the different tectonic structures/phases to the exhumation of the Central Menderes Massif.

REFERENCES

Bozkurt, E., Park, G.R., 1994*. Southern Menderes massif: an incipient metamorphic core complex in western Anatolia, Turkey.* Journal of the Geological Society of London, 151, 213–216.

Brun, J.P., Faccenna, C., 2008. *Exhumation of high-pressure rocks driven by slab rollback*. Earth Planet. Sci. Lett., 272, 1–7.

Brun, J.-P., Sokoutis, D., 2012. *45 m.y. of Aegean crust and mantle flow driven by trench retreat*. Geol. Soc. Am., 38, 815–818.

Coney, P.J., 1974. *Structural analysis of the Snake Range "décollement," east-central Nevada*. Geological Society of America Bulletin, 88, 1237–1250.

Coney, P.J., 1980. *Cordilleran metamorphic core complexes: An overview*, *in* Crittenden, M.D., Coney, P.J., and Davis , G.H., eds., Cordilleran Metamorphic Core Complexes: Geological Society of America Memoir, 153, 7–34.

Crittenden, M.D., Jr., Coney, P.J., Davis, G.H., eds., 1980. *Cordilleran Metamorphic Core Complexes*. Geological Society of America Memoir, 153, 490 p.

Davis, G.A., Anderson, J.L., Frost, E.G., and Shackelford, T.J., 1980. *Mylonitization and detachment faulting in the Whipple-Bucksin-Rawhide Mountains terrane, southeastern California and western Arizona*. in Crittenden, M.D., Coney, P.J., and Davis, G.H., eds., Cordilleran Metamorphic Core Complexes: Geological Society of America Memoir, 153, 9-129.

Davis G. H., Constenius K. N., Dickinson W. R., Rodríguez E. P., Cox L. J., 2004. *Fault and fault-rock characteristics associated with Cenozoic extension and core-complex evolution in the Catalina–Rincon region, southeastern Arizona*. Geological Society of America Bulletin, 116, 128-141.

Dinter, D.A., Royden, L., 1993. *Late Cenozoic extension in northeastern Greece: Strymon Valley detachment system and Rhodope metamorphic core complex*. Geology, 21, 45–48.

Ersoy E.Y., Çemen İ., Helvacı C., Billor Z., 2014 - *Tectono-stratigraphy of the Neogene basins in Western Turkey: Implications for tectonic evolution of the Aegean Extended Region*. Tectonophysics, 635, 33–58.

Friedmann S. J. & Burbank D. W., 1995. *Rift basins and supradetachment basins: intracontinental extensional end-members*. Basin Research, 7, 109-127.

Jolivet, L., Brun, J.P., 2010. *Cenozoic geodynamic evolution of the Aegean*. International Journal of Earth Sciences, 99, 109–138.

Lister G. S. & Baldwin S. L., 1993. *Plutonism and the origin of metamorphic core complexes*. Geology, 21, 607-610.

Lister, G.S., and Davis, G.A., 1989. *The origin of metamorphic core complexes and detachment faults formed during Tertiary continental extension in the northern Colorado River region, USA*. Journal of Structural Geology, 11, 65–94, doi:10.1016/0191-8141(89)90036-9.

Parsons T. & Thompson G. A., 1993. *Does magmatism influence low-angle normal faults?* Geology, 21, 247-250

Platt et al., 2015

Şengör A. M. C. & Yilmaz Y., 1981. *Tethyan evolution of Turkey: a plate tectonic approach*. Tectonophysics, 75, 181–241.

Sengör, A.M.C., Satir, M., Akkök, R., 1984. *Timing of the tectonic events in the Menderes massif, western Turkey: implications for tectonic evolution and evidence for Pan- African basement in Turkey*. Tectonics, 3, 693–707.

Wernike, B., 1985. *Uniform-sense normal simple shear of the continental lithosphere*. Canadian Journal of Earth Sciences, 22(1), 108-125.

Whitney D. L., Teyssier C., Rey P. & Buck W. R., 2013: *Continental and oceanic core complexes*. Geological Society of America Bulletin, 125 (3/4), 273-298.

CHAPTER 2

UNRAVELING THE TECTONO-SEDIMENTARY EVOLUTION OF A SUPRADETACHMENT BASIN BY DETRITAL APATITE FISSION TRACK THERMOCHRONOLOGY – THE GEDIZ GRABEN, MENDERES MASSIF, WESTERN TURKEY

Riccardo Asti[1], **Marco Giovanni Malusà**[2] and **Claudio Faccenna**[1]

1) Università degli Studi Roma Tre, Department of Sciences, Rome, Italy

2) University of Milano-Bicocca, Department of Earth and Environmental Sciences, Milan, Italy

Abstract: The Menderes Massif is an outstanding example of Tertiary metamorphic core complex, exhumed in the upper Oligocene – Miocene time, during the deposition of a series of E-W trending basins. Several studies address to the exhumation history of the massif, but the depositional history of this basins is still poorly defined. The aim of this study is to reconstruct the source-to-sink evolution of the Gediz Graben, defining the exhumation/cooling pattern of the Central Menderes Massif at the footwall of the Gediz Detachment Fault and reconstructing the sedimentary evolution of the basin. We used low-temperature detrital thermochronology to unravel the sedimentary history of the basin and the erosion pattern of the study area on short-term and long-term timescales. We integrated fission track dating of detrital apatite from the modern Alaşehir/Gediz river and from some of its tributaries with a careful assessment of hydraulic sorting effects and mineral fertility in the source rocks. We additionally performed detrital apatite fission track analyses on the ancient sedimentary succession to better constrain the age of the Neogene sedimentary fill of the graben. We found that a Late Miocene major event of bedrock exhumation localized at the northern margin of the Central Menderes Massif have been recorded in the basin, following the Upper Oligocene/Lower Miocene main cooling event that involved the whole Menderes Massif. A second and more recent cooling event involved only the western portion of the southern margin of the basin, leading the Gediz Detachment and the Salihli Granodiorite to the surface in very recent times in the Bozdağ area (Early Pleistocene). The modern short term erosion

pattern closely reflects this event, showing higher erosion rates in the exposure area of the Gediz Detachment than in the rest of the investigated region.

1. INTRODUCTION

The Aegean region is an outstanding example of an area where a phase of intense crustal extension followed an orogenic phase of shortening and thickening of the continental crust (e.g. Jolivet & Faccenna, 2000); here, late to post-orogenic extension is ongoing since Eocene time (e.g. Brun & Sokoutis, 2007). In regions of intense post-orogenic extension, tectonics can commonly lead to exhumation of upper-to-middle crustal rocks, usually by extensional ductile-to-brittle detachment faults that eventually put in contact deeply buried mylonitic metamorphic rocks at the footwall with unmetamorphosed upper crustal rocks at the hanging wall (e.g. Gibbs, 1984; Lister & Davis, 1989). Nevertheless, it is always important to take into account the fact that exhumation results from the combination of tectonic processes and erosion at the surface (e.g. England & Molnar, 1990). In highly extended continental terrains, supradetachment basins with high sedimentation rates associated to the main tectonic structures may record phases of tectonic activity and erosion, giving important constrains on the exhumation history of the region (e.g. Friedmann & Burbank, 1995).

Along-strike variations of the cooling pattern are seldom taken into account; their identification, together with careful field analysis of structures, is fundamental to discriminate between local and regional exhumation events, thus avoiding misinterpretation in tectonic reconstructions. This kind of variation might also be reflected in the erosion pattern that onset after exhumation.

Despite many study addressed to the sedimentary fill of the basin, the chronology of sedimentation in the Gediz Graben is still poorly defined; detrital apatite fission-track analysis can be then an invaluable tool to define the maximum age of sedimentary deposits where constrains from other sources (like paleontology, or datable volcanic deposits) are lacking (e.g. Baldwin et al., 1986; Gallagher et al., 1998).

In this study, the analysis of detrital apatite fission-track from both modern river sediments and from the Neogene-to-Quaternary sedimentary fill of the Gediz Graben allowed us to

reconstruct the exhumation and sedimentary history of the study area since the formation of the basin until present times, drawing a geologic evolution in which the succession of the main sedimentary and exhumation events is unraveled and the contribution of the different structures (among which the Gediz Detachment Fault) is determined.

2. GEOLOGICAL SETTING

2.1. *The Menderes Massif*

The Menderes Massif is exposed along the Western Turkey sector of the Alpine-Himalayan belt which has experienced during the Cenozoic an orogenic phase and post-orogenic collapse (e.g. Şengör et al., 1984; Şengör, 1987; Gessner et al., 2013). It is built up of continental fragments with African affinity accreted along the southern margin of Laurasia and separated by major suture zones (Şengör et al., 1984). The Menderes Massif is located in the southernmost among these continental blocks, namely the Tauride-Anatolide Platform, according to Şengör & Yilmaz (1981). This block is separated from the Sakarya zone to the North by the Izmir-Ankara Suture Zone.

Rocks outcropping in the Menderes Massif recorded a complex tectono-metamorphic history, preserving traces of Pan-African, Variscan and Alpine tectono-metamorphic events (e.g. Ring et al., 1999; Lips et al., 2001; Oberhänsli et al., 2010 and references therein). The Alpine nappe stack of the Menderes Massif represents the lowermost tectonic unit of the Anatolide Belt (e.g. Ring et al., 1999, 2001; Gessner et al., 2013 and references therein), and is composed of 4 nappes: 1) the Selimiye Nappe is the structurally uppermost unit and is composed of low-grade metabasites, metapelites and marble with protolith ages spanning from Precambrian to Devonian/Carboniferous times (e.g. Ring at al., 1999, 2001 and references therein; Régnier et al., 2003); 2) the underlying Çine Nappe is composed mainly of orthogneiss and undeformed metagranite with intrusion age of the protolith around 530-560 Ma (e.g. Zlatkin et al., 2013 and references therein) and minor pelitic gneiss, eclogite and amphibolite (e.g. Ring et al., 1999, 2001); 3) the Bozdağ Nappe occurs structurally below and is mainly composed of metapelite with minor lens of marble, amphibolite and eclogite (Ring et al., 1999, 2001); the Bayındır Nappe is the lowermost tectonic unit and consists of Alpine

greenschist facies phyllite, quartzite and marble (e.g. Lips et al., 2001; Ring et al., 2001).

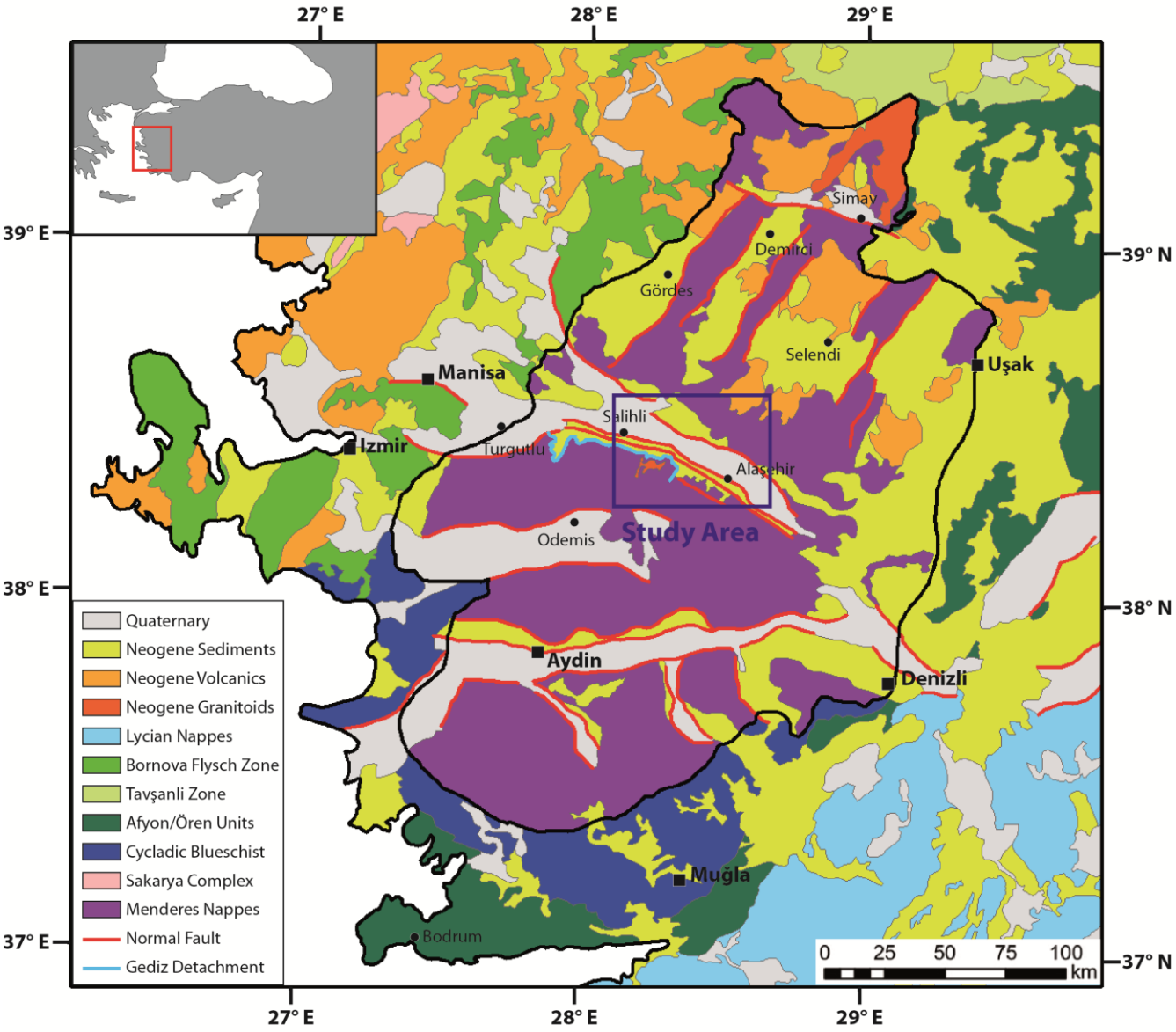

Figure 1: *Schematic tectonic map of SW Turkey. The black line delimitates the Menderes Massif; the blue box show the location of the study area represented in Fig. 2.*

The NNE-SSW directed extensional phase that affects the Anatolide Belt since the latest Oligocene and related retreat of the Aegean subduction system (e.g. Şengör, 1987; Seyitoğlu & Scott, 1996a; Thomson & Ring, 2006; Jolivet & Brun, 2010) led to the Miocene formation of two major E-W trending grabens (Büyük Menderes and Gediz graben) that divided the Menderes Massif in three sub-massifs (i.e. Northern, Central and Southern Menderes Massif).

During this phase the gently dipping (~20°) ductile-to-brittle Gediz Detachment Shear Zone was formed; it separates mylonitic gneiss deformed under greenschist conditions at its footwall from unmetamorphosed Neogene sediments of the Gediz Graben at its hanging wall (e.g. Hetzel et al., 1995). The mylonitic foliation of the detachment dips gently to the NNE and shows a well-developed stretching lineation oriented ~N30 and kinematic indicators always reporting a top-to-the-NNE sense of shear (e.g. Işik et al., 2003).

Two syn-extensional intrusive bodies outcrop at the footwall of the Gediz Detachment, namely the Salihli and Turgutlu granodiorite; the intrusion age of these plutons has been suggested to be early-middle Miocene, around 15-16 Ma (Glodny & Hetzel., 2007).

At the hanging wall of the Gediz Detachment the Neogene-to-present deposits of the Gediz Graben lay on top of the detachment's surface in tectonic contact, with strata tilted to the SSW cut by high-angle normal faults that root on the detachment.

Existing thermochronological data for the Menderes Massif (Gessner et al., 2001, 2013; Ring et al., 2003; Thomson & Ring, 2006; Buscher et al., 2013) highlighted two major episodes of cooling during the Cenozoic, a first one during late Oligocene – early Miocene and a second one from late Miocene to Quaternary, with the latter involving only the Central Menderes Massif and showing a clear rejuvenation trend of the cooling ages from S to N in the Gediz Detachment's area.

2.2. The Gediz Graben

The formation of the Gediz Graben is related to the activity of the Gediz Detachment and the other major normal faults bounding the northern margin of the Central Menderes Massif (e.g. Çiftçi & Bozkurt, 2009; Öner & Dilek, 2011), but clear age constrains for the beginning of the sedimentation and for the main sedimentary events are lacking. The basin's formation and the sedimentation of the lower half of the fill have been inferred to be early-middle Miocene in age, on the base of palynological data (e.g. Seyitoğlu and Scott, 1992; Ediger et al., 1996). Çiftçi & Bozkurt (2009) suggested that the basin developed as an half-graben with an active southern margin during Miocene and changed its geometry during post-Miocene with the activation of the northern margin.

In the Gediz Graben, major differences in the cooling pattern exist between the northern and southern margin of the basin, the former being exhumed in Late Oligocene – Early Miocene times and the latter between Late Miocene and Early Quaternary (Gessner et al., 2001, 2013; Ring et al., 2003; Thomson & Ring, 2006, Buscher et al., 2013).

Many studies in the last two decades have addressed the sedimentary evolution of the Gediz Graben, but most of these used different names and subdivisions for the lithostratigraphic units of the basin fill (e.g. Iztan & Yazman, 1991; Cohen et al., 1995; Emre, 1996; Koçyiğit et al., 1999; Sarica, 2000; Yilmaz et al., 2000; Seyitoğlu et al., 2002; Purvis & Robertson, 2005; Çiftçi & Bozkurt, 2009), thus making difficult to unravel the stratigraphy of this area and generating controversies on the age of different formations. In this study we use the nomenclature proposed by Çiftçi & Bozkurt (2009), with some modifications due to field observations and differences in the stratigraphic sequence in outcrop between western and the eastern sectors of the study area, who divided the sedimentary sequence outcropping at the southern margin of the basin in 4 different lithostratigraphic formations: the oldest one is represented by the Alaşehir Fm., which is made of grey-to-brownish continental conglomerates and sandstones (Evrenli Mbr.) heteropic with lacustrine shales and siltstones (Zeytinçayi Mbr.); above this, are the concordant continental red sandstones and conglomerates of the Çaltilik Fm., that are characterized in their lower part by a few-tens of meters thick limestone interval; the above Gediz Fm. is represented by yellowish continental sandstones and conglomerates with an overall coarsening-upward trend; the uppermost unit is the discordant Plio-Quaternary Kaletepe Fm., generally made of brown continental conglomerates and sandstones. On top of this Neogene-to-Quaternary sedimentary sequence are the Quaternary alluvial deposits of the modern graben.

For what concerns the distribution in outcrop of the different formations of the sedimentary sequence, major differences exist between the eastern (Alaşehir area) and the western (Salihli area) sector of the study area; the older deposits (i.e. the Alaşehir Fm. and the lower part of the Çaltilik Fm.) outcrop only in the former area, whereas in the latter the oldest outcropping deposits are represented by the middle part of the Çaltilik Fm.

3. METHODS

Apatite fission-track dating method relies on the damages produced in the crystal lattice by fission decay of radioactive elements and that are preserved in the mineral below the closure temperature of ~110/120°C, providing useful information on cooling and exhumation through the upper 3-4 Km of the crust (Gallagher et al., 1998).

Apatite fission-track analysis from detrital samples represents a powerful tool to quantify the sedimentary budget from main river's tributaries draining rocks that experienced contrasting cooling history (e.g. Resentini & Malusà, 2012). The determination of apatite budget from each source area in this kind of study is a key issue, because slowly eroding apatite-rich rocks can provide comparable amounts of apatite of apatite-poor rocks eroding fast, thus representing a major and unneglectable source of bias (Resentini & Malusà, 2012; Malusà et al., 2015). In general, by integrating detrital apatite fission track analysis from modern sediments and from the ancient sedimentary fill of a basin it is possible to build a solid dataset to unravel the erosional/sedimentary history allowing to:

- constrain the maximum age of ancient sedimentary deposits by dating the exhumation of their source rocks, when other constrains are lacking;
- estimate average long-term exhumation rates of the source areas of modern sediments by calculating their age-peaks;
- reconstruct the modern short-term erosion pattern by evaluating the relative erosion rates of the different source areas alimenting the main river's sediment load.
- reconstruct the ancient short-term erosion patterns by identifying major exhumation events recorded in the ancient basin sedimentary fill;

3.1. *Sampling strategy*

In order to reconstruct the modern erosion pattern of the study area we use the method proposed by Resentini & Malusà (2012). We collected 5 samples of sorted bedload sediment along the trunk of Alaşehir /Gediz river (MAIN1-4 inside the study area from Sarigöl to Salihli in the Alaşehir river and MAIN5 far away in the direction of the river flow after the confluence of the Alaşehir river in the Gediz river) for apatite fission-track dating (Fig. 2). To identify the AFT age signal of the source areas and to determine their apatite fertility, we also collected 5 bedload samples from some of the left tributaries (SX1-5; draining the southern margin of the basin) and 3 from some of the right tributaries (DX1-3; draining the northern margin of the

basin); these latter 8 samples were taken in catchments draining only the bedrock of the basin, avoiding influences in the detrital signal and in fertility determination of sediments provided by the Neogene-to-Quaternary basin fill (Fig. 2). Samples SX3-5 were collected in catchments draining the Salihli granodiorite, the mylonitic shear zone of the Gediz Detachment and its footwall (Bayındır nappe), while samples SX1-2 were collected in catchments draining mainly rocks at the hanging-wall of the detachment related to the Çine nappe of the Menderes metamorphic basement. Samples DX1-3 were collected in catchments draining rock related to the Çine and the Selimiye nappe.

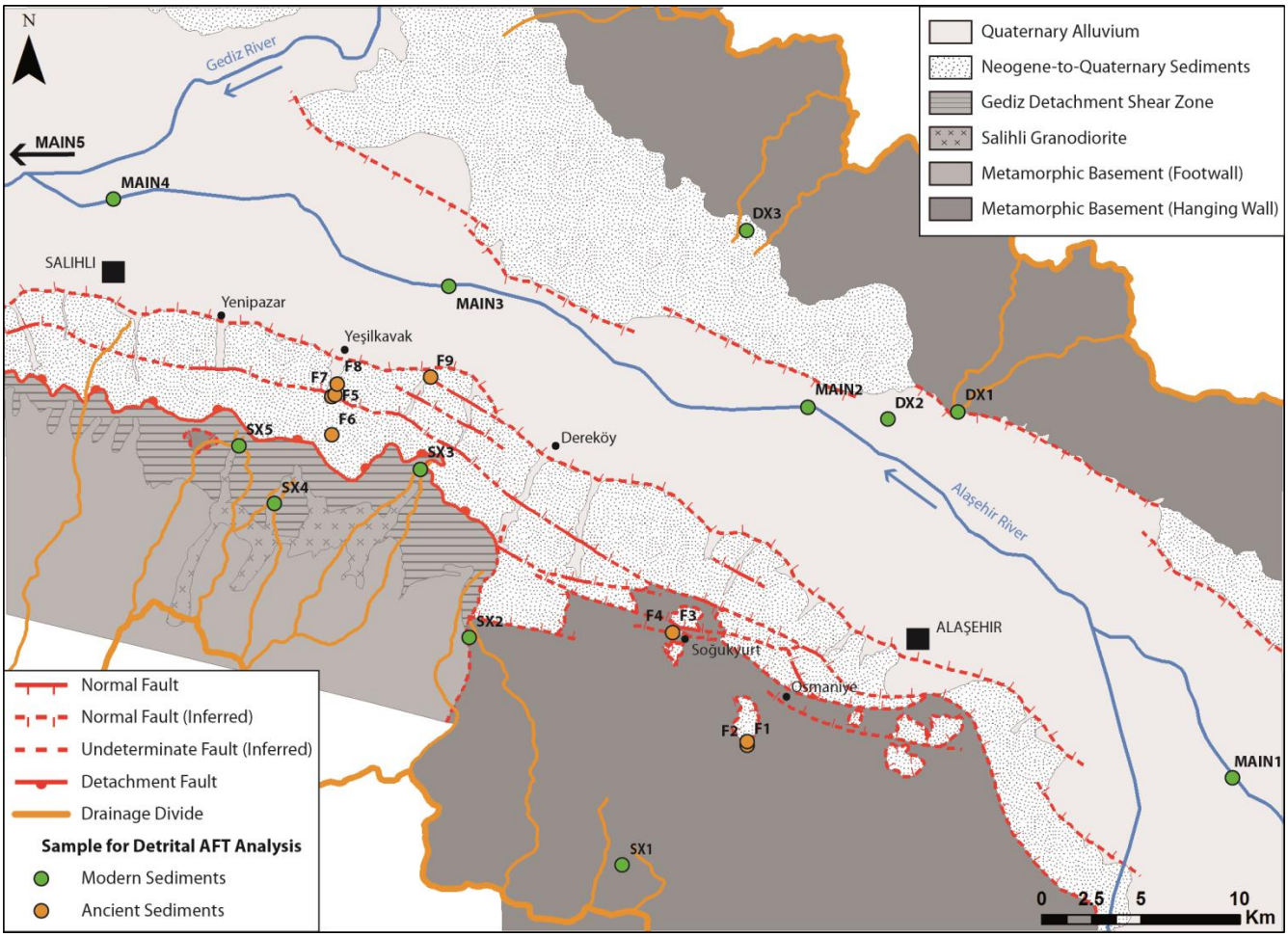

Figure 2: *Simplified geologic map of the study area with location of the samples for detrital apatite fission track analysis.*

For this study we took samples from strata close to the southern edge of the basin, in order to avoid possible problems with thermal resetting of AFT ages that could be expected in a more central and deeply buried portion of the graben (Garver et al., 1999).

In diagenesized sedimentary succession the abundance of any mineral species is not only function of mineral fertility and hydraulic sorting, but also of the stability of minerals to diagenetic dissolution (e.g. Morton, 1985); moreover, disaggregation processes during sample preparation might alter the original grain-size signature of sediments. All this makes impossible the determination of original mineral fertility of the source rocks from ancient sediments (Malusà et al., 2015).

Sample	Lab Code	River	Site	Lat.	Long.
MAIN1	DTR6	Alaşehir	Bağlica	N 38° 18' 09.9"	E 28° 39' 27.2"
MAIN2	DTR7	Alaşehir	Şendurak	N 38° 26' 04.6"	E 28° 27' 55.4"
MAIN3	DTR8	Alaşehir	Yeşilova	N 38° 28' 37.8"	E 28° 18' 09.1"
MAIN4	DTR9	Alaşehir	Salihli	N 38° 30' 29.6"	E 28° 09' 02.7"
MAIN5	DTR13	Gediz	Yeniharmandali	N 38° 38' 22.4"	E 27° 32' 32.6"
SX1	DTR1	S tributary	Kestanelik	N 38° 16' 18.9"	E 28° 22' 53.2"
SX2	DTR2	S tributary	Karadağ	N 38 ° 21' 09.0"	E 28° 18' 43.2"
SX3	DTR3	S tributary	Karadut	N 38° 24' 45.2"	E 28° 17' 25.2"
SX4	DTR5	S tributary	Çatak	N 38° 24' 00.6"	E 28° 13' 25.9"
SX5	DTR4	S tributary	Damatli	N 38° 25' 13.7"	E 28° 12' 27.4"
DX1	DTR12	N tributary	Türkmen	N 38° 25' 58.3"	E 28° 32' 01.1"
DX2	DTR11	N tributary	Matarli	N 38° 24' 41.9"	E 28° 30' 03.0"
DX3	DTR10	N tributary	Gülpinar	N 38° 29' 50.0"	E 28° 26' 13.8"

Table 1: *Location of samples from the modern Alaşehir /Gediz river and its tributaries.*

We sampled for detrital AFT analysis the Neogene-to-Quaternary basin fill (Fig. 2 and 7) in order to reconstruct the long-term exhumation history of the area and to find constrains on the maximum age of the different deposits. We took 9 samples from the whole sedimentary succession: 2 samples from the oldest Alaşehir Fm. (Zeytinçayi Mbr., F1-2), 4 samples from the Çaltilik Fm. (F3-4 from the lower part with limestone intercalations and F5-6 from the upper part), 2 from the Gediz Fm. (F7-8) and 1 from the Kaletepe Fm. (F9).

Sample	Lab Code	Formation	Site	Lat.	Long.
F1	ALA04	Alaşehir Fm.	Güldere	N 38° 18' 51.8"	E 28° 26' 18.2"
F2	DTR ALA1	Alaşehir Fm.	Güldere	N 38° 18' 49.4"	E 28° 26' 15.8"
F3	DTR CAT2	Çaltilik Fm.	Soğukyurt	N 38° 21' 16.4"	E 28° 24' 15.2"
F4	DTR CAT1	Çaltilik Fm.	Soğukyurt	N 38° 21' 16.4"	E 28° 24' 15.2"
F5	DTR RED2b	Çaltilik Fm.	Kocayar	N 38° 26' 18.4"	E 28° 14' 59.1"
F6	DTR RED1	Çaltilik Fm.	Degirmendere	N 38° 24' 48.2"	E 28° 17' 55.2"
F7	DTR YEL1	Gediz Fm.	Kocayar	N 38° 26' 19.5"	E 28° 15' 04.4"
F8	DTR YEL2	Gediz Fm.	Kocayar	N 38° 26' 33.7"	E 28° 15' 09.6"
F9	DTR YEL3	Kaletepe Fm.	Erendali	N 38° 26' 42.8"	E 28° 17' 40.0"

Table 2: *Location of samples from the Neogene-to-Quaternary basin fill of the Gediz Graben.*

3.2. Samples preparation and analysis

For all samples from modern catchments, in order to recover the highest amount of apatite grains, we used MinSORTING (Resentini et al., 2013) to model the mineral distribution and sorting in different grain-size windows, defining in this way the grain-size classes with the highest probability to retrieve apatite grains.

To determine apatite fertility in the source areas while separating apatite grains from the bulk sediment we applied to the samples collected in the main river's tributaries (SX1-5 and DX1-3) the procedure described in Malusà et al. (2015) that allows to determine the apatite concentration in the bulk sediment and to determine if it reflects mineral concentration in the source rocks (Fig. 3).

In samples coming from the Alaşehir /Gediz river (MAIN1-5) and from the Neogene-to-Quaternary basin fill apatite grains were separated from the bulk sediment using standard techniques: 1) pre-concentration of the denser component by GEMINI shaking table processing separately different grain-size classes to minimize the effect of grain-size during hydrodynamic sorting (Malusà et al., 2013); 2) centrifugation of the heavier part in sodium polytungstate with density δ = 2.90 kg/dm3; 3) refinement of the fraction denser than 2.90 kg/dm3 by using a Frantz magnetic separator to remove the magnetic minerals; 4) dense-liquid processing of the dense diamagnetic fraction in diiodomethane (δ = 3.32 kg/dm3).

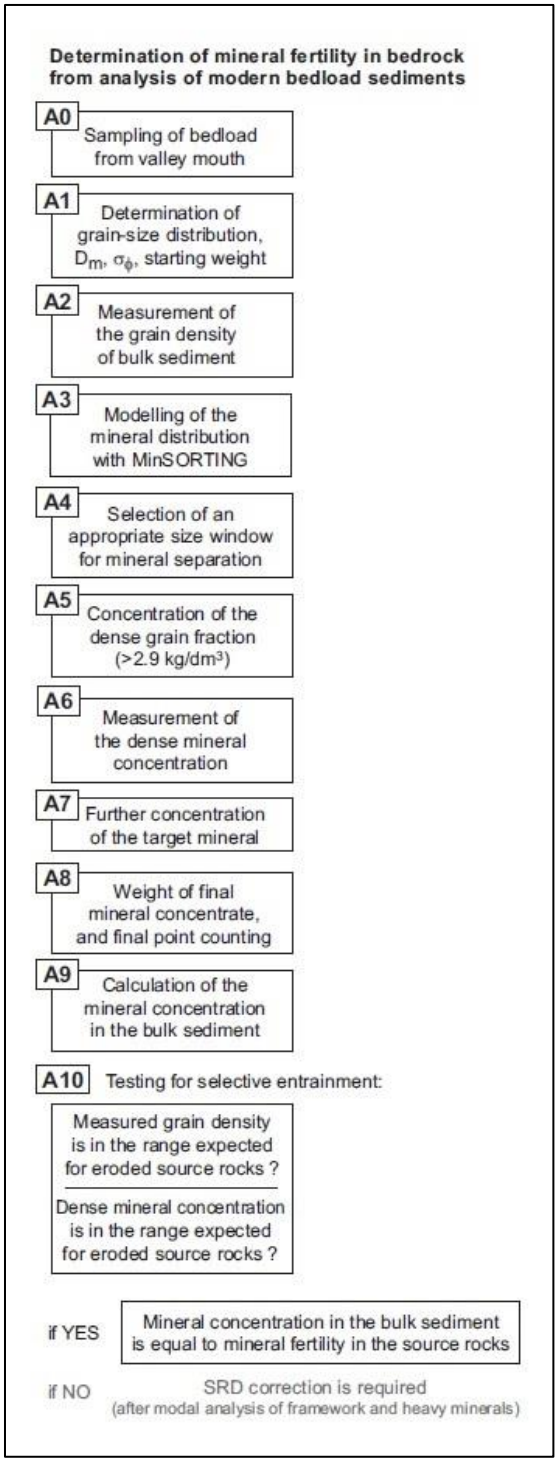

Figure 3: *Flowchart for the determination of mineral fertility in bedrock from detrital samples (Malusà et al., 2015; modified).*

All the samples were prepared for nuclear irradiation following the External Detector Zeta (ζ) Calibration Method (Hurford, 1990) and were then irradiated in the TRIGA-II nuclear reactor at

Oregon State University (USA). Fission-track counting was carried on in the Laboratory of Milano Bicocca University (Italy) with an Olympus microscope (1250X magnification) equipped with FT-Stage software (Dumitru, 1993). For each counted grain, we documented several features, such as size, shape, the presence of defects and fluid inclusions (in clusters or in plans), and we investigated their potential relationship with fission-track age by using Radial Plotter (Vermeesch, 2009). Grain age was determined by using Trackkey software (Dunkl, 2002), while decomposition of grain-age distribution was carried out with BinomFit software (Brandon, 2002).

4. RESULTS

4.1. *Modern rivers*

No apparent relationship have been found between grain-age and grain-size and between grain-age and grain-shape in all the samples analyzed (Fig. 4), showing that grain age distributions are not vulnerable to hydraulic sorting effects. Moreover, grain density of the detrital samples from tributaries of the main river (Fig. 5) show values consistent with those expected for deposits with geologically analog source areas, thus suggesting that selective entrainment did not affect their composition and allowing their use to infer the composition of the parent bedrock (Malusà et al., 2015).

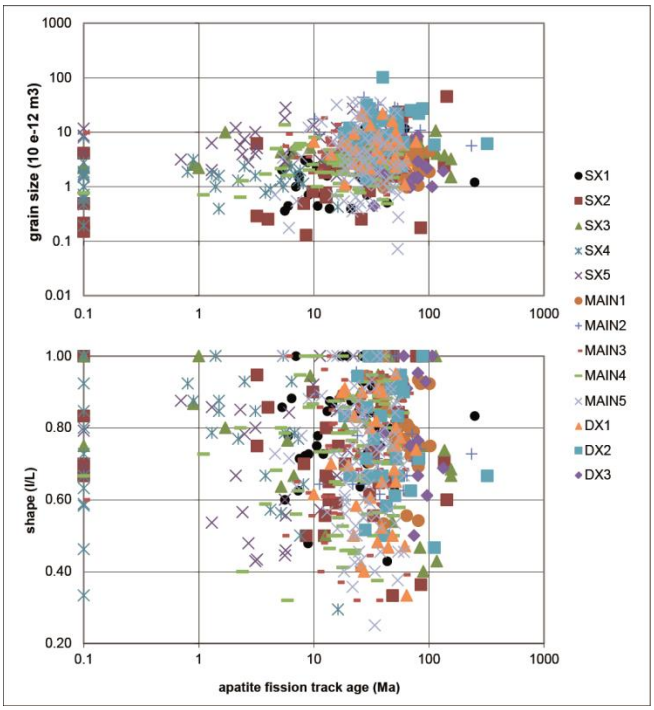

Figure 4: *Diagrams showing the relationship between AFT grain-ages and grain size (top) and between AFT grain-ages and grain shape (bottom) in the detrital samples collected in the modern rivers. No apparent correlation raised in the correlation between these parameters, showing that the grain-age distributions are not vulnerable to hydraulic sorting effects.*

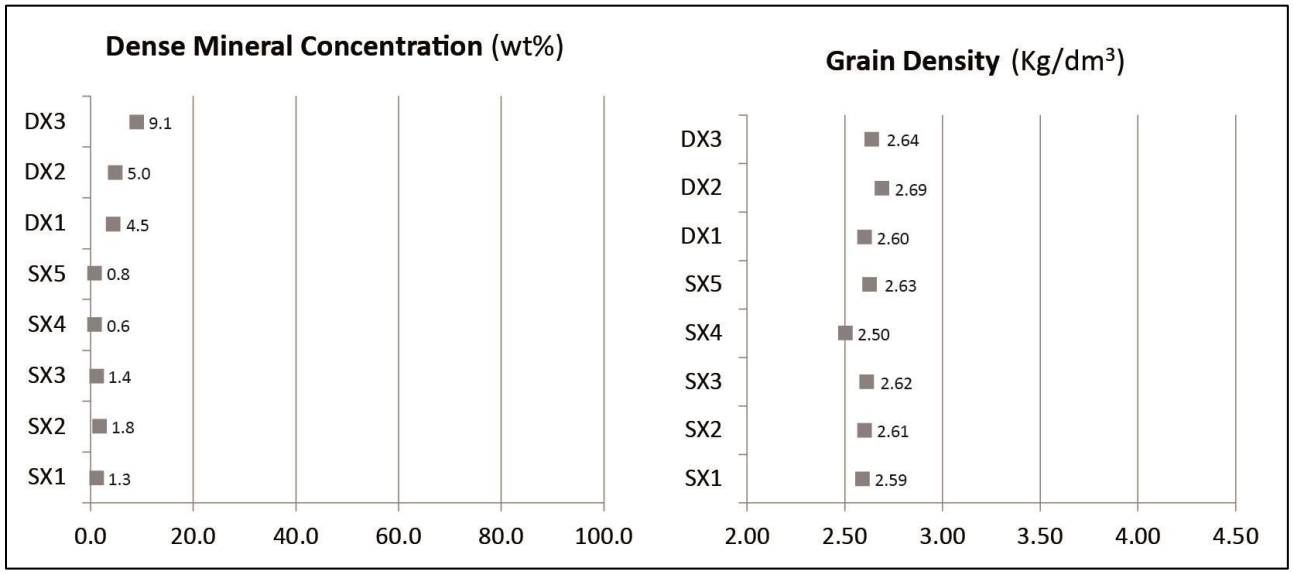

Figure 5: *Dense Mineral Concentration (left) and Grain Density values (right) in samples from the northern (DX) and southern (SX) tributaries of the main river. Dense Mineral Concentration is always <10% and Grain Density is always <2.70 Kg/dm^3: these values show that the analyzed samples are not affected by anomalous enrichment of dense minerals due to hydraulic effects during transport.*

By measuring apatite abundance in processed sediments form tributaries draining the basin's margin (samples SX1-5 and DX1-3), we found that mean apatite fertility in the outcropping area of the Salihli granodiorite and of the milonitized shear zone of the Gediz Detachment and its footwall (186 ppm) is three times less than the mean fertility of the rest of the source area (551 ppm) (Fig. 6).

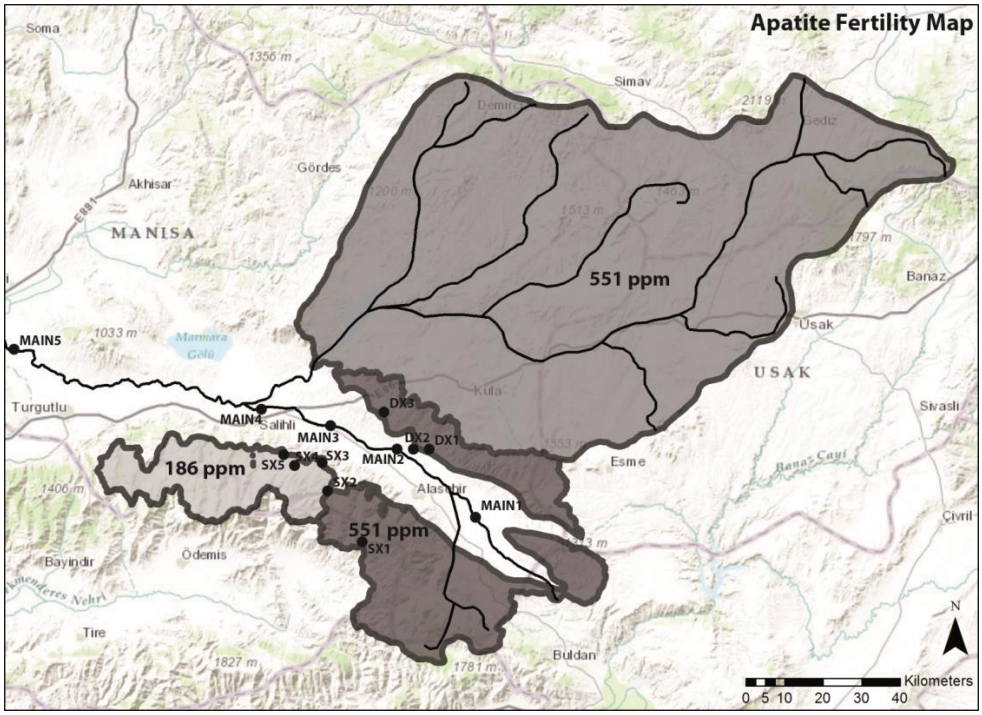

Figure 6: *Apatite fertility map of the study area. Apatite fertility is expressed in ppm.*

Sample	River	Site	Drainage Area (km^2)	Textural parametrs mean size (phi)	sorting (phi)	skewness (phi)	selected window (μm)	relative amount (%)	dense mineral (%)	grain density (kg/dm^3)	Apatite size distribution coarser (%)	in selected window (%)	finer (%)	Apatite Fertility > 63 μm (ppm)
SX1	Kestanelik	Kestanelik	7	2.63	1.26	-0.06	63-500	61.47	1.3	2.59	7.3	78.5	14.2	312.0
SX2	Ozan	Karadağ	56	2.40	1.27	-0.05	63-500	55.55	1.8	2.61	10.2	78.9	11	734.0
SX3	Dariyeri	Karadut	21	1.70	0.98	0.19	125-500	28.97	1.4	2.62	2.2	70.7	16.7	179.0
SX4	Kisik	Çatak	17	2.50	1.20	-0.14	63-500	56.56	0.6	2.50	6.6	80.7	11.6	259.0
SX5	Karanohut	Damatli	28	1.90	1.14	0.04	125-500	41.66	0.8	2.63	15.9	63.2	20.9	120.0
DX1	-	Türkmen	31	2.57	1.24	-0.11	63-500	59.34	4.5	2.60	7.6	79.2	13.1	563.0
DX2	-	Matarli	29	1.83	0.85	-0.08	125-500	40.59	5.0	2.69	10.2	77.5	12.2	569.0
DX3	Sarikaya	Gülpinar	22	2.00	1.42	-0.11	63-500	49.79	9.1	2.64	19.5	72.4	8.1	577.0

Table 3: *Apatite fertility in samples from the main river's tributaries.*

In Fig. 9 we reported the results of grain-age distribution of samples from modern rivers, represented in radial plots, with their relative position with respect to the drainage network, showing the confluences of the sampled tributaries in the Alaşehir /Gediz river in order to highlight the influence of their age-signal along the trunk of the main river. All the results for detrital AFT from modern rivers are listed in Table 4.

Sample	**Age**	**Error**	**%**	**Age**	**Error**	**%**	**Age**	**Error**	**%**
	1st population			2nd population			3rd population		
SX1	9.3	+3.3/-2.4	44.5	25.5	+9.1/-6.7	47.6	47.6	+23.5/-15.7	7.9
SX2	6.4	+2.2/-1.6	44.5	40.8	+7.3/-6.2	55.5	-	-	-
SX3	3.8	+2.4/-1.5	31.4	32.2	+13.9/-9.7	42.4	110.4	+56.3/-37.4	26.2
SX4	0.5	+1/-0.3	61	4.8	+4.1/-2.2	39	-	-	-
SX5	2.4	+0.6/-0.5	69.8	16.7	+3.6/-3	30.2	-	-	-
DX1	26.8	+10/-7.3	62.6	44.1	+23.7/-15.4	37.4	-	-	-
DX2	35.7	+6.8/-5.7	82.8	80.8	+27.5/-20.6	17.2	-	-	-
DX3	68.9	± 11.7	100	-	-	-	-	-	-
MAIN1	55.2	± 5.4	100	-	-	-	-	-	-
MAIN2	33	+8.1/-6.5	83.2	74.9	+31.6/-22.3	16.8	-	-	-
MAIN3	14.3	+5.4/-3.9	20.9	32.2	+5.9/-5	79.1	-	-	-
MAIN4	11.6	+3.4/-2.7	35.4	37.5	+7.1/-6	64.6	-	-	-
MAIN5	6.6	+5.7/-3	4.6	26.1	+5.7/-4.7	70.5	48.8	+19.3/-13.8	24.9

Table 4: *(on the previous page) Apatite grain-age populations of samples from the modern Alaşehir /Gediz river (MAIN1-5) and its soutern (SX1-5) and northern (DX1-3) tributaries; age and error are expressed in Ma.*

In most of the cases, decomposition of grain-are distribution yielded more than one distinct population. Samples from catchments draining the southern margin of the basin yielded much younger age peaks (less tha 9.3 Ma for their younger peaks) with respect to those found in catchments draining the northern margin (more than 26.8 Ma for their younger peaks), confirming that the latter have not been exhumed by the same structures responsible for the exhumation in the former sector. We also noticed that variations in the younger age peak occur along the strike of the structures bounding the southern margin (Fig. 10), with the westernmost samples yielding ages younger than 5 Ma (light-grey boxes in Fig. 9) and the easternmost ones yielding ages in the range between 6 and 10 Ma (dark-grey boxes of the southern tributaries in Fig. 9).

Samples SX3-5 yielded the youngest age peaks of the whole study area, while samples SX1-2 provided slightly older ages for the youngest age peak. Samples DX1-3, from catchments draining the northern margin, yielded older ages for their youngest age peaks. All these ages are consistent with bedrock low-T thermochronology ages from northern and southern margin of the basin. Samples MAIN1-5, collected in the Alaşehir /Gediz river, show a rejuvenation of the younger age peak in the direction of the river flow (see radial plots in the central column in Fig. 9).

For what concerns detrital-apatite flux in the main Alaşehir /Gediz river, on sample MAIN3 the contribution from the Gediz Detachment and its footwall (i.e. apatite grains with grain-age >5 Ma) is 2%, for sample MAIN4 it increases to 14% and in sample MAIN5 it decreases again to 3%. Our dataset does not allow to discriminate between the contribution to the apatite flux in the main river from the norther margin of the Gediz Graben and from the eastern portion of the southern margin (Alaşehir area), because of their similar age signal. Furthermore, it is not possible to distinguish the contribution to the main river's apatite flux of the exposed Neogene-to-Quaternary deposits from that of the metamorphic bedrock at the hanging wall of the Gediz Detachment, because these are characterized by similar AFT ages (see below).

4.2. *Neogene-to-Quaternary basin fill*

Results for detrital AFT from the Neogene-to-Quaternary sedimentary sequence are listed in Table 5. In Fig. 7 are reported the results of grain-age distribution of samples from ancient sediments of the Gediz Graben sedimentary fill, represented in radial plots, with their position with respect to the Neogene-to-Quaternary stratigraphy of the basin. In the lower part of the stratigraphic sequence, in samples from the Alaşehir Fm. (F1-2) and the lower part of the Çaltilik Fm. (F3-4), all the age-peaks obtained after decomposition of grain-age distribution are characterized by ages older than Middle Miocene. Starting from the upper part of the Çaltilik Fm. until the youngest deposits of the Kaletepe Fm. (samples F5-9), a younger age-peak is obtained in all the samples, with a Late Miocene age.

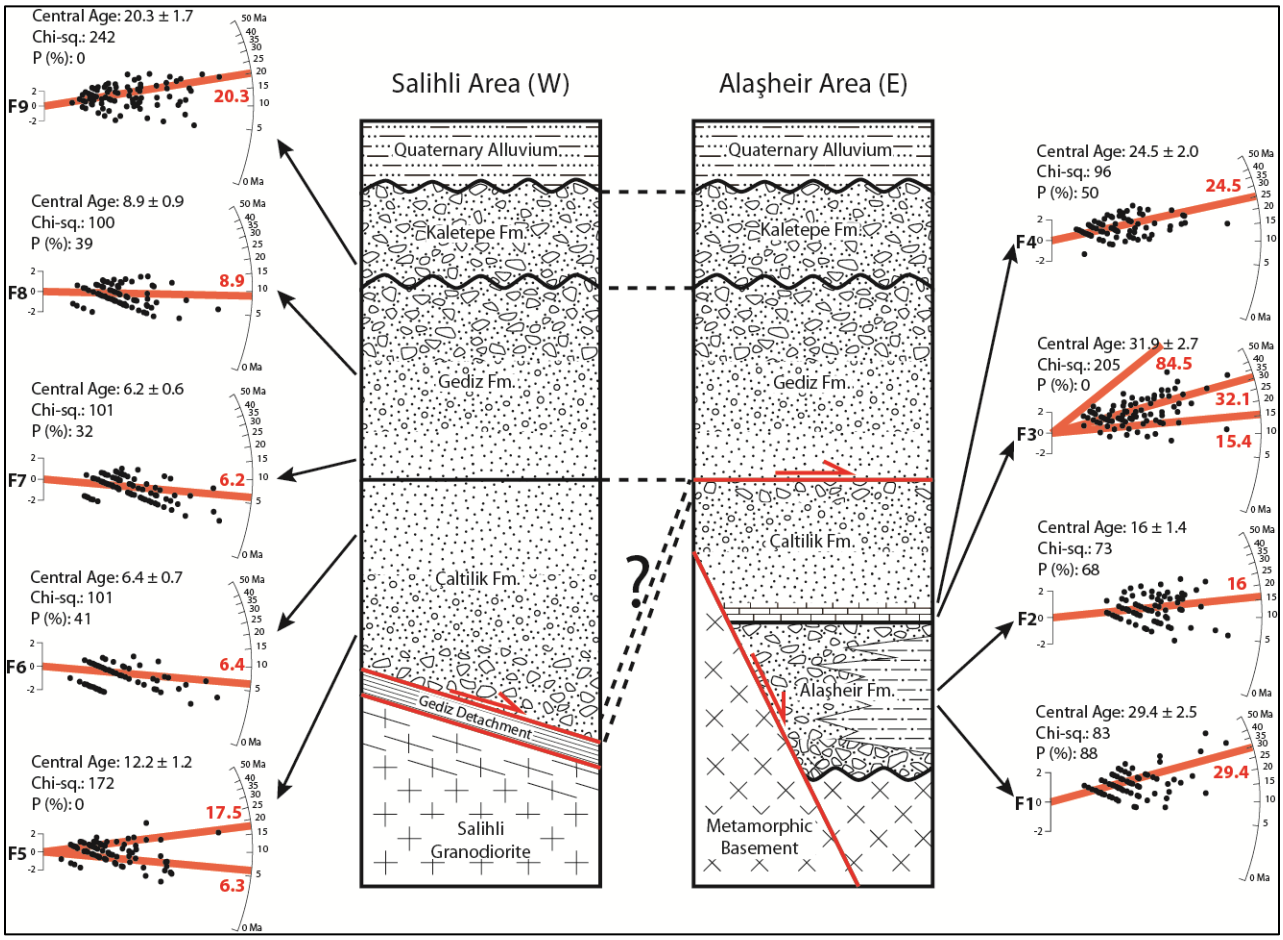

Figure 7: *Stratigraphy of the Gediz Graben and radial plots reporting apatite fission track grain-age distribution for detrital samples from the Neogene-to-Quaternary sedimentary sequence (F1-9), with relative stratigraphic position indicated by black arrows. Light-red lines in the radial plots show age peaks (with relative value in red expressed in Ma) for the different populations retrieved after grain-age deconvolution with BinomFit software (Brandon, 2002).*

Sample	Formation	Age	Error	%	Age	Error	%	Age	Error	%
		1st population			2nd population			3rd population		
F1	Alaşehir	29.4	± 2.5	100	-	-	-	-	-	-
F2	Alaşehir	16	± 1.4	100	-	-	-	-	-	-
F3	Çaltilik	15.4	+9.1/-5.7	18.2	32.1	+6.9/-5.7	74.4	84.5	+35.1/-24.9	7.3
F4	Çaltilik	24.5	± 2	100	-	-	-	-	-	-
F5	Çaltilik	6.3	+2.6/-1.8	45	17.5	+5.1/-3.9	55	-	-	-
F6	Çaltilik	6.4	± 0.7	100	-	-	-	-	-	-
F7	Gediz	6.2	± 0.6	100	-	-	-	-	-	-
F8	Gediz	8.9	± 0.9	100	-	-	-	-	-	-
F9	Kaletepe	9.3	+3.4/-2.5	23.3	21.1	+5.5/-4.3	61.3	36.2	+19.8/-12.8	15.4

Table 5: *Apatite grain-age populations of samples from the Neogene-to-Quaternary sedimentary succession of the Gediz Graben; age and error are expressed in Ma.*

5. DISCUSSION

5.1. *Detrital AFT age evolution of the Neogene-to-Quaternary sedimentary sequence*

The lowest sample of the whole stratigraphic succession analyzed (F1) (Fig. 7) yielded a single age-peak at 29.4 ± 2.5 Ma compatible with existing bedrock AFT ages in the region. The same is for sample F2 (16 ± 1.4 Ma), that was sampled ~20m above the former. This data show that at the beginning of the sedimentary history of the Gediz graben there is no evidence for an episode of major exhumation of the source areas. Moreover, this data yielded a maximum age for the deposition of the Zeytinçayi Mbr. of the Alaşehir Fm. corresponding to the lower-middle Miocene boundary, refining the weak existing age data based on the palynological association that pointed to a lower-middle Miocene age (20-14 Ma) for the deposition of this formation (Iztan & Yazman, 1991; Seyitoğlu & Scott, 1992; Ediger et al., 1996).

Also samples taken in sandy layers intercalated to limestone layers at the base of the Çaltilik Fm. (F3-4), yielded age-peaks comparable with existing upper Oligocene to middle Miocene bedrock AFT ages, thus confirming that no major synchronous event of bedrock exhumation is represented in the lower part of the stratigraphic succession. The maximum age for these deposits furnished by the younger age-peak of sample F3 (15.4 ± 7.4 Ma) is comparable with the one of the underlying Alaşehir Fm.

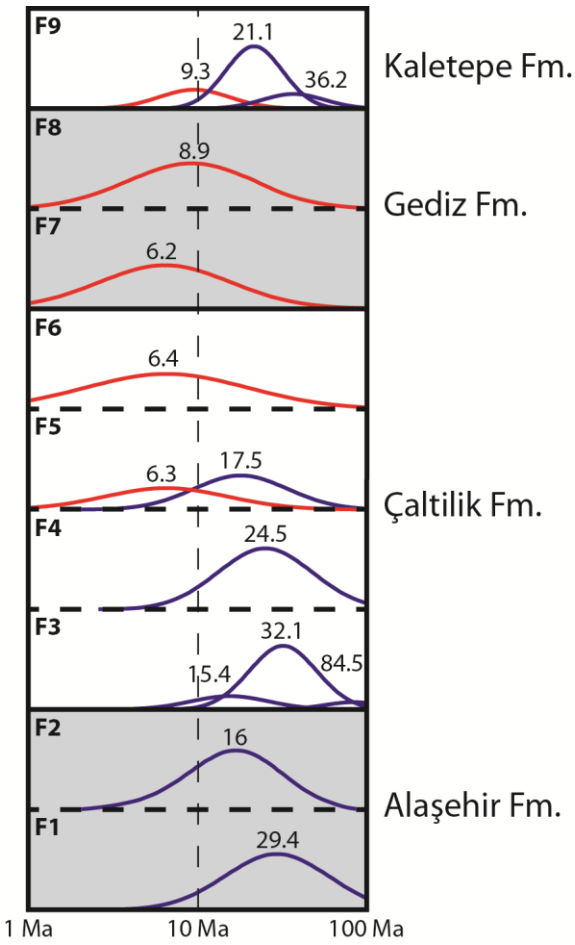

Figure 8: *Diagram reporting probability density plots for samples from the Neogene-to-Quaternary basin fill in stratigraphic order. Ages are expressed in Ma. After the first upper Oligocene-to-lower Miocene exhumation phase of the Menderes Massif recorder in the lower part of the stratigraphic succession (samples F1-4) and here represented by the blue peaks, a second major exhumation event, upper Miocene (Tortonian-Messinian) in age, is recorded in the basin from the middle part of the Çaltilik Fm. to the Gediz Fm. (samples F5-8), here represented by the red peaks. Sample F8 yield a slightly older age for its younger peak (8.9 ± 0.9 Ma) with respect to those of the lower samples, probably because its age-peak is influenced by grain-ages yielding both Messinian ages and older ages related to other source areas that the software used for deconvolution was not able to separate in two different populations.*

Starting from the upper part of the Çaltilik Fm., a new and younger episode of bedrock exhumation is recorded in the sedimentary fill of the basin (Fig. 7 and 8). Samples F5 (6.3 ± 2.2 Ma and 17.5 ± 4.5 Ma) and F6 (6.4 ± 0.7 Ma) both yielded Messinian AFT age-peaks, indicating that the source area of this deposits experienced a cooling/exhumation phase in this period. Moreover, samples from the overlaying Gediz fm. (F7-8) yielded detrital AFT age-peaks spanning from upper Tortonian to Messinian time. The fact that sample F8 yield a slightly older age of the younger peak (8.9 ± 0.9 Ma) with respect to the lower samples can be explained considering that its age-peak might be influenced by grain-ages yielding Messinian ages and older ages related to other source areas that the software used for deconvolution was not able to distinguish. All these data suggest that, after the first upper Oligocene-to-lower Miocene exhumation phase of the Menderes Massif recorder in the lower part of the stratigraphic succession, a second major exhumation event, upper Miocene (Tortonian-Messinian) in age, is recorded in the basin (Fig. 8).

The fact that the sample related to the Kaletepe Fm. (F9) yielded a young age-peak older than the lower samples reflects the fact that this formation is separated from the older ones by an unconformity (Fig. 7) and that was fed by sediments coming from the older sedimentary fill of the basin, thus not representing a discrepancy in the stratigraphic distribution of detrital ages.

In terms of maximum age of the deposition of these formations, data from the upper part of the Çaltilik Fm. represent a breakthrough: the only existing age determination in the literature for these deposits relies on the Eskihisar sporomorph association (20–14 Ma) of Benda & Meulenkamp (1979, 1990), while our new dataset significantly makes younger this age, pointing to a depositional age more recent than 6.3 ± 2.2 Ma (i.e. not before Messinian time). On the contrary, detrital AFT age data from the Gediz and Kaletepe Fm. do not give any significant new information on the age of these deposits, with respect to existing literature data, pointing to an age of deposition younger than 6.2 ± 0.6 Ma; Emre (1996) already assigned a Dacian age (Mio-Pliocene boundary) to the Göbekli Fm., that in our interpretation, based on field observation, can be correlated to the lower part of the Gediz Fm.

Basing on our detrital AFT data and on paleontological data by Emre (1996), it is possible to reconstruct a mean exhumation rate for the source area during the upper Messinian by using

the lag time method (e.g. Brandon & Vance 1992, Garver & Brandon 1994): considering a closure temperature of the AFT system at 110°C, a paleogeothermal gradient of 100°C/Km (roughly calculated by using pressure-temperature condition for the crystallization of the Salihli granodiorite proposed by Erkül et al., [2013] that occurred in the latest Early Miocene, according to Glodny & Hetzel [2007]) and a lag time of 0.9 ± 0.6 Ma between the deposition of the lower part of the Gediz Fm. and the exhumation of its source area, we obtained a mean exhumation rate of 2.2 ± 1.47 Km/Ma (or mm/a) during the late Messinian. If we use for the same interval the paleogeothermal gradient of 40°C/Km proposed by Buscher et al. (2013), calculated from the mean modern surface heat flow in the Menderes Massif, we would obtain a mean exhumation rate of 5 ± 3.33 Km/Ma (or mm/a) during the late Messinian, which is in our opinion unreasonably high.

In terms of sedimentation rate, it is possible to reconstruct a minimum value for the upper part of the Çaltilik Fm. by crossing our data with those of Emre (1996). Considering a stratigraphic difference of at least ~500m between sample F5, that yielded a young age-peak at 6.3 ± 2.2 Ma, and the sediments dated by Emre (1996) as Dacian (i.e. Mio-Pliocene boundary), we obtained a mean sedimentation rate of at least 500 m/Ma (0.5 mm/a) for the upper Messinian, which is comparable as order of magnitude with similar basins (e.g. Friedmann & Burbank, 1995). If this sedimentation rate have been constant (or didn't vary much) through time since the beginning of the sedimentation, it is likely that formation of the Gediz Graben is not older than Middle Miocene.

5.2. *Information from main river's tributaries detrital AFT ages and along-strike variations of the cooling pattern of the southern margin of the basin*

Considering that the samples collected in the main river's tributaries (SX1-5 and DX1-3) drain relatively small and lithologically uniform areas, and that their mineralogical composition and grain-age distribution have not been significantly modified by hydrodynamic processes compared to that of their source rock (Fig. 4 and 5), it is reasonable to assume that their grain-age distribution closely reflects the cooling age of their relative source areas. From this point of view, these detrital samples' data represents also new bedrock cooling-age data and provide new information with respect to the exhumation-age data existing in the literature (i.e. Gessner et al., 2001, 2013; Ring et al., 2003; Thomson & Ring, 2006; Buscher et al., 2013).

Samples from the northern tributaries show two different trends in their age-peaks (Fig. 9): some of them are consistent with the exhumation-ages known from the literature (see younger peaks in samples DX1-2), whereas some other are contrasting, because of their older ages (see sample DX3 and older peaks in samples DX1-2). This age distribution indicates that in the small source areas of these samples the thermal history of the bedrock did not completely reset the AFT system during the Cenozoic, preserving some older exhumation ages with respect to those known in the area.

These older ages are preserved also in the older peaks of samples from most of the tributaries draining the southern margin of the basin, particularly in those draining the bedrock at the hanging wall of the Gediz detachment (samples SX1-2) and klippen laying of top of the detachment surface (sample SX5 and probably sample SX3).

Samples from the southern margin provide interesting information also on variations in the cooling pattern along the strike of the main graben bounding structures that are involved in the exhumation of this sector (Fig. 9 and 10). Samples SX3-5, from catchments draining the Salihli granodiorite, the mylonitic-to-ultracataclastic Gediz detachment shear zone and the footwall of the detachment, yielded very young AFT cooling-ages (Pliocene or younger) for their drainage areas that are consistent with the existing bedrock low-T thermochronology in the same area, that also show a rejuvenation trend in the direction of the dipping of the detachment (Gessner et al., 2001; Buscher et al., 2013). On the contrary, sample SX1, from a catchment draining only Menderes metamorphic rocks (Çine nappe) at the hanging wall of the Gediz detachment, yielded an older age (9.3 ± 2.8 Ma) for its younger age-peak, confirming the structural relationship between this sector and the detachment fault and pointing to a different cooling/exhumation history for this portion for the southern margin. Moreover, in sample SX2, whose drainage area comprehends both rocks at the hanging wall of the detachment and partially rocks at its footwall, the younger age-peak (6.4 ± 1.9 Ma) seems to be influenced by the younger grain-ages of both sectors (around 10 Ma to the SE and less than 5 Ma to the NW), toughening this interpretation. All these data seems to suggest that the western portion of the southern margin (the Salihli area, where the Salihli granodiorite and the mylonitic-to-ultracataclastic Gediz detachment outcrop) experienced a younger and independent phase of exhumation with respect to the eastern portion (the Alaşehir area).

In our opinion, the cooling pattern of the southern margin is somehow strongly influenced by the presence of the early-middle Miocene granodioritic Salihli pluton. In this light, bedrock exhumation ages calculated on the granodiorite are not extendible along the whole strike of the southern margin, because these are probably related to an extremely localized event.

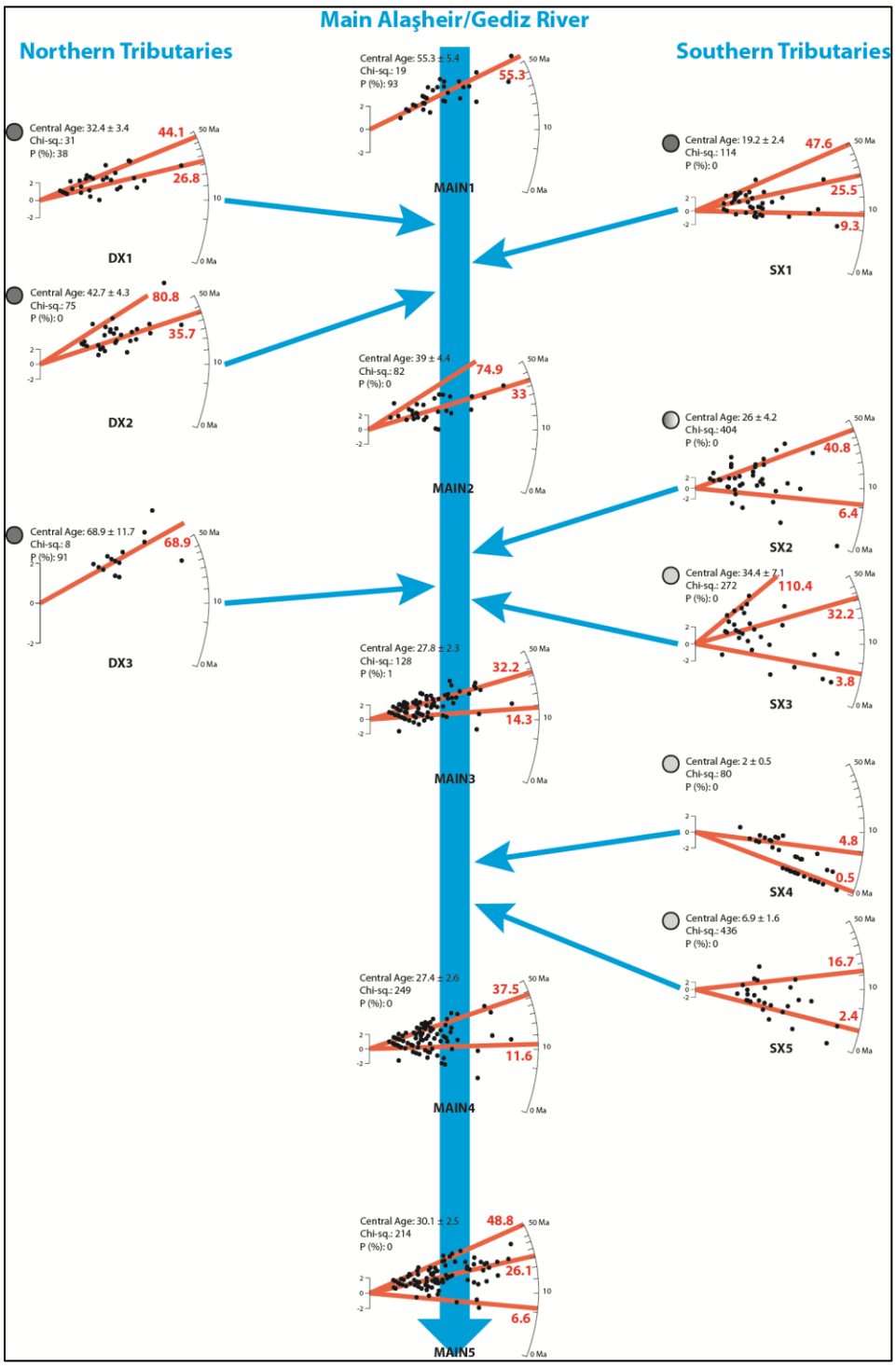

Figure 9: *(on the previous page) Radial plots reporting apatite fission track grain-age distribution for the modern rivers' detrital samples. In the central column samples from the modern Alaşehir /Gediz river (MAIN1-5), in the left column samples from the northern (right) tributaries (DX1-3) and in the right column samples from the southern (left) tributaries (SX1-5). Radial plots with a light-grey circle to the left of the central age are relative to tributaries draining the footwall of the Gediz Detachment (SX3-5), while those with a dark-grey circle to the left of the central age are relative to tributaries draining its hanging wall (SX1 and DX1-3); radial plot with a shaded dark-to-light-grey circle to the left of the central age is relative to the southern tributary draining both the footwall and the hanging wall of the detachment (SX2).The thick blue arrow indicate the direction of the main river flow, while the thin blue arrows show the position of the confluence of the sampled tributaries in the main river with respect to the position of the samples from the modern Alaşehir /Gediz river. Light-red lines in the radial plots show age peaks (with relative value in red expressed in Ma) for the different populations retrieved after grain-age deconvolution with BinomFit software (Brandon, 2002).*

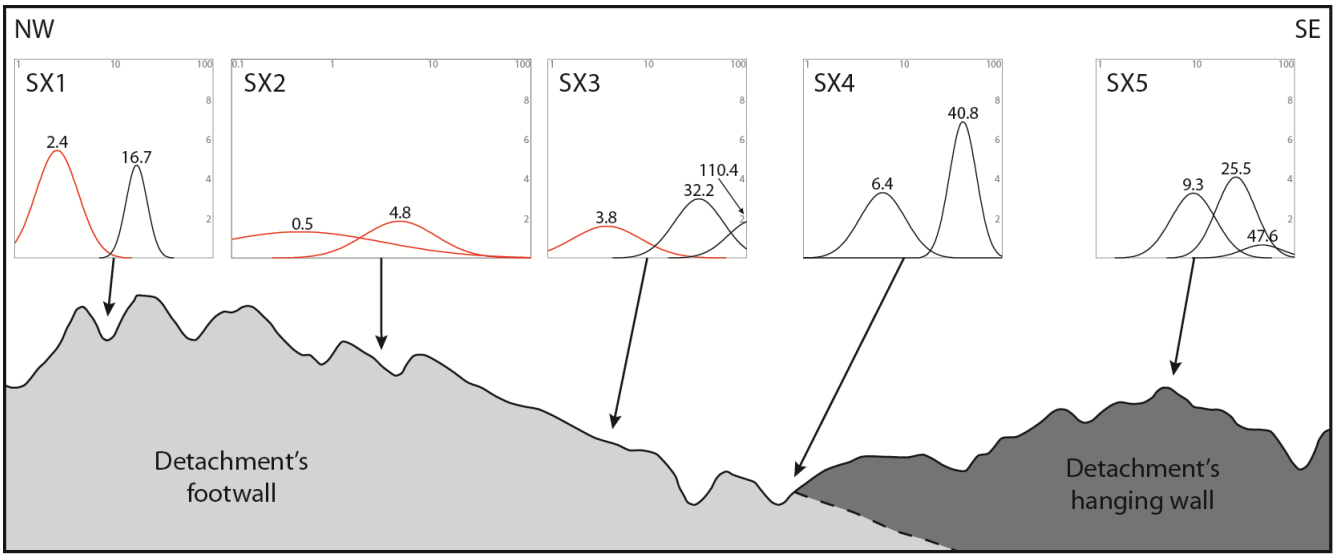

Figure 10: *Schematic cross-section (see Fig. 11 for the location) showing the relative position of samples collected in tributaries draining the southern margin of the basin (Gediz Detachment side) and the structural relationship between their drainage areas. Results for detrital apatite fission track grain-age distribution is represented in probability density plots with age-peaks expressed in Ma; red peaks are those relative to the youngest exhumation event. It is clearly visible that this last event involved only the footwall of the Gediz Detachment (western part of the margin), confirming that this structure does not bound the whole southern margin of the basin.*

5.3. *Considerations on apatite fertility and short-term erosion pattern*

By measuring apatite fertility in the different source areas, we found that there is a strong difference in the mean fertility between the outcropping area of the Neogene Salihli granodiorite and the Gediz detachment (186 ppm) and in the rest of the source area (551

ppm) (Fig. 6). This means that in the evaluation of the sediment contribution on the main Alaşehir /Gediz river, the number of apatite grains with a grain-age signal ascribed to the detachment's area should be multiplied by a factor of 3 in order to properly estimate its contribution to the whole sediment load.

Considering that the lithologies outcropping in the drainage area of the Gediz river upstream the confluence of the Alaşehir river (i.e. the Northern Menderes Massif) are the same that outcrop at the northern margin of the Gediz graben, we found reasonable to extrapolate the apatite fertility value calculated from the left tributaries (551 ppm) to this area.

Considering relative apatite contribution from each drainage area and their mean apatite fertility, we defined the contribution to the total sediment load in the Alaşehir /Gediz river of the outcropping area of the Gediz Detachment and its footwall (including the Salihli Granodiorite); we found that it represents 6% of the total sediment load in sample MAIN3, 33% in sample MAIN4 and 8% in sample MAIN5, while all the remaining contribution is related to the Menderes metamorphic basement. These values can be divided by the relative drainage area to get relative (nondimensional) erosion rate (Fig. 11). For sample MAIN3 we found that the erosion rate of the easternmost portion of the detachment's area is more or less equal to the one of Menderes metamorphic basement at the margins of the Gediz Graben. For sample MAIN4, that is much more representative of the contribution of the Gediz Detachment to the total sediment load of the Alaşehir /Gediz river, we calculated that the erosion rate of detachment's area and its footwall is ~3.5 times higher than in the rest of the drainage area. The difference in the erosion rate of the Gediz Detachment area between its central part and its eastern termination (i.e. between sample MAIN4 and MAIN3) is in our opinion related to the fact that the latter area is in close proximity of the hanging wall, thus being uplifted and eroded less than the rest of the structure. For sample MAIN5 we could finally calculate also the ratio of the erosion rate of the Northern Menderes Massif with respect to the other drainage areas. In fact, between sample MAIN4 and MAIN5 the drainage area of the Menderes metamorphic basement in the Gediz Graben remains almost the same; in this way the difference in the contribution to the sediment load of the Menderes metamorphic basement above the Gediz Detachment between the two samples is related only to the contribution of the drainage of the Northern Menderes Massif. Hence, we found that the erosion rate of the Northern Menderes Massif drained by the Gediz river is ~3 times

higher than in the metamorphic basement at the margins of the Gediz Graben and slightly lower than in the Gediz Detachment area.

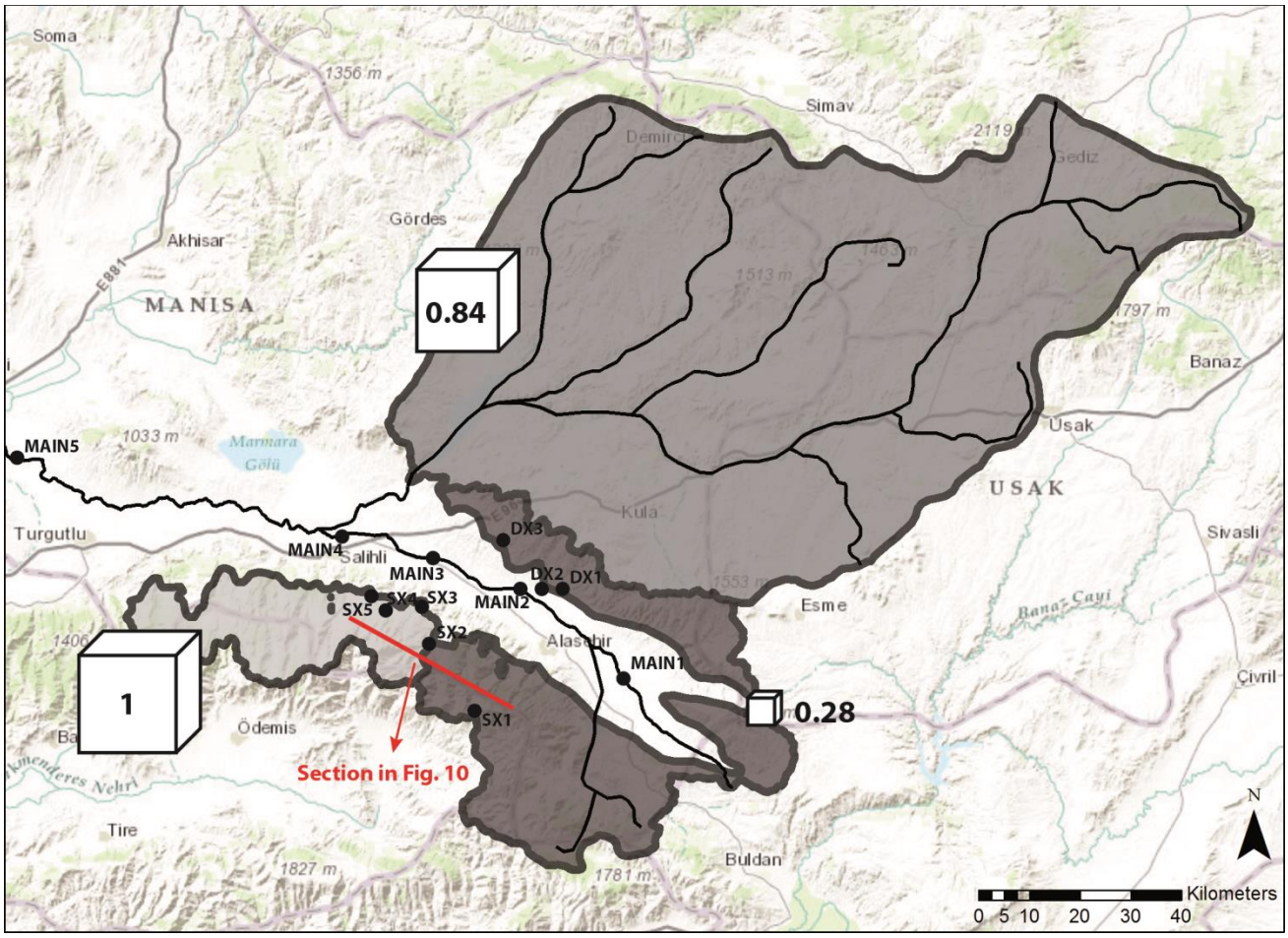

Figure 11: *Short-term erosion pattern of the drainage area of the Alaşehir /Gediz river; relative dimension of the white cubes represents the relative short-term erosion rate (nondimensional) of each sub-basin; the red line indicates the trace of the schematic cross-section of Fig. 10. The erosion is now focused on the outcropping area of the Gediz Detachment and of its footwall (including the Salihli granodiorite).*

Buscher et al. (2013) quantified the erosion rate of the Gediz Detachment area by using cosmogenic ^{10}Be, obtaining a mean value of 110 ± 10 mm/Ka. By integrating this value with our results and we obtained an erosion rate of 31 ± 2.8 mm/Ka for the Menderes metamorphic basement at the hanging wall of the Gediz Detachment at the Gediz Graben margins, and a rate of 93 ± 8.4 mm/Ka for the Northern Menderes Massif drained by the Gediz river.

The fact that the erosion rate of western part of the southern margin of the basin is much higher than in the eastern part and in the northern margin might be related to the fact that the youngest exhumation event that lead to the surface the Gediz Detachment (revealed by its younger AFT ages) generated a localized recent uplift that did not affect its hanging wall, thus reflecting on the short-term erosion pattern. The fact that the highest peaks of the region (the Bozdağ range) are located right at the footwall of the detachment seems to support this interpretation. In our opinion, this is another evidence that the presence of the granodioritic Salihli pluton might have played a major role in the exhumation of the Gediz Detachment's ductile-to-brittle shear zone.

The relatively high erosion rate of the Northern Menderes Massif with respect to that of metamorphic basement surrounding the Gediz Graben is, in our opinion, related to the fact that in this region the Gediz river drains also Neogene NE-trending continental basins that are reasonably eroding much faster than their metamorphic basement.

5.4. *Schematic evolution of the Gediz Graben*

To summarize our results, in Fig. 12 we schematically represented the evolution of Gediz Graben. Previously published bedrock apatite fission track data (Gessner et al., 2001), together with our detrital ages from the northern modern tributaries, show that the northern margin of the basin was already exhumed during Oligocene or Early Miocene at the latest, so did not experienced relevant exhumation during the whole evolution of the graben.

The detrital apatite fission track ages recorded in the lower part of the stratigraphic sequence (i.e. Alaşehir Fm. and lower Çaltilik Fm.) reflect the fact that the source areas of these deposits where not undergoing major exhumation by the time of the first phases of basin formation (i.e. Middle Miocene: Çiftçi & Bozkurt, 2009; this study. Fig. 12a).

During Late Miocene, a major phase of exhumation involves the southern margin of the basin and is recorded in the detrital apatite fission track ages of all the upper part of the Neogene-to-Quaternary sedimentary sequence (Fig. 12b), starting from the middle Çaltilik Fm. This phase is controlled by the brittle high-angle normal faults bounding the southern margin of the basin, that lead to exhumation of their footwall and produced significant accommodation space at their hanging wall for the deposition of the upper Çaltilik Fm. and Gediz Fm. between

Late Miocene and Pliocene. These normal faults rooted on the detachment shear zone at depth, that at that time was not already exposed at the surface (e.g. Gessner et al., 2001; Buscher et al., 2013; this study) and was rather under conditions for ductile deformation at least until Messinian time (Lips et al., 2001).

The last exhumation phase recorded in the southern margin by both bedrock and detrital apatite fission track data (Gessner et al., 2001; Ring et al., 2003; Buscher et al., 2013; this study) occurred during Late Pliocene – Early Pleistocene and involved only the western part (Salihli area) of the margin, where it is presently exposed to the surface the Gediz Detachment ductile-to-brittle shear zone and rocks at its footwall, including the latest Early Miocene Salihli granodiorite (Fig. 12c). It is likely that this differential exhumation produced a differential uplift between the eastern and the western sectors, which is closely reflected by many present-day features such as the topography, the short-term erosion pattern and the rocks exposed at the surface. As a matter of fact, the sector of the margin that experienced the last exhumation phase (to the W) is topographically much higher than the eastern part and, in general, than the whole Menderes Massif, with the peaks of the Bozdağ Range located in this area representing the highest elevations reached in the present-day Menderes Massif's topography. Moreover, the short-term erosion pattern (Fig. 11) show much higher erosion rates in the Gediz Detachment area, which might likely be related to the highest relief produced by the last exhumation event. Basement rocks outcropping in the eastern sector of the basin margin do not show any ductile deformation related to the Neogene extensional phase that generated the basin, thus suggesting that in this portion is exposed an higher crustal level than the in the western sector; finally, in the Alaşehir area are visible in outcrop the oldest sedimentary units of the Gediz Graben fill which might have been more uplifted in the Salihli area above the Gediz Detachment and then eroded, thus explaining the differences in the outcropping stratigraphic sequence between the two sectors (see Fig. 7).

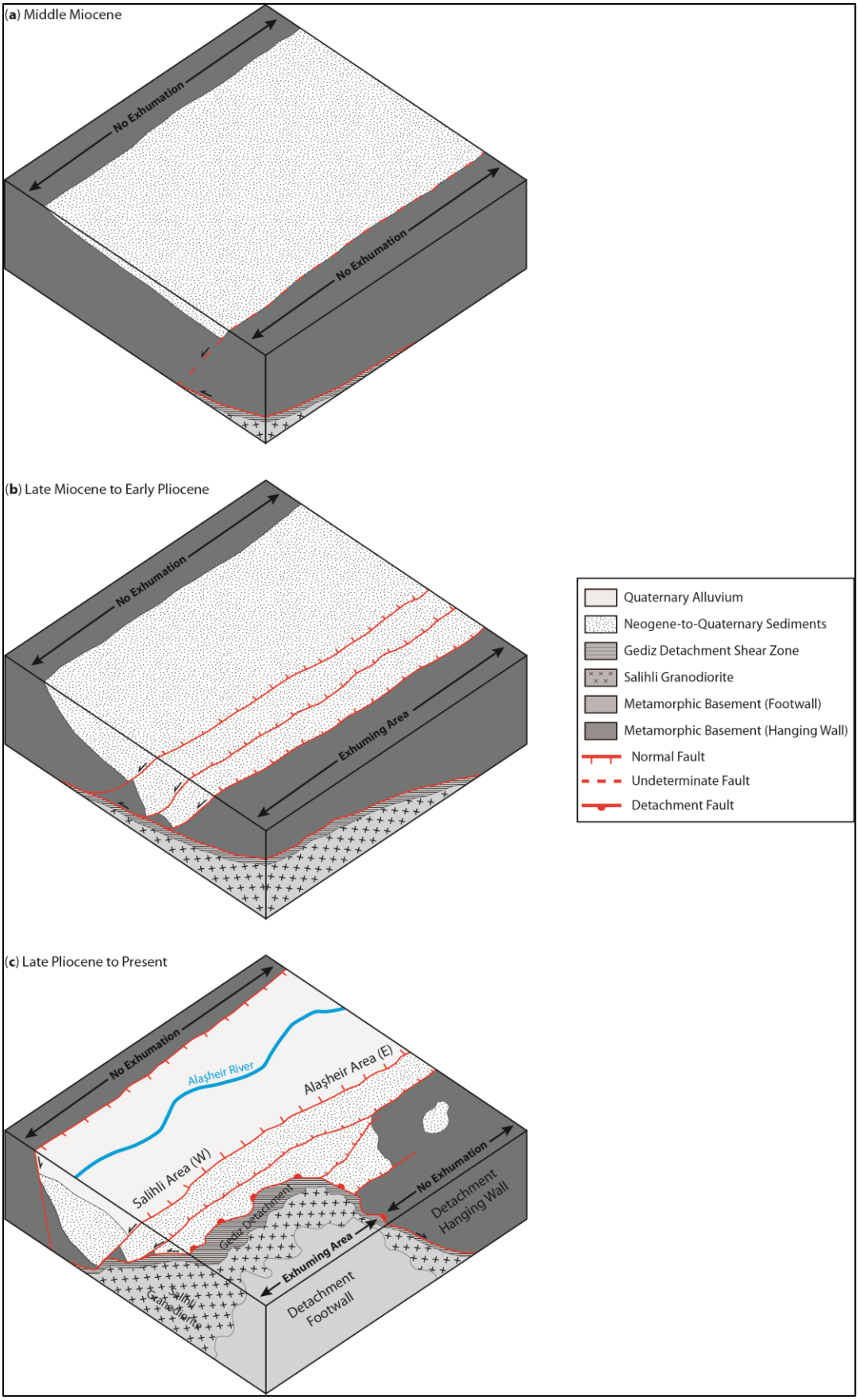
(a) Middle Miocene
No Exhumation
No Exhumation
(b) Late Miocene to Early Pliocene
No Exhumation
Exhuming Area
(c) Late Pliocene to Present
No Exhumation
Alaşheir River
Alaşheir Area (E)
Salihli Area (W)
Gediz Detachment
No Exhumation
Detachment Hanging Wall
Exhuming Area
Salihli Granodiorite
Detachment Footwall
Quaternary Alluvium
Neogene-to-Quaternary Sediments
Gediz Detachment Shear Zone
Salihli Granodiorite
Metamorphic Basement (Footwall)
Metamorphic Basement (Hanging Wall)
Normal Fault
Undeterminate Fault
Detachment Fault

Figure 12: *(on the previous page) Schematic block-diagram showing the geologic evolution of the Gediz Graben since the beginning of the formation of the basin: a) no exhumation occurs at the margins of the basin during Middle Miocene (i.e. beginning of basin formation); all the detrital ages recorded in the lower part of the stratigraphic sequence (i.e. Alaşehir Fm. and lower Çaltilik Fm.) reflects older exhumation ages of the Menderes Massif metamorphic basement; b) a major exhumation phase of the southern margin of the basin at the footwall of the graben bounding faults takes place during Late Miocene; syn- and post-Late Miocene deposits (i.e. upper Çaltilik Fm. and Gediz Fm.) recorded detrital ages related to this exhumation event. c) a last exhumation event involves only the footwall of the Gediz Detachment, including the Salihli granodiorite, in the western part of the southern margin of the basin since Late Pliocene; this last phase is recorded in modern sediments of the catchments draining the southern margin and witnessed also by the modern short-term erosion pattern that shows higher exhumation rates at the footwall of the Gediz Detachment (see Fig. 11).*

6. CONCLUSION

In this work, by integrating detrital apatite fission track analysis from modern rivers' sediments and from ancient sediments of the basin's sedimentary fill, we reconstructed the exhumation history of the northern margin of the Central Menderes Massif, the Neogene-to-Present evolution of the Gediz Graben and the modern erosion pattern of the surrounding bedrock.

A Tortonian/Messinian major event of bedrock exhumation localized at the northern margin of the Central Menderes Massif have been recorded in the basin, following the Upper Oligocene/Lower Miocene main cooling event that involved the whole Menderes Massif. Detrital AFT data point to an age of formation for the Gediz Graben not older than Middle Miocene. A second and more recent cooling event involved only the western portion of the southern margin of the basin, leading the Gediz Detachment and the Salihli Granodiorite to the surface in very recent times in the Bozdağ area. The modern short term erosion pattern closely reflects this event, showing higher erosion rates in the area of the Gediz Detachment than in the rest of the investigated region.

It is likely, in our opinion, that these exhumation events involved only the northern margin of the Central Menderes Massif, so we reject the idea that the structures that controlled the Gediz Graben have been responsible for the exhumation of the whole Central Menderes Massif. We also suggest that the presence of the Salihli Granodiorite might have played a major role in the exhumation pattern of this area, at least for the most recent event.

This study highlight the importance of considering along-strike variation of the cooling pattern to identify the role of different structures in the exhumation of an area, and show once again the crucial importance of carefully evaluating the mineral fertility in detrital thermochronology studies in order to properly estimate the erosional contribution of different source areas.

REFERENCES

Baldwin S. L., Harrison T. M. & Burke K., 1986. *Fission track evidence for the source of accreted sandstones, Barbados*. Tectonics, 5 (3), 457-468.

Benda L. & Meulenkamp J. E., 1979. *Biostratigraphic correlations in the Eastern Mediterranean Neogene: 5. Calibration of sporomorph associations, marine microfossils and mammal zones, marine and continental stages and radiometric scale*. VII International Congress of Mediterranean Neogene, Athens, 61–70.

Benda L. & Meulenkamp J. E., 1990. *Biostratigraphic correlation in the Eastern Mediterranean Neogene, 9. Sporomorph associations and event stratigraphy of the Eastern Mediterranean*. Newsletters on Stratigraphy, 23, 1–10.

Brandon M. T. & Vance J. A., 1992. *Tectonic Evolution of the Cenozoic Olympic Subduction Complex, Western Washington State, as Deduced from Fission Track Ages for Detrital Zircon*. American Journal of Science, 292, 565–636.

Brandon M. T., 2002. *Decomposition of mixed grain age distributions using Binomfit*. On Track, 24, 13–18.

Brun J.P. & Sokoutis D., 2007. *Kinematics of the southern Rhodope core complex (North Greece)*. International Journal of Earth Sciences, 96 (6), 1079-1099.

Buscher J. T., Hampel A., Hetzel R., Dunkl I., Glotzbach C., Struffert A., Akal C. & Rätz M., 2013. *Quantifying rates of detachment faulting and erosion in the central Menderes Massif (western Turkey) by thermochronology and cosmogenic 10Be*. Journal of the Geological Society of London, 170, 669–683.

Çiftçi N. B. & Bozkurt E., 2009. *Evolution of the Miocene sedimentary fill of the Gediz Graben, SW Turkey*. Sedimentary Geology, 216, 49–79.

Cohen H. A., Dart C. J., Akyüz H. S. & Barka A. A., 1995. *Syn-rift sedimentation andstructural development of Gediz and Büyük Menderes graben, western Turkey*. Journal of the Geological Society, London 152, 629–638.

Dumitru T. A., 1993. *A new computer-automated microscope stage system for fission-track analysis*. Nuclear Tracks and Radiation Measurements, 21, 575–580.

Dunkl I., 2002. *Trackkey: a Windows program for calculation and graphical presentation of fission track data*. Computers & Geosciences, 28, 3–12

Ediger V. Ş., Batı Z., Yazman M., 1996. *Paleopalynology of possible hydrocarbon source rocks of the Alaşehir-Turgutlu area in the Gediz Graben (western Anatolia)*. Turkish Association of Petroleum Geologists, 8, 94–112.

Emre T., 1996. *Geology and tectonics of Gediz Graben*. Turkish Journal of Earth Sciences, 5, 171–185.

England P. & Molnar P., 1990. *Surface uplift, uplift of rocks, and exhumation of rocks*. Geology, 18, 1173-1177.

Erkül F., Erkül S.T., Ersoy Y., Uysal I., Krötzli U., 2013. *Petrology, mineral chemistry and Sr–Nd–Pb isotopic compositions of granitoids in the central Menderes metamorphic core complex: Constraints on the evolution of Aegean lithosphere slab*. Lithos, 180-181, 74-91.

Friedmann S. J. & Burbank D. W., 1995. *Rift basins and supradetachment basins: intracontinental extensional end-members*. Basin Research, 7, 109-127.

Gallagher K., Brown R. & Johnson C., 1998. *Fission track analysis and its application to geological problems*. Annual Reviews Earth Planetary Science, 26, 519-572.

Garver J. I. & Brandon M. T., 1994. Fission-Track Ages of Detrital Zircon from Mid-Cretaceous Sediments of the MethowTyaughton Basin, Southern Canadian Cordillera. Tectonics, 13 (2), 401–420.

Garver J. I., Brandon M. T., Roden-Tice M. & Kamp P. J. J., 1999. *Exhumation History of Orogenic Highlands Determined by Detrital Fission-Track Thermochronology*. In: Exhumation Processes: Normal Faulting, Ductile Flow and Erosion, Ring, U., Brandon, M.T., Lister, G.S., and Willett, S.D., Eds., Geological Society of London Special Publication, 154, 283–304.

Gessner K., Ring U., Johnson C., Hetzel R., Passchier C.W. & Gungor, T., 2001. *An active bivergent rolling-hinge detachment system: Central Menderes metamorphic core complex in western Turkey*. Geology, 29, 611–614.

Gessner K., Gallardo L. A., Markwitz V., Ring U. & Thomson S. N., 2013. *What caused the denudation of the Menderes Massif: Review of crustal evolution, lithosphere structure, and dynamic topography in southwest Turkey*. Gondwana Research, 24(1), 243–274.

Gibbs A. D., 1984. *Structural evolution of extensional basin margins*. Journal of the Geological Society, 141, 609-620.

Glodny J. & Hetzel R., 2007. *Precise U–Pb ages of syn-extensional Miocene intrusions in the central Menderes Massif, western Turkey*. Geological Magazine, 144, 235–246.

Hetzel R., Ring U., Akal C. & Troesch M., 1995. *Miocene NNE-directed extensional unroofing in the Menderes massif, southwestern Turkey*. Journal of the Geological Society of London, 152, 639–654.

Hurford A. J., 1990. *Standardization of fission-track dating calibration: Recommendation by the Fission Track Working Group of the I.U.G.S.: Subcommission on Geochronology*. Chemical Geology, 80, 171–178.

Işik V., Seyitoğlu G. & Çemen I., 2003. *Ductile–brittle transition along the Alas_ehir detachment fault and its structural relationship with the Simav detachment fault, Menderes massif, western Turkey*. Tectonophysics, 374, 1–18.

Iztan H. & Yazman M., 1991. *Geology and hydrocarbon potential of the Alaşehir (Manisa) area, western Turkey*. Proceedings of the International Earth Sciences Congress on Aegean Regions, Izmir, 327–338.

Lips A. L. W., Cassard D., Sözbilir H., Yilmaz H. & Wijbrans, J. R., 2001. *Multistage exhumation of the Menderes Massif, western Anatolia (Turkey)*. International Journal of Earth Sciences (Geologische Rundschau), 89, 781–792.

Jolivet L. & Faccenna C., 2000. *Mediterranean extension and the Africa-Eurasia collision*. Tectonics, 19 (6), 1095–1106.

Jolivet L. & Brun J. P., 2010. *Cenozoic geodynamic evolution of the Aegean*. International Journal of Earth Sciences, 99, 109–138.

Koçyiğit A., Yusufoğlu H. & Bozkurt, E., 1999. *Evidence from the Gediz Graben for episodic two-stage extension in western Turkey*. Journal of the Geological Society, London 156, 605–616.

Lips A. L. W., Cassard D., Sözbilir H., Yilmaz H. & Wijbrans J.R., 2001. *Multistage exhumation of the Menderes Massif, western Anatolia (Turkey)*. International Journal of Earth Sciences (Geologische Rundschau), 89, 781–792.

Lister G. S. & Davis G. A., 1989. *The origin of metamorphic core complexes and detachment faults formed during Tertiary continental extension in the northern Colorado River region, U.S.A.* Journal of Structural Geology, 11 (1/2), 65-94.

Malusà M.G., Carter A., Limoncelli M., Villa I.M. & Garzanti E., 2013. *Bias in detrital zircon geochronology and thermochronometry*. Chemical Geology, 359, 90-107.

Malusà M.G., Resentini A. & Garzanti E. (IN PRESS). *Hydraulic sorting and mineral fertility bias in detrital geochronology*.

Morton A.C., 1985. *Heavy minerals in provenance studies*. In. Zuffa, G.G. (Ed.), Provenance of arenites. Reidel, Dordrecht, 249-277.

Oberhänsli R., Candan O. & Wilke F., 2010. *Geochronological evidence of Pan-African eclogites from the central Menderes Massif, Turkey*. Turkish Journal of Earth Sciences, 19, 431–447.

Öner Z. & Dilek Y., 2011. *Supradetachment basin evolution during continental extension: the Aegean province of western Anatolia, Turkey*. Geological Society of America Bulletin, 123, 2115–2141.

Purvis M. & Robertson A. H. F., 2005. *Sedimentation of the Neogene–Recent Alaşehir (Gediz) continental graben system used to test alternative tectonic models for western (Aegean) Turkey*. Sedimentary Geology, 173, 373–408.

Régnier J. L., Ring U., Passchier C. W., Gessner K. & Gungor T., 2003. *Contrasting metamorphic evolution of metasedimentary rocks from the Cine and Selimiye nappes in the Anatolide belt, western Turkey*. Journal of Metamorphic Geology, 21, 699–721.

Resentini A. & Malusà M.G., 2012. *Sediment budgets by detrital apatite fission-track dating (Rivers Dora Baltea and Arc, Western Alps)*. Geological Society of America Special Papers, 487, 125-140.

Resentini A., Malusà M.G. & Garzanti E., 2013. *MinSORTING: An Excel® worksheet for modelling mineral grainsize distribution in sediments, with application to detrital geochronology and provenance studies*. Computers & Geosciences, 59, 90-97.

Ring U., Gessner K., Gungor T. & Passchier C.W., 1999. *The Menderes Massif of western Turkey and the Cycladic Massif in the Aegean — do they really correlate?* Journal of the Geological Society, 156, 3–6.

Ring U., Willner A. P. & Lackmann W., 2001. *Stacking of nappes with unrelated pressure–temperature paths: an example from the Menderes nappes of western Turkey*. American Journal of Science, 301, 912–944.

Ring U., Johnson C., Hetzel R. & Gessner K., 2003. *Tectonic denudation of a Late Cretaceous–Tertiary collisional belt: regionally symmetric cooling patterns and their relation to extensional faults in the Anatolide belt of western Turkey*. Geological Magazine, 140, 421–441.

Sarıca N., 2000. *The Plio–Pleistocene age of Büyük Menderes and Gediz grabens and their tectonic significance on N–S extensional tectonics in West Anatolia: mammalian evidence from the continental deposits*. Geological Journal 35, 1–24.

Şengör A. M. C. & Yilmaz Y., 1981. *Tethyan evolution of Turkey: a plate tectonic approach*. Tectonophysics, 75, 181–241.

Şengör A. M. C., Satir M. & Akkök R., 1984. *Timing of the tectonic events in the Menderes massif, western Turkey: implications for tectonic evolution and evidence for Pan- African basement in Turkey*. Tectonics, 3, 693–707.

Şengör A.M.C., 1987. *Cross faults and differential stretching of hangingwalls in regions of low-angle normal faulting: examples from Western Turkey*. In: Coward, M.P.,Dewey, J.F., Hancock, P.L. (Eds.), Continental Extensional Tectonics, 575–589.

Seyitoğlu G. and Scott B. C., 1992. *The age of the Büyük Menderes graben (west Turkey) and its tectonic implications*. Geological Magazine, 129, 239–242.

Seyitoğlu G. & Scott B. C., 1996a. *The cause of N–S extensional tectonics in western Turkey: tectonic escape vs back-arc spreading vs orogenic collapse*. Journal of Geodynamics, 22, 145–153.

Seyitoğlu G. & Scott B. C., 1996b. *Age of the Alaqehir graben (west Turkey) and its tectonic implications*. Geological Journal, 31, 1–11.

Seyitoğlu G., Tekeli O., Çemen İ., Şen Ş. & Işık V., 2002. *The role of flexural rotation/rolling hinge model in the tectonic evolution of the Alaşehir Graben, western Turkey*. Geology Magazine, 139, 15–26.

Thomson S. N. & Ring U., 2006. *Thermochronologic evaluation of post-collision extension in the Anatolide Orogen, western Turkey*. Tectonics, 25, TC3005.

Vermeesch P., 2009. *RadialPlotter: a Java application for fission track, luminescence and other radial plots*. Radiation Measurements, 44 (4), 409-410.

Yılmaz Y., Genç S. C., Gürer Ö. F., Bozcu M., Yılmaz K., Karacık Z., Altunkaynak Ş. & Elmas A., 2000. *When didwesternAnatolian grabens begin to develop*. In: Bozkurt, E.,Winchester, J.A., Piper, J.D.A. (Eds.), Tectonics and Magmatism in Turkey and the Surrounding Area. Geological Society, London, Special Publications, 173, p. 353-384.

Zlatkin O., Avigad D. & Gerdes A., 2013. *Evolution and provenance of Neoproterozoic basement and Lower Paleozoic siliciclastic cover of the Menderes Massif (western Taurides): Coupled U–Pb–Hf zircon isotope geochemistry*. Gondwana Research, 23, 682–700.

CHAPTER 3

MAGMATISM EMPLACEMENT AND CRUSTAL EXTENSION: CONSTRAINING THE ACTIVATION OF DUCTILE SHEARING ALONG THE GEDIZ DETACHMENT, MENDERES MASSIF (WESTERN TURKEY)

Federico Rossetti[1], Riccardo Asti[1], Federico Lucci[1], Axel Gerdes[2], Thomas Theye[3] and **Claudio Faccenna[1]**

1) Università degli Studi Roma Tre, Department of Sciences, Rome, Italy

2) Geozentrum der Goethe-Universität, Institut für Geowissenschaften, Facheinheit Mineralogie - Petrologie und Geochemie, Frankfurt am Main, Germany

3) Universität Stuttgart, Institut für Mineralogie und Kristallchemie, Stuttgart, Germany

Abstract: The role of magmatism in core complex formation is hot topic in geology; the question whether is magmatism that facilitates detachment faulting (and core complex formation in general) or the other way around, is a fundamental issue in the tectonic evolution of highly extended terrains. The Menderes Massif of western Turkey is a key area to study feedback relationships between Neogene magma generation/emplacement and activation of extensional detachment tectonics. Here, we present new textural analysis and in situ U-Th-Pb titanite dating from selected samples collected in the transition from the undeformed to the mylonitized zones of the Salihli granodiorite at the footwall of the Gediz detachment fault outcropping at the northern margin of the Central Menderes Massif. The bimodal distribution of the $^{206}Pb/^{238}U$ titanite ages records the transition from magma crystallization and emplacement (at ca. 17-16 Ma) to the syn-tectonic, solid-state recrystallization (at ca. 14 Ma) of the Salihli granodiorite, with a minimum time lapse of ca. 2 Ma between the crustal emplacement of the Salihli granodiorite and the activation of the ductile top-to-the-NNE extensional tectonics along the Gediz detachment. The reconstruction of the cooling pattern of the Salihli granodiorite showed a punctuated cooling history and highlighted two phases of rapid cooling (~100°C/Ma), one between ~17 Ma and ~12 Ma following its emplacement and

one between ~3 Ma and ~2 Ma. We relate the first phase to post-emplacement cooling and the second to high-angle brittle faults related rapid exhumation. Our dataset suggests that in the Menderes Massif the activation of ductile extension was a consequence, rather than the cause, of magma emplacement in the extending crust.

1. INTRODUCTION

Detachment faults are high-strain, ductile-to-brittle, low-angle extensional shear zones, typically constituted by an upper cataclastic or ultracataclastic horizon, underlain by a ductile, hundreds of meters thick, mylonitic to ultramylonitic zone (e.g. Lister and Davis, 1989). When exposed at the surface, these shear zones generally separate a non-metamorphosed or slightly metamorphosed hanging wall, from a higher grade metamorphic footwall, also known as metamorphic core complexes (Coney, 1974, 1980; Critteden et al., 1980; Wernike, 1985; Lister and Davis, 1989; Davis et al., 2004; Withney et al., 2013 and references therein). The role of magmatism in core complex formation is still debated. In particular, it is a key issue to understand whether is magmatism that facilitates detachment faulting (and core complex formation in general) or the other way around, because despite extension-driven decompression may cause melting, melting itself may promote and guide the extensional process (e.g. Parson and Thompson 1993; Teyssier & Withney, 2002; Corti et al., 2003). In particular, crustal heating induced by pluton emplacement at shallow depths may generate a time-dependent variation in the rheological properties of the crust by causing an upward migration of the (regional) brittle-ductile transition and allowing shear strain localization facilitated by thermal softening (Lister & Baldwin, 1993; Caggianelli et al., 2013). The thermal softening induced by magmatism may also facilitates the slip on low-angle normal faults by inducing rotation of the principal stresses (Parsons & Thompson, 1993). As a matter of fact, the general chronological relationship between the onset of extension and magmatism is not straightforward: it has been documented that one can alternatively pre-date the other, or these may even be synchronous (e.g. Metcalf & Smith, 1995; Lister and Baldwin, 1993; Aoya et al., 2005; Rabillard et al., 2015).

The Menderes Massif of western Turkey (Fig. 1) is a key area to study feedback relationships between Neogene magma generation/emplacement and activation of extensional detachment

tectonics (Bozkurt and Park, 1994; Hetzel et al., 1995a,b, 1996; Işik et al., 2003; Ring and Collins, 2005; Çemen et al., 2006; Thomson and Ring, 2006; Glodny and Hetzel, 2007; Dilek et al., 2009: Öner et al., 2010; Erkül et al., 2013). Pluton emplacement is commonly considered as syn-extensional (e.g. Glodny and Hetzel, 2007; Dilek et al., 2009; Erkül et al., 2013 and references therein), but some uncertainty still persists on the timing of magma crystallization and ductile shearing (Catlos et al., 2010; 2011). In this study we report new textural and in situ U-Th-Pb titanite dating results from selected samples collected in the transition from the undeformed to the mylonitized zones of the Salihli granodiorite at the footwall of the Gediz detachment fault (GDF; Hetzel et al., 1995a; Işik et al., 2003), documenting a minimum time lapse of ca. 2 Ma between magma crystallization/emplacement and activation of ductile shearing associated with the development of the GDF. We conclude that Neogene ductile extension was a consequence, rather than the cause, of magma emplacement in the Menderes Massif.

2. GEOLOGICAL BACKGROUND

The Menderes Massif of western Turkey (Fig. 1) is an Alpine extensional province, which has been affected by post-orogenic crustal stretching since the Oligocene-Miocene times as a part of the Tertiary Aegean extensional system (e.g. Gessner et al., 2001a; Ring et al., 2003; Thomson & Ring, 2006; Jolivet and Brun, 2010). The Menderes Massif is currently interpreted as metamorphic core complex (Menderes Metamorphic Core Complex, MMCC), whose exhumation was dominantly assisted by ductile-to-brittle extensional detachment tectonics and closely associated with emplacement of syn-tectonic granitoids and formation of supradetachment basins (Bozukurt and Park, 1994; Hetzel et al., 1995a,b, 1996; Işık et al., 2003; Bozkurt and Sözbilir, 2004; Thomson and Ring, 2006; Glodny and Hetzel, 2007; Dilek et al., 2009; Öner et al., 2010; Öner and Dilek, 2011; Erkül et al., 2013).

Activity of the extensional detachment tectonics in the MMCC is chiefly constrained by the age of crystallization and cooling of the syn-extensional magmatism in the immediate footwall of the detachment faults. In particular, a two-stage extensional detachment tectonics has been reconstructed (Çemen et al., 2006). The early stage is associated with the activity of the early Miocene (~ 21-19 Ma) top-to the-N Simav detachment in the northern part of the

Menderes Massif, as constrained by the syn-tectonic Alaçamdağ magmatic suite (Işik et al., 2003; Erkül, 2010; Ring and Collins, 2005, Bozkurt et al., 2011). The second stage is associated with the middle Miocene (16-7 Ma) activity of the north-dipping Gediz and the south-dipping Büyük Menderes detachment faults, associated with the emplacement and ductile shearing of the Salihli and Turgutlu granodiorites in the central part of the Menderes Massif (Hetzel et al., 1995a; Lips et al., 2001; Glodny and Hetzel, 2007).

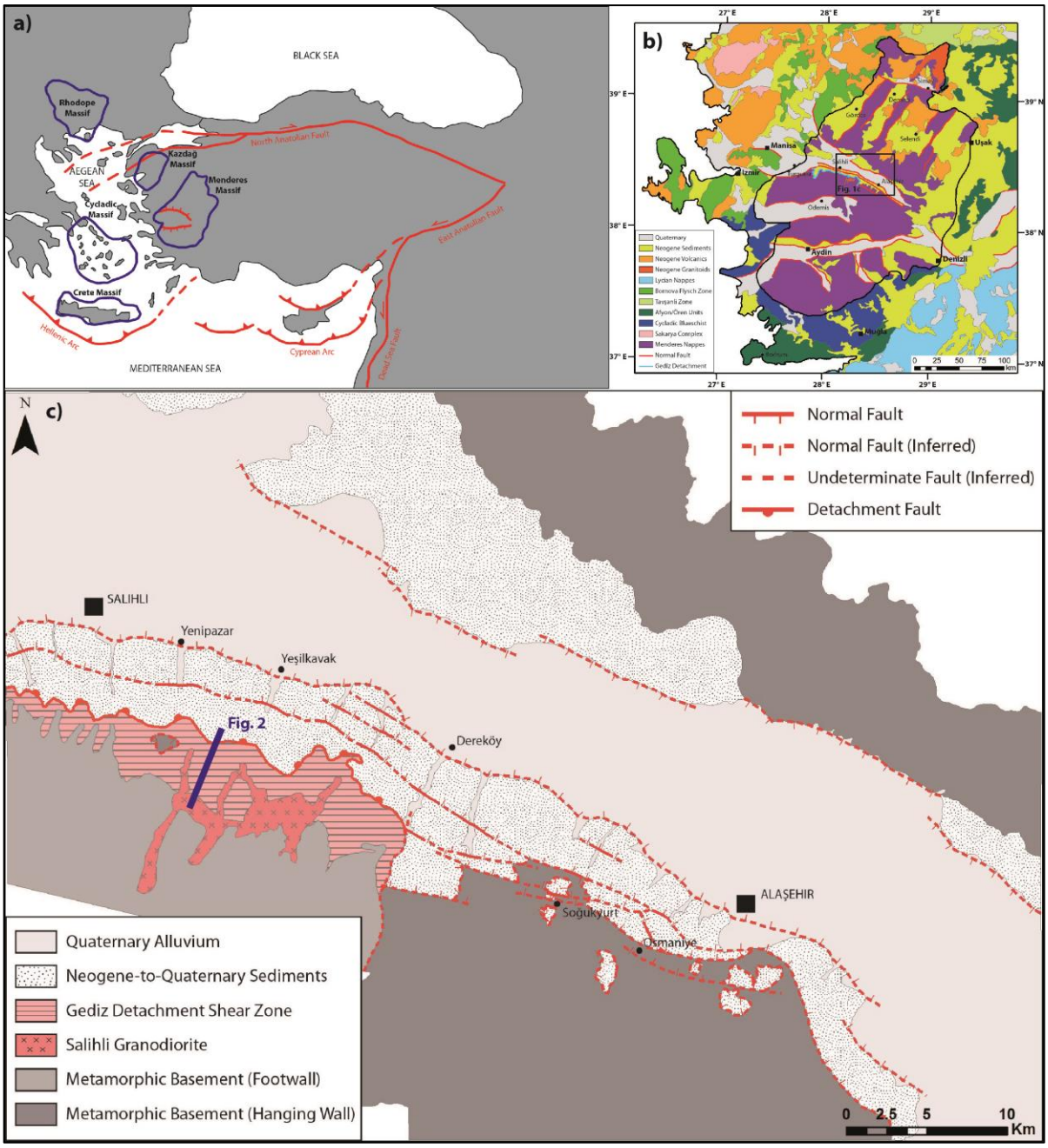

Figure1: *(on the previous page) (a) Schematic tectonic map of northeastern Mediterranean with main metamorphic core complex of the Aegean Extensional Province marked by blue lines. (b) Schematic tectonic map of southwestern Turkey; the black line delimitates the Menderes Massif, the black box show the location of the study area represented in Fig. 1c. (c) Simplified geologic map of the study area; the blue line show the location of the schematic cross-section represented in Fig.2.*

Between these two detachment systems, a series of NE-trending basins developed during Neogene, hosting continental clastic, volcano-clastic and volcanic deposition in unconformity on top of the metamorphic basement of the Menderes Massif (Ersoy et al., 2011 and references therein). Early volcanic activity recorded in the lower part of these basins has been constrained by various studies to have occurred between ~22 and ~14 Ma (Seyitoğlu et al., 1992; Ercan et al., 1996; Seyitoğlu et al., 1997; Purvis et al., 2005; Ersoy et al., 2008, 2012, 2014; Karaoğlu et al., 2010), suggesting that the Northern Menderes Massif was already exhumed during early Miocene . These basins terminate to the South against the E-W trending Gediz Graben, which developed between middle Miocene and Quaternary as a consequence of the activity of the Gediz Detachment (e.g. Çiftçi & Bozkurt, 2009), and to the North against the E-W trending Plio-Quaternary Simav Graben (Seyitoğlu, 1997).

Geochemical signatures of the syn-tectonic granitoids document for I- and S-type magmatism, derived from heterogeneous sub-continental lithospheric mantle sources (Dilek et al., 2009; Öner et al., 2010; Catlos et al., 2010; Erkül & Erkül, 2012; Erkül et al., 2013) with a strong crustal fingerprint (Altunkaynak et al., 2012). Igneous thermobarometry documents shallow crustal emplacement conditions for the Miocene granitoids, with crystallization temperatures ranging 700-800°C over 0.2-0.3 GPa (Catlos et al, 2010; Erkül et al., 2013).

The Miocene Turgutlu and Salihli granitoids (e.g. Hetzel et al., 1995a; Işik et al., 2003; Glodny and Hetzel, 2007; Erkül et al., 2013) outcrop at the footwall of the NNE dipping GDF, a ductile-to-brittle gently dipping (~20°) extensional fault that separates the crystalline rocks of the MMCC at the footwall from the supradetachment Neogene deposits of Gediz graben at the hanging wall (e.g. Hetzel et al., 1995a,b; Gessner et al., 2001a; Işik et al., 2003; Öner and Dilek, 2011). The crystallization age of these granodioritic intrusions is constrained to the middle Miocene, based on TIMS U-Pb dating of monazite (16.1±0.2 Ma; Turgutlu) and allanite (15.0±0.3 Ma; Salihli) aliquots (Glodny and Hetzel, 2007). The $^{40}Ar/^{39}Ar$ biotite ages of 13.1±0.2 Ma from Turgutlu and 12.2±0.4 Ma from Salihli indicate slow cooling and

continuous deformation to the late Miocene (Hetzel et al., 1995a,b; Glodny & Hetzel, 2007). A relatively wide range of ages spanning between 21.7 ± 4.5 and 9.6 ± 1.6 Ma was obtained through in situ ion microprobe monazite Th-Pb dating from the Salihli granodiorite (Catlos et al. 2008, 2010). The youngest among these ages, obtained from a monazite grain located in the outer edge of an altered plagioclase crystal, was interpreted as a deformation age, rather than a crystallization age, also suggesting that this range of ages most likely dates episodes of deformation and tectonic exhumation (Catlos et al., 2010). $^{40}Ar/^{39}Ar$ dating of syn-kinematic withe micas from the top of the detachment fault zone yielded ages of 7 ± 1 Ma (Lips et al., 2001), interpreted as the time when the shear zone crossed the brittle-ductile transition (Glodny and Hetzel, 2007). Furthermore, textural evidence from the protomylonitic assemblages along the ADF (Catlos et al., 2011) and the sedimentary record in the Gediz graben indicate that activity of the GDF was pulsed and hence the region experienced episodes of pulsed extension reflecting on both structural and stratigraphic evolution of the basin (Bozkurt and Sözbilir, 2004 ; Purvis and Robertson, 2005). Finally, low-temperature thermochronology data (AHe, AFT, ZHe and ZFT) on the Salihli granodiorite and on the GDF shows a Messinian event of rapid cooling that reduced after 2 Ma (Buscher et al., 2013).

3. METHODS

To constrain the age of activation of ductile shearing along the GDF, textural and petrographic observations were carried out in selected S-L tectonites developed at the expenses of the Salihli granodiorite. Representative samples were chosen for the U-(Th)-Pb geochronological study in order to constrain timing of the ductile shear strain along the GDF (Fig. 2) in the transition from magma crystallization to solid-state shearing. Sample selection was based on the structural architecture at outcrop scale and on meso- and micro-scale textural and mineralogical features. Samples are shown in their structural context in Figure 2 and in Table 1, where their location, fabrics, and constituent mineralogy are detailed.

Electron microprobe analyses were used to define compositions of the constituent mineral assemblages. Details on the analytical methods and protocols adopted in this study are provided in the Appendix. In the following, mineral abbreviations are after Withney and Evans (2010).

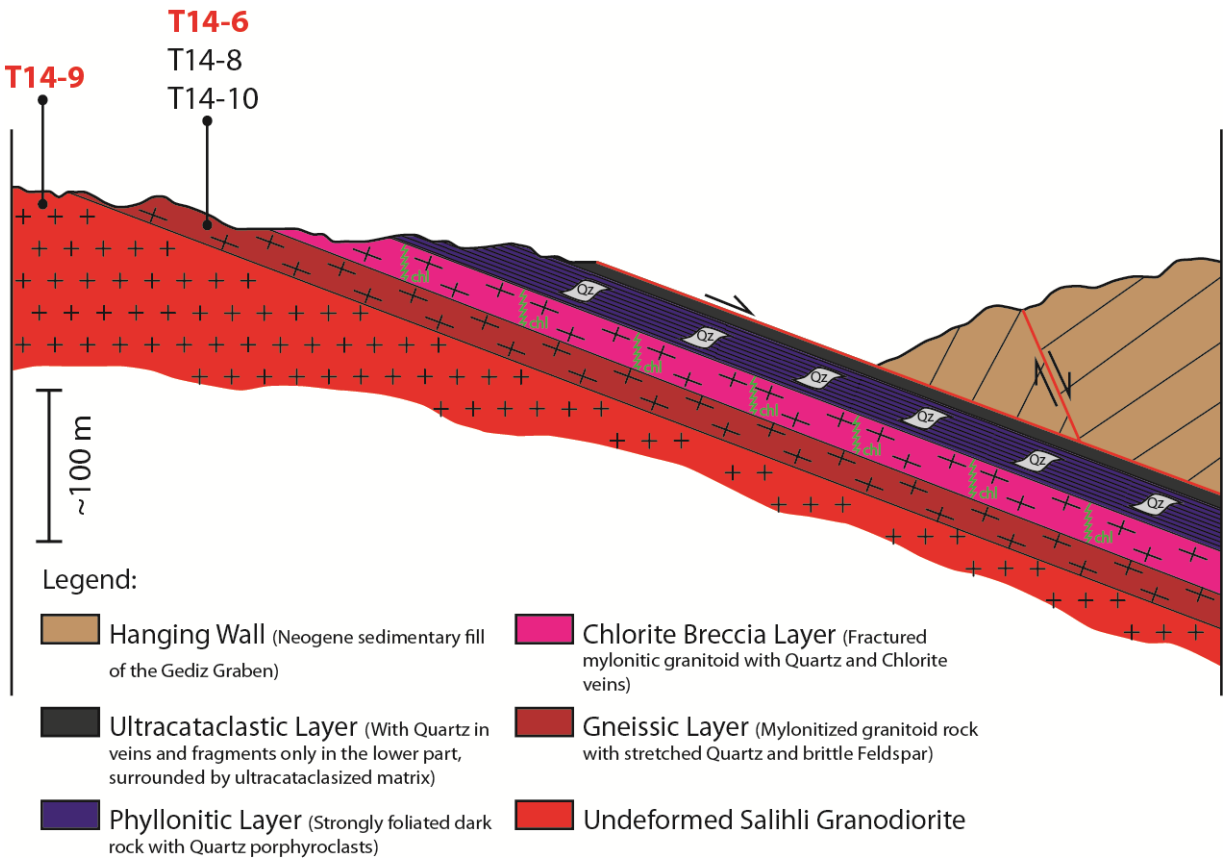

Figure 2: *Schematic cross-section through the Gediz Detachment Shear Zone with representation of the main structural facies and relative location of the studied samples; samples indicated in red are those used for U-(Th)-Pb dating. See Fig. 1c for the location.*

4. RESULTS

4.1. *Structures, textures and petrography*

The NNE dipping GDF consists of a flat-lying (10° to 30° dip) ductile-to-brittle shear zone with variable thickness (generally not exceeding ~100 m). The shear zone formed at the expenses of the Miocene Salihli Granodiorite and consists of a basal (up to 30 m thick) mylonite that gradually transition upward into a very fine grained ultra-cataclasite (Hetzel et al., 1995a; Işik et al., 2003; Catlos et al., 2011; Buscher et al., 2013). Within the mylonitic horizon, the stretching lineation's attitude is dip-slip and they are provided by Qz-Fsp-Bt aggregates trending between N20°E and N40°E. Sense of shear as defined in the X-Z sections of the

finite strain ellipsoid, systematically point to top-to-the-NNE sense of shear (Hetzel et al., 1995a; Işik et al., 2003).

Our samples are from the protomylonitic (T14-09) and mylonitic (T14-06, T14-08 and T14-10) zones. Magmatic mineralogy consists of Kfs + Pl_1 + Qz + Amp (Mg-horneblende) + Bt and Ttn_1, All, Ap (up to 3% in vol.) and minor Zrc as accessory minerals. Ductile shearing is responsible for the transformation of the original igneous texture into a plano-linear gneissic fabric (S-L tectonite), defined by the preferred orientation of ribbon Qz, secondary plagioclase (Pl_2) and especially biotite (Bt_2), that together with Ep and secondary titanite (Ttn_2) define strong oblique foliations (Figs. 3a-b).

The rock microtextures attests for heterogeneous strain during progressive development of the shear zone fabrics. Tectonic foliations wrap around Fsp porphyroclasts to produce augen, which typically show a σ-type geometry with the sense of shear indicating top to the NNE (Figs. 3a-c). Ttn_1 grains also form σ -shaped poryroclasts and occurs as boudinaged and stretched grains within the shear foliation (Fig. 3c). Feldspar porphyroclasts commonly show recrystallized grains at their boundaries, producing a core-and-rim structure diagnostic of dynamic recrystallization, compatible with medium- to high-grade temperature conditions (600–400 °C) during deformation (e.g., Gapais, 1989a, 1989b; Leloup et al., 1995; Passchier and Trouw, 2005). Albite-rich plagioclase also commonly occur as rims of Pl_1 (Fig. 3a-d). Myrmekite growth along the boundaries of K-Fsp porphyroclasts and albite flame pertites suggests a fluid-assisted deformation under medium-grade temperature conditions (400–600 °C) (Passchier and Trouw, 1996; Menegon et al. 2006) (Fig. 3e). Bent twin lamellae, undulose extinction, and microfracturing suggest deformation under lower-grade temperature conditions (300–400 °C; e.g., Passchier and Trouw, 2005) (Fig. 3d). Quartz shows dynamic recrystallization, dominantly assisted by subgrain rotation that resulted in pronounced grain size reduction (average grain size of 20 μm in the higher strain domains). Healed textures are also observed with evidence of static recrystallization accommodated by grain boundary migration (Figs. 3f-g). These structures are typical at medium- to high-grade conditions (600–400 °C; Drury and Urai; 1990; Hirth and Tullis, 1992; Stipp et al., 2002; Passchier and Trouw, 2005). Quartz grains also exhibit undulose extinctions and subgrain formation typical of strain-enhanced low-grade conditions (below 300 °C; Passchier and Trouw, 1996). Biotite

and amphibole fishes are ubiquitous (Fig. 3h). Biotite also shows undulose extinction and, in some samples, kink folding.

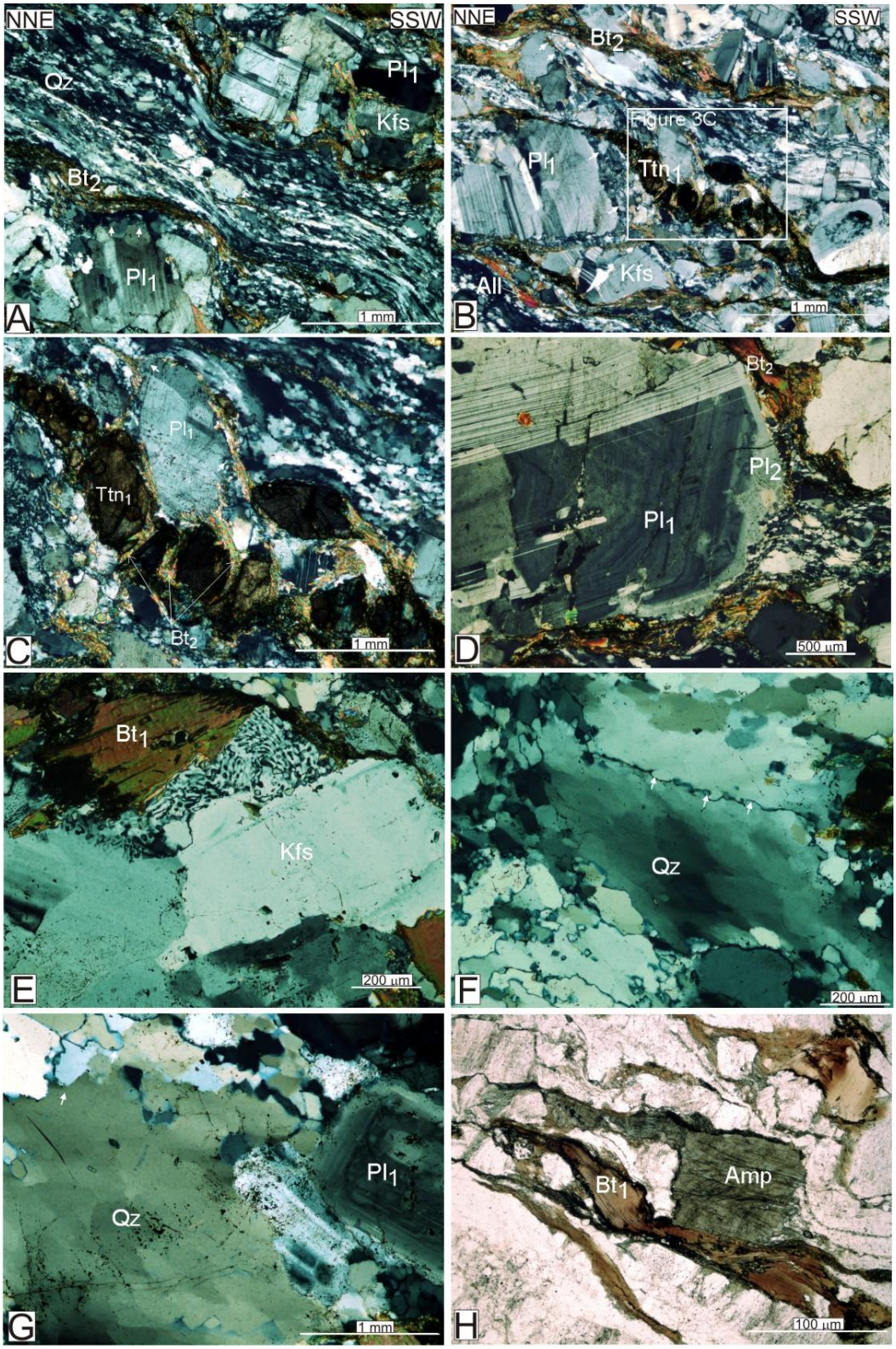

Figure 3: *(on the previous page) Microtextural evidences in thin section. Tectonic foliations wrap around Fsp porphyroclasts to produce augen, which typically show a σ-type geometry with the sense of shear indicating top to the NNE (a-c). Ttn_1 grains also form σ -shaped poryroclasts and occurs as boudinaged and stretched grains within the shear foliation (c). Albite-rich plagioclase commonly occur as rims of Pl_1 (a-d). Myrmekite growth along the boundaries of K-Fsp porphyroclasts (e). Quartz shows dynamic recrystallization, dominantly assisted by subgrain rotation, healed textures are also observed with evidence of static recrystallization accommodated by grain boundary migration (f-g). Biotite and amphibole fishes are ubiquitous (h).*

4.2. *Titanite crystallisation*

Ttn makes up to 1-2% of the rock and shows evidence of a polyphasic crystallization, in a continuum from magma crystallization to solid-state, syn-metamorphic shear zone enucleation and development. Magmatic Ttn_1 occurs as isolated grains with euhedral, rhomboid to elongate and rounded shapes (300–500 μm across; Fig. 4a). Magmatic origin is indicated by: (i) equilibrium textures with magmatic Fsp-Qz-Amp assemblages; (ii) Ttn inclusion in igneous Fsp and Amp; (iii) bright oscillatory and sector zoning in back-scattered electron (BSE) imaging (cfr. Wintsch et al., 2005) (Fig. 4b); and (iv) the pre-kinematic crystallization relative to the shear foliation (Fig. 3c). Metamorphic Ttn occurs within metamorphic folia both as (i) the replacement product of igneous Bt and Amp in conjunction with Ep during syn-tectonic re-crystallization and (ii) as minute subhedral grains (10–30 μm across) associated and intergrowth with metamorphic Ep and fabric-forming Bt (Fig. 4c). Metamorphic Ttn_2 also occurs as overgrowth onto magmatic Ttn_1 as outlined by uniform dark grey BSE domains that truncate oscillatory zoning patterns (Fig. 4b).

The two titanite types are chemically distinct (see Appendix for analytical details), as documented by differences in concentrations of Al_2O_3, Fe_2O_3 (Al^{3+}/Fe^{3+} ratios of 4–6) , REE, Y (Table 2) plus Th/U (see below). The oscillatory zoned domains in Ttn_1 are characterised by higher in Al_2O_3, Fe_2O_3 and Th/U (up to 1.2) with up to 6 wt.% of total REE and yttrium, whereas overgrowth and matrix Ttn_2 contain less than 0.3 wt.% of total REE + Y and Th/U down to 0.05 (Figs. 4d).

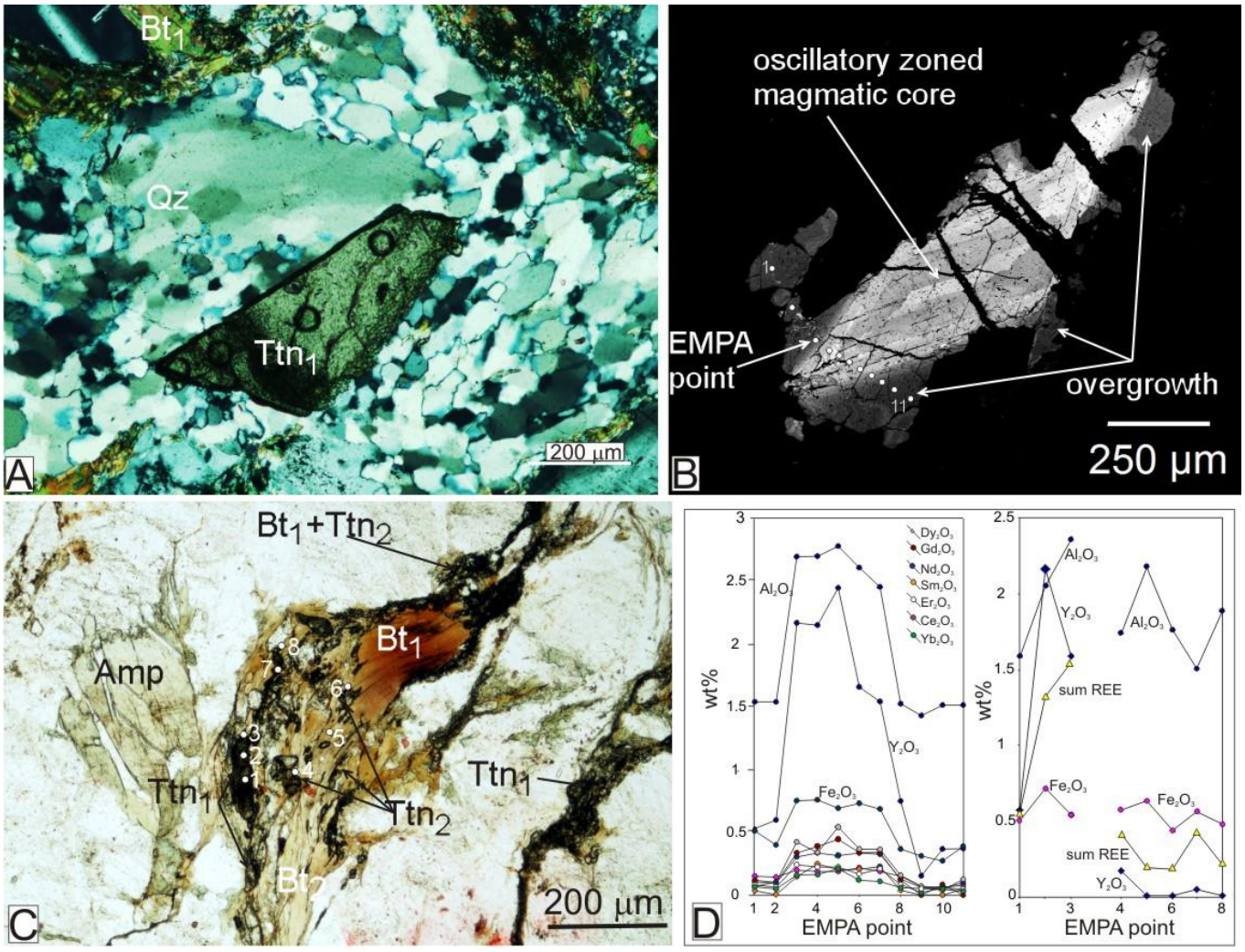

Figure 4: *(a) Euhedral titanite grain in a recrystallized quartz matrix (crossed polars; sample T14-09). (b) BSE image of a titanite grain showing oscillatory zoned cores (richer in REE) and metamorphic nerly homogeneous overgrowth (poorer in REE). The points indicate the EMPA compositional line traverse. (c) Secondary titanite (Ttn2) growing at the expenses of igneous biotite (Bt1) and boundinaged igneous titanite (Ttn1). The EMPA points are indicated in yellow. (d) Left: EMPA composition profile of the titanite grain shown in (b); Right: EMPA compositional data of the titanite grains shown in (c).*

4.3. *Titanite U-Pb geochronology*

An in situ laser ablation induction-coupled mass spectrometry (LA-ICPMS) U-Pb dating approach was adopted in this study to constrain age of shearing on selected samples from the protomylonitic (T14-09 sample) and mylonitic (T14-06 sample) zones of the GDF. Analytical protocols and method adopted in this study are detailed in the Appendix. Analytical results are listed in Table 3. Plots and age calculations were made using the ISOPLOT

software (Ludwig, 2003). Selected spots (*n* =180) of 30–43 μm in diameter show the Ttn grains have generally low concentrations of U (11–830 ppm), low concentrations of radiogenic ^{206}Pb (1–13 ppm), and high common Pb (up to 90% of total Pb).

Collectively, the ^{206}Pb/^{238}U ages span 18.1 ± 0.7 to 11.2 ± 0.7 Ma (Table 2). In both samples, all spots cluster near the Concordia line on a Tera-Wasserburg Concordia diagram, yielding nearly coincident lower intercept ages of 15.68 ± 0.65 Ma and 15.42 ± 0.32 Ma, for the proto-mylonitic (T14-09) and mylonitic (T14-06) sample, respectively (Fig. 5a-b). It is worth nothing that the ^{206}Pb/^{238}U ages correlate with Th/U ratios and zoning domains in Ttn, with the oldest ages from the oscillatory zoned high Th/U domains and the youngest ages from the homogeneous overgrowth low Th/U domains, respectively (Fig. 6). Best fit Gaussian ^{206}Pb/^{238}U age plots for the two samples consistently shows a bimodal distribution with peaks at 17.1 ± 0.2 (73% of the data population; *n* = 54) Ma and 14.4 ± 0.3 Ma (27% of the data population) and 16.1 ± 0.1 Ma (63% of the data population; *n* = 126) and 14.5 ± 0.1 Ma (37% of the data population), for sample T14-09 and T14-06, respectively (Figs. 5a-b).

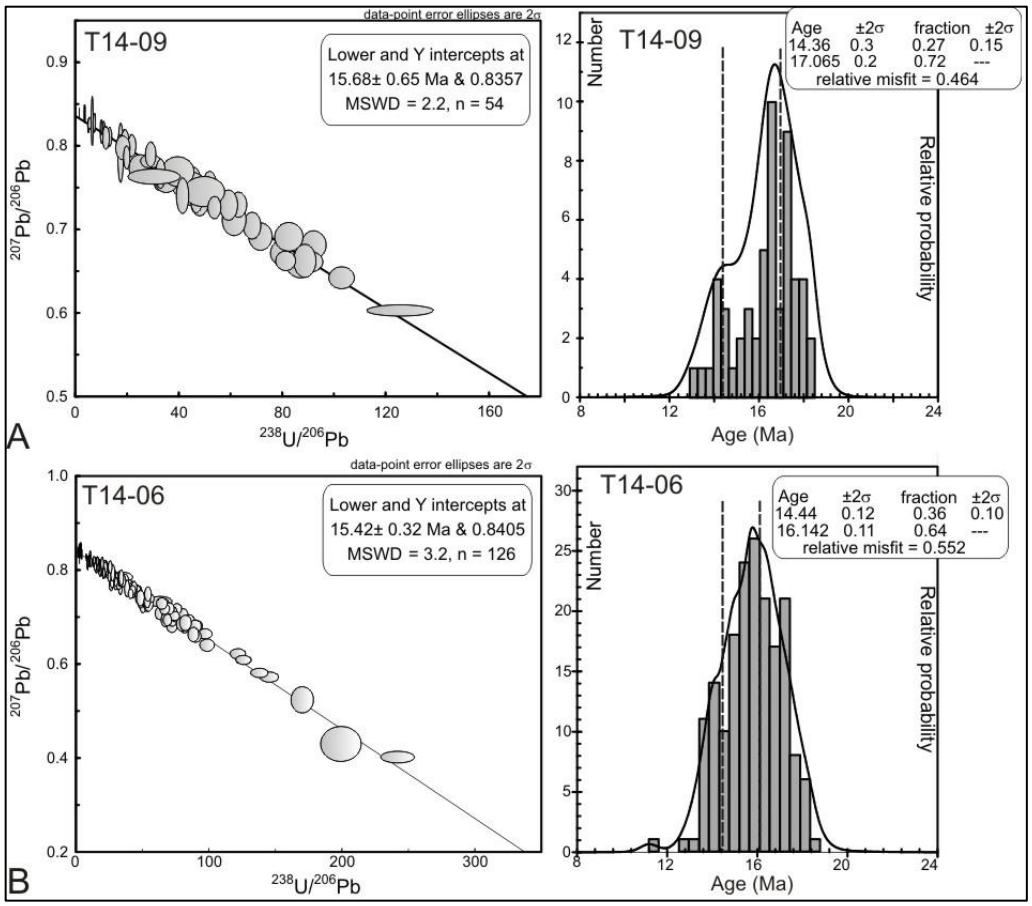

Figure 5: *(on the previous page) Left: Tera-Wassemburg Concordia diagrams for the study samples. Right: Probability density distributions of $^{206}Pb/^{238}U$ dates for the study samples.*

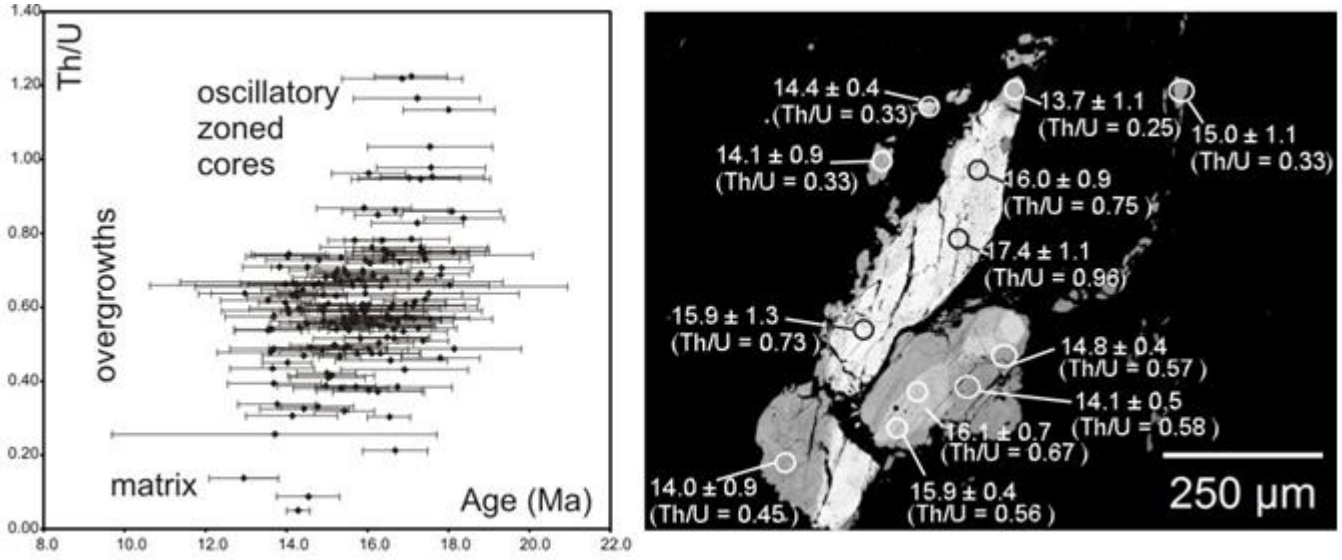

Figure 6: *Left: Plot of the cumulative $^{206}Pb/^{238}U$ dates vs. the Th/U data for the studied titanite grains. Right: Comparison of $^{206}Pb/^{238}U$ dates and Th/U zoning in a titanite grain from sample T14-06.*

5. DISCUSSION

The textural and petrographic features described in this study are compatible with a fluid-mediated syn-tectonic metamorphic/metasomatic overprint (Wintsch et al, 2005; Catlos et al., 2010), that operated below the solidus temperature of the Salihli granodiorite during the onset of dynamic re-crystallization and transformation of the granodiorite to orthogneiss. In particular solid-state fabrics attests for upper-greenschist to amphibolite facies metamorphic conditions (T = 500-600 °C), indicating that mylonitization in the investigated rocks took place mostly at medium to high temperature conditions, dominantly assisted by retrograde hydrate reaction at the expenses of the pristine igneous assemblage (Wintsch et al., 2005).

Occurrence of REE-rich magmatic and REE-poor metamorphic Ttn in the same samples allows possibility to constrain time of magma crystallization and solid-state shearing through U-Th-Pb geochronology. The spread of $^{206}Pb/^{238}U$ dates along the Concordia (Fig. 5), together with (i) the textural evidence documenting fluid assisted re-crystallization (Catlos et al., 2010; this study), and (ii) the REE re-distribution in Ttn that spatially correlates with the

Th/U zoning in Ttn (Figs. 4 and 6) (see also Bonamici et al., 2015) collectively suggest that the Ttn from the Salihli granodiorite preserve predominantly open-system dates and radiogenic Pb diffusion during fluid-assisted syn-tectonic Ttn re-crystallization. This evidence suggests that the U-Pb TIMS ages of 16.1 ± 0.2 Ma (monazite, Turgutlu granodiorite) and 15.0 ± 0.3 Ma (allanite, Salihli granodiorite) (Glodny and Hetzel, 2007) dominantly record mixed ages, resulting from the analytical mixing of multiple (magmatic and metamorphic) age domains. We therefore propose that the bimodal distribution of the $^{206}Pb/^{238}U$ Ttn ages (Figs. 5a-b) records the transition from magma crystallization and emplacement (with a minimum age at ca. 17-16 Ma) to the syn-tectonic, solid-state recrystallization (at ca. 14 Ma) of the Salihli granodiorite. A minimum time lapse of ca. 2 Ma is therefore highlighted between the crustal emplacement of the Salihli granodiorite and the activation of the ductile top-to-the-NNE extensional tectonics along the GDF.

5.1. *Cooling history of the Salihli granodiorite: linking exhumation to extensional shearing*

Assuming (i) the crystallization temperatures of the Salihli granodiorite around 750-800 °C (Catlos et al. 2010) at ~17 Ma (sample T14-09), (ii) the thermal environment associated with the solid-state syn-metamorphic overprint during ductile shearing as occurred under the upper greenschist- amphibolite-grade conditions (temperature around 500-600 °C) at ~14 Ma, and (iii) taking into account published age data and thermochronological constraints (i.e. Hetzel et al., 1995a, 2013; Gessner et al., 2001; Lips et al., 2001; Ring et al., 2003; Glodny & Hetzel, 2007; Catlos et al., 2008, 2010; Buscher et al., 2013), it is possible to reconstruct the time-temperature (*T-t*) evolution of the Salihli granodiorite and of the associated GDF (Fig. 7). In particular, the following key thermochronological constrains are assumed here: (i) cooling below 350 ± 50 °C (McDougall and Harrison, 1999) is assumed at ~12 Ma based on Ar-Ar dating on biotite from the Salihli granodiorite (Hetzel et al., 1995a), and (ii) zircon and apatite fission track and U-Th/He thermochronology (Gessner et al., 2001a; Ring et al., 2003; Bucher et al., 2013). The reconstructed *T-t* diagram shows three distinct phases of cooling since the early/middle Miocene boundary, with different cooling rates. The first one, following the emplacement of the Salihli Granodiorite at ~ 17 Ma, lasted until ~12 Ma and operated with a mean cooling rate of ~90 °C/Ma. After ~12 Ma, cooling rate dramatically decreased until 3 Ma, with a mean value of 18 °C/Ma. The final phase corresponds to a renewed fast cooling

phase between 3 and 2 Ma, with a mean rate of ~120 °C/Ma during the final exhumation event that drove the Salihli granodiorite and the GDF to the surface.

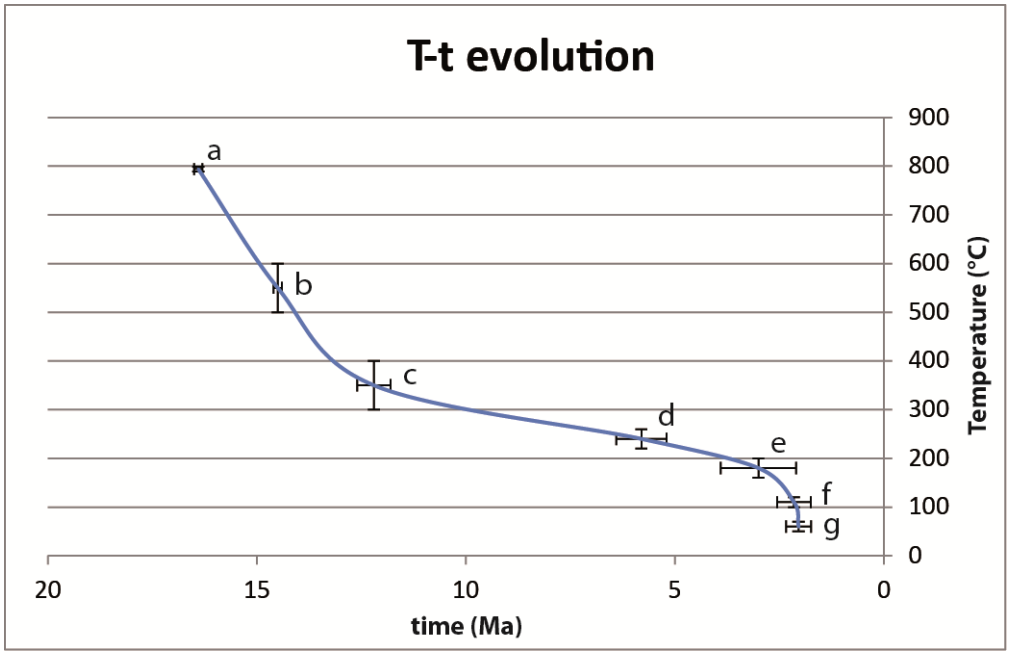

FIGURE 7: *T-t evolution of the Salihli granodirite and of the associated Gediz Detachment Fault. Time and temperature constrains are from: (a) Catlos et al., 2010 for temperature (Zr-saturation) + this study for the age (U-(Th)-Pb on Ttn); (b) this study (U-(Th)-Pb on Ttn); (c) Hetzel et al., 1995a ($^{40}Ar/^{39}Ar$ on Bt); (d) Gessner et al., 2001 + Ring et al., 2003 + Buscher et al., 2013 (zircone fission track); (e) Buscher et al., 2013 (U-Th/He on zircon); (f) Gessner et al., 2001 + Ring et al., 2003 + Buscher et al., 2013 (apatite fission track); (g) Buscher et al., 2013 (U-Th/He on apatite).*

The first implication of the reconstructed *T-t* evolution is that the thermal perturbation associated with crystallization, emplacement and deformation of the Salihli granodiorite in the crustal section of the MMCC was a long-lasting event that operated at temporal scales in the order of 10^6 years. Thermo-rheological modeling of the post-intrusive scenario in the crust predicts that the conditions for ductile deformation should last for a much shorter time interval, in the order of 10^4-10^5 years (Caggianelli et al., 2013). A similar long-lasting thermal perturbation associated with granite emplacement in an extending crustal section has been documented in the Larderello geothermal field of Central Italy, where anomalous high gradient geothermal conditions were documented in the last 3 Ma in concomitance with multiple granite intrusion ad depth (Bertini et al., 2006; Rossetti et al., 2008). This suggests

that the Salihli and Turgutlu granodiorites were the upper crustal apophyses of a deeper magma chamber responsible for the maintenance of the regional positive thermal anomaly.

The second implication is that the *T-t* diagram points to a pulsed nature of the cooling/exhumation history of the Salihli granodiorite, which also influences the space-time rheological evolution of the GDF. In particular, the reconstructed T-t evolution suggests that the transition from ductile to brittle behavior along the GDF did not occur as a continuous process, but was instead punctuated in time, with a direct impact on the stratigraphic arrangement and structural evolution of the supradetachement Gediz Graben (Purvis and Robertson, 2005; Öner and Dilek, 2010). An upper bound for the transition to brittle conditions along the GDF can be placed at ~7 ± 1 Ma, as derived from the $^{40}Ar/^{39}Ar$ dating of syn-kinematic withe micas from the topmost horizons of the GDF (Lips et al., 2001). This is in line with the published low-*T* thermochronological data, showing that variations in the exhumation rates of the Salihli granodiorite have occurred in the last 6 Ma, ranging between 0.6 and 2.2 km/Ma (Buscher et al., 2013). Within this scenario, the last rapid cooling/exhumation phase starting at ~3 Ma was related to brittle extensional faulting, active in the hanging wall of the GDF. Structurally-controlled fluid circulation and percolation of meteoric fluids assisted by brittle faulting could have favored heat extraction by advection, hence enhancing cooling of the exhuming rock section (e.g. Morrison & Anderson, 1998).

6. CONCLUDING REMARKS

The textural and Ttn geochronological data presented in this study provides evidence that crustal magma emplacement predated onset of extensional detachment faulting. This evidence suggests that activation of ductile extension was a consequence, rather than the cause, of magma emplacement in the extending crust. This evidence reinforces the importance of the rheological perturbation produced by magma intrusion in the crust and the rheological control operated by transient ductile-to-brittle transition and strain softening processes associated with pluton emplacement (e.g. Parsons and Thompson, 1993; Lister and Baldwin, 1993; Brun et al., 1994; Caggianelli et al., 2013) in controlling localization and enucleation of ductile extension and extensional detachment tectonics in extensional provinces.

REFERENCES

Altunkaynak, Ş., Dilek, Y., Genç, C.Ş., Sunal, G., Gertisser, R., Furnes, H., Foland, K.A., Yang, J., 2012. *Spatial, temporal and geochemical evolution of Oligo-Miocene granitoid magmatism in western Anatolia, Turkey*. Gondwana Research, 21, 961–986.

Aoya, M., Wallis, S.R., Terada, K., Lee, J., Kawakami, T., Wang, Y. & Heizler, M., 2005. *North–south extension in the Tibetan crust triggered by granite emplacement*. *Geology*, 33, 853–856.

Bertini G., Casini M., Gianelli G., Pandeli E., 2006. *Geological structure of a long-living geothermal system, Larderello, Italy*. Terra Nova, 18 (3), 163–169.

Bonamici C.E., Fanning C.M., Kozdona R., Fournellea J.H., Valleya J.W., 2015. *ombined oxygen-isotope and U-Pb zoning studies of titanite: New criteria for age preservation*. Chemical Geology, 398, 70–84.

Bozkurt, E., Park, G.R., 1994*. Southern Menderes massif: an incipient metamorphic core complex in western Anatolia, Turkey.* Journal of the Geological Society of London, 151, 213–216.

Bozkurt, E., Sözbilir, H., 2004. *Tectonic evolution of the Gediz Graben: field evidence for an episodic, two-stage extension in western Turkey*. Geological Magazine 141, 63–79.

Bozkurt, E., Satır, M., Buğdaycıoğlua, Ç., 2011. *Surprisingly young Rb/Sr ages from the Simav extensional detachment fault zone, northern Menderes Massif, Turkey*. Journal of Geodynamics, 52, 406– 431.

Brun, J. P., Sokoutis, D., and Van Den Driessche, J., 1994. *Analogue modelling of detachment fault systems and core complexes*. Geology, 22, 319–322.

Buscher J.T., Hampel A., Hetzel R., Dunkl I., Glotzbach C., Struffert A., Akal C., Ratz M., (2013). *Quantifying rates of detachment faulting and erosion in the central Menderes massif*

(western Turkey) by thermochronology and cosmogenic 10Be. J. Geol. Soc. London, 170, 669–683.

Caggianelli A., Ranalli G., Lavecchia A., Liotta D. & Dini A., 2013. *Post-emplacement thermo-rheological history of a granite intrusion and surrounding rocks: the Monte Capanne pluton, Elba Island, Italy*. Geological Society, London, Special Publications, 394, http://dx.doi.org/10.1144/SP394.1.

Candan, O., Dora, O.Ö., Oberhänsli, R., Çetinkaplan, M., Partzsch, J.H., Warkus, F.C., Dürr, S., 2001. *Pan-African high-pressure metamorphism in the Precambrian basement of the Menderes Massif, western Anatolia, Turkey*. International Journal of Earth Sciences (Geologische Rundschau), 89, 793–811.

Catlos, E.J., Baker, C., Sorensen, S.S., Cemen, I., Hancer, M., 2008. *Monazite geochronology, magmatism and extensional dynamics within the Menderes massif, Western Turkey*. IOP Conf. Series: Earth and Environmental Science, 2, paper 012015, 2 pp, doi:10.1088/1755-1307/2/1/012015.

Catlos, E.J., Baker, C., Sorensen, S.S., Çemen, I., Hancer, M., 2010. *Geochemistry, geochronology, and cathodoluminescence imagery of the Salihli and Turgutlu granites (central Menderes Massif, western Turkey): implications for Aegean tectonics*. Tectonophysics, 48, 110-130.

Catlos, E.J., Baker, C.B., Sorensen, S.S., Jacob, L., Çemen, I., 2011 - *Linking microcracks and mineral zoning of detachment-exhumed granites to their tectonomagmatic history: Evidence from the Salihli and Turgutlu plutons in western Turkey (Menderes Massif)*. Journal of Structural Geology, 33 (5), 951-969.

Çemen, I., Catlos, E.J., Gögüs, O., Özerdem, C., 2006. *Postcollisional extensional tectonics and exhumation of the Menderes massif in the Western Anatolia extended terrane, Turkey*. In: Dilek, Y., Pavlides, S. (Eds.), Postcollisional Tectonics and Magmatism in the Mediterranean Region and Asia: Geological Society of America Special Paper, 409, 353–379.

Çiftçi, N.B., Bozkurt, E., 2009 - *Evolution of the Miocene sedimentary fill of the Gediz Graben, SW Turkey*. Sedimentary Geology, 216, 49–79.

Coney, P.J., 1974. *Structural analysis of the Snake Range "décollement," east-central Nevada*. Geological Society of America Bulletin, 88, 1237–1250.

Coney, P.J., 1980. *Cordilleran metamorphic core complexes: An overview*, *in* Crittenden, M.D., Coney, P.J., and Davis , G.H., eds., Cordilleran Metamorphic Core Complexes: Geological Society of America Memoir, 153, 7–34.

Corti, G., Bonini, M., Conticelli, S., Innocenti, S., Manetti, P., Sokoutis, D., 2003. *Analogue modelling of continental extension: a review focused on the relations between the patterns of deformation and the presence of magma*. Earth-Science Reviews, 63, 169–247.

Crittenden, M.D., Jr., Coney, P.J., Davis, G.H., eds., 1980. *Cordilleran Metamorphic Core Complexes*. Geological Society of America Memoir, 153, 490 p.

Davis G. H., Constenius K. N., Dickinson W. R., Rodríguez E. P., Cox L. J., 2004. *Fault and fault-rock characteristics associated with Cenozoic extension and core-complex evolution in the Catalina–Rincon region, southeastern Arizona*. Geological Society of America Bulletin, 116, 128-141.

Dilek, Y., Altunkaynak, S., Öner, Z., 2009. *Syn-extensional granitoids in the Menderes core complex and the late Cenozoic extensional tectonics of the Aegean province*. In: Ring, U., Wernicke, B. (Eds.), Extending a Continent: Architecture, Rheology and Heat Budget. Geological Society of London Special Publications, 321, 197-223.

Drury M.R., Urai J.L., 1990. *Deformation related recrystallization processes*. Tectonophysics, 172: 235-253.

Ercan, E., Satır, M., Sevin, D., Türkecan, A., 1996 - *Batı Anadolu'daki Tersiyer ve Kuvaterner yaşlı volkanik kayaçlarda yeni yapılan radyometrik yaş ölçümlerinin yorumu [Some new radiometric ages from Tertiary and Quaternary volcanic rocks from West Anatolia]*. Miner. Res. Explor. Bull. (Turkey), 119, 103–112.

Erkül, F., 2010. *Tectonic significance of synextensional ductile shear zones within the Early Miocene Alacamdag granites, northwestern Turkey*. Geological Magazine, 147, 611–637.

Erkül, S.T., Erkül, F., 2012. *Magma interaction processes in syn-extensional granitoids: the Tertiary Menderes metamorphic core complex, western Turkey*. Lithos, 142–143, 16–33.

Erkül F., Erkül S.T., Ersoy Y., Uysal I., Krötzli U., 2013. *Petrology, mineral chemistry and Sr–Nd–Pb isotopic compositions of granitoids in the central Menderes metamorphic core complex: Constraints on the evolution of Aegean lithosphere slab*. Lithos, 180-181, 74-91.

Ersoy, Y., Helvacı, C., Sözbilir, H., Erkül, F., Bozkurt, E., 2008 - *A geochemical approach to Neogene–Quaternary volcanic activity of western Anatolia: an example of episodic bimodal volcanism within the Selendi Basin, Turkey*. Chem. Geol., 255, 265–282.

Ersoy, E.Y., Helvacı, C., Palmer, M.R., 2011 - *Stratigraphic, structural and geochemical features of the NE–SW-trending Neogene volcano-sedimentary basins in western Anatolia: implications for associations of supradetachment and transtensional strike-slip basin formation in extensional tectonic setting*. J. Asian Earth Sci., 41, 159–183.

Ersoy, E.Y., Helvacı, C., Palmer, M.R., 2012 - *Petrogenesis of the Neogene volcanic units in the NE–SW-trending basins in western Anatolia, Turkey*. Contrib. Mineral. Petrol., 163, 379–401.

Ersoy E.Y., Çemen İ., Helvacı C., Billor Z., 2014 - *Tectono-stratigraphy of the Neogene basins inWestern Turkey: Implications for tectonic evolution of the Aegean Extended Region*. Tectonophysics, 635, 33–58.

Famin V., Philippot P., Jolivet L. & Agard P., 2004*. Evolution of hydrothermal regime along a crustal shear zone, Tinos Island, Greece*. Tectonics, 23, TC5004, doi:10.1029/2003TC001509.

Gébelin A., Mulch A., Teyssier C., Heizler M., Vennemann T. & Seaton N. C. A., 2011. *Oligo-Miocene extensional tectonics and fluid flow across the northern Snake Range detachment system, Nevada*. Tectonics, 30, TC5010, doi:10.1029/2010TC002797.

Gapais Denis, 1989a. *Les orthogneiss: structures, mécanismes de déformation et analyse cinématique*. Mémoire et documents du Centre Armoricain d'Etudes Structurale des Socles, 28, 382 pp.

Gapais Denis, 1989b. *Shear structures within deformed granites: mechanical and thermal indicators*. Geology, 17 (12), 1144-1147.

Gessner, K., Ring, U., Johnson, C., Hetzel, R., Passchier, C.W., Gungor, T., 2001a. *An active bivergent rolling-hinge detachment system: Central Menderes metamorphic core complex in western Turkey*. Geology, 29, 611–614.

Gessner, K., Piazolo, S., Gungor, T., Ring, U., Kroener, A., Passchier, C.W., 2001b. *Tectonic significance of deformation patterns in granitoid rocks of the Menderes nappes, Anatolide Belt, Southwest Turkey*. International Journal of Earth Sciences, 89, 766–780.

Gessner, K., Ring, U., Passchier, C.W., Gungor, T., 2001c. *How to resist subduction: evidence for large-scale out-of-sequence thrusting during Eocene collision in western Turkey*. Journal of the Geological Society 158, 769–784.

Gessner, K., Gallardo, L.A., Markwitz, V., Ring, U., Thomson, S.N., 2013. *What caused the denudation of the Menderes Massif: Review of crustal evolution, lithosphere structure, and dynamic topography in southwest Turkey*. Gondwana Research, 24 (1), 243-274.

Glodny, J., Hetzel, R., 2007. *Precise U-Pb ages of syn-extensional Miocene intrusions in the central Menderes Massif, western Turkey*. Geological Magazine, 144, 235-246.

Hetzel, R., Ring, U., Akal, C., Troesch, M., 1995a. *Miocene NNE-directed extensional unroofing in the Menderes Massif, southwestern Turkey*. Journal of the Geological Society of London, 152, 639-654.

Hetzel, R., Passchier, C.W., Ring, U., Dora, O.Ö, 1995b. *Bivergent extension in orogenic belts; the Menderes Massif (southwestern Turkey)*. Geology, 23, 455-458.

Hetzel, R., Reischmann, T., 1996. *Intrusion age of Pan-African augen gneisses in the southern Menderes massif and the age of cooling after Alpine ductile extensional deformation*. Geological Magazine, 133, 565–572.

Hetzel, R., Romer, R.L., Candan, O., Passchier, C.W., 1998. *Geology of the Bozdağ area, central Menderes massif, SW-Turkey: Pan African basement and Alpine deformation*. Geologische Rundschau, 87, 394–406.

Hirth, G., Tullis, J., 1992. *Dislocation creep regimes in quartz aggregates*. Journal of Structural Geology, 14 (2), 145-159.

Işik, V., Seyitoğlu, G., Çemen, I., 2003. *Ductile-brittle transition along the Alaşheir detachment fault and its structural relationship with the Simav detachment fault, Menderes massif, western Turkey*. Tectonophysics, 374, 1-18.

Jolivet, L., Brun, J.P., 2010. *Cenozoic geodynamic evolution of the Aegean*. International Journal of Earth Sciences, 99, 109–138.

Karaoğlu, Ö., Helvacı, C., Ersoy, E.Y., 2010 - *Petrogenesis and 40Ar/39Ar geochronology of the volcanic rocks of the Uşak–Güre basin, western Türkiye*. Lithos, 119, 193–210.

Leloup, P. H., R. Lacassin, P. Tapponnier, U. Schärer, D. Zhong, X. Liu, L. Zhang , S. Ji and P. T. Trinh, 1995. *The Ailao Shan-Red River shear zone (Yunnan, China), Tertiary transform boundary of Indochina*. Tectonophysics, 251, 2-84.

Lips, A.L.W., Cassard, D., Sözbilir, H., Yilmaz, H., Wijbrans, J.R., 2001. *Multistage exhumation of the Menderes Massif, western Anatolia (Turkey)*. International Journal of Earth Sciences (Geologische Rundschau), 89, 781–792.

Lister G. S. & Baldwin S. L., 1993. *Plutonism and the origin of metamorphic core complexes*. Geology, 21, 607-610.

Lister, G.S., and Davis, G.A., 1989. *The origin of metamorphic core complexes and detachment faults formed during Tertiary continental extension in the northern Colorado River region, USA*. Journal of Structural Geology, 11, 65–94, doi:10.1016/0191-8141(89)90036-9.

Ludwig, K.R., 2003. *Isoplot/EX version 3.0, A geochronological toolkit for Microsoft Excel*. Berkeley Geochronology Center Special Publication.

McDougall I., Harrison T.M., 1999. *Geochronology and Thermochronology by the 40Ar/39Ar method*. Oxford University Press, New York, 212 pp.

Metcalf R. V. & Smith E. I., 1995. *Introduction to special section: Magmatism and extension*. Journal of Geophysical Research, 100 (10), 249-253.

Morrison, J., and J. L. Anderson, 1998*. Footwall refrigeration along a detachment fault: Implications for the thermal evolution of core complexes*. Science, 279, 63–66.

Oberhänsli, R., Candan, O., Wilke, F., 2010. *Geochronological evidence of Pan-African eclogites from the central Menderes Massif, Turkey*. Turkish Journal of Earth Sciences, 19, 431–447.

Öner, Z., Dilek, Y., Kadıoğlu, Y.K., 2010. *Geology and geochemistry of the synextensional Salihli granitoid in the Menderes core complex, western Anatolia, Turkey*. International Geology Review, 52, 336–368.

Öner Z. & Dilek Y., 2011. *Supradetachment basin evolution during continental extension: the Aegean province of western Anatolia, Turkey*. Geological Society of America Bulletin, 123, 2115–2141.

Menegon, L., 2006. *Ductile deformation of granitic rocks: selected examples from the Western Alps*. Unpublished PhD Thesis, Universita` degli Studi di Padova, Italy.

Parsons T. & Thompson G. A., 1993. *Does magmatism influence low-angle normal faults?* Geology, 21, 247-250

Passchier C. W., Trouw R. A. J., 1996. *Microtectonics*. Berlin, Springer-Verlag, 289 pp.

Passchier, C., Trouw, R. A. J., 2005. *Microtectonics*. Berlin, Springer Verlag, 366pp.

Purvis, M., Robertson, A.H.F., 2005. *Sedimentation of the Neogene–Recent Alaşehir (Gediz) continental graben system used to test alternative tectonic models for western (Aegean) Turkey*. Sedimentary Geology 173, 373–408.

Purvis, M., Robertson, A., Pringle, M., 2005 - *40Ar–39Ar dating of biotite and sanidine in tuffaceous sediments and related intrusive rocks: implications for the early Miocene evolution of the Gördes and Selendi basins, W Turkey*. Geodin. Acta, 18, 239–253.

Rabillard, A., L. Arbaret, L. Jolivet, N. Le Breton, C. Gumiaux, R. Augier, and B. Grasemann, 2015. *Interactions between plutonism and detachments during metamorphic core complex formation, Serifos Island (Cyclades, Greece)*. Tectonics, 34, 1080–1106. doi: 10.1002/2014TC003650.

Régnier, J.L., Ring, U., Passchier, C.W., Gessner, K., Gungor, T., 2003. *Contrasting metamorphic evolution of metasedimentary rocks from the Cine and Selimiye nappes in the Anatolide belt, western Turkey*. Journal of Metamorphic Geology 21, 699–721.

Régnier, J.L., Metzger, J.E., Passchier, C.W., 2007. *Metamorphism of Precambrian–Palaeozoic schists of the Menderes core series and contact relationships with Proterozoic orthogneisses of the western Çine Massif, Anatolide belt, western Turkey*. Geological Magazine, 144, 67–104.

Rimmelé, G., Oberhänsli, R., Goffé, B., Jolivet, L., Candan, O., Cetinkaplan, M., 2003. *Deformation history of the high-pressure Lycian Nappes and implications for tectonic evolution of SW Turkey*. Tectonics, 22, 1007.

Ring, U., Gessner, K., Gungor, T., Passchier, C.W., 1999. *The Menderes Massif of western Turkey and the Cycladic Massif in the Aegean - do they really correlate?* Journal of the Geological Society, 156, 3–6.

Ring, U., Johnson, C., Hetzel, R., Gessner, K., 2003. *Tectonic denudation of a Late Cretaceous– Tertiary collisional belt: regionally symmetric cooling patterns and their relation to extensional faults in the Anatolide belt of western Turkey*. Geological Magazine, 140, 421–441.

Ring, U., Collins, A.S., 2005. *U–Pb SIMS dating of synkinematic granites: timing of core–complex formation in the northern Anatolide belt of western Turkey*. Journal of the Geological Society, 162, 289–298.

Rossetti, F., Balsamo, F., Villa, I.M., Bouybaouenne, M., Faccenna, C. & Funiciello, R., 2008. *Pliocene–Pleistocene HT–LP metamorphism during multiple granitic intrusions in the southern branch of the Larderello geothermal field (southern Tuscany, Italy)*. Journal of the Geological Society, London, 165, 247–262.

Sengör, A.M.C., Satir, M., Akkök, R., 1984. *Timing of the tectonic events in the Menderes massif, western Turkey: implications for tectonic evolution and evidence for Pan- African basement in Turkey*. Tectonics, 3, 693–707.

Seyitoğlu, G., Scott, B.C., Rundle, C.C., 1992 - *Timing of Cenozoic extensional tectonics in west Turkey*. J. Geol. Soc., 149, 533–538.

Seyitoğlu, G., Anderson, D., Nowell, G., Scott, B., 1997 - *The evolution from Miocene potassic to Quaternary sodic magmatism in Western Turkey: implications for enrichment processes in the lithospheric mantle*. J. Volcanol. Geotherm. Res., 76, 127–147.

Seyitoğlu, G., 1997 - *The Simav graben: an example of young E–W trending structures in the late Cenozoic extensional system of Western Turkey*. Turk. J. Earth Sci., 6, 135–141.

Stip M., Stunitz H., Heilbronner R., Schmid S.M., 2002. *The eastern Tonale fault zone: a "natural laboratory" for crystal plastic deformation for quartz over a temperature range from 250 to 700°C*. Journal of structural geology, 24, 1861-1884.

Teyssier C. & Withney D. L., 2002. *Gneiss domes and orogeny*. Geology, v. 30, p. 1139–1142

Thomson, S.N., Ring, U., 2006. *Thermochronologic evaluation of post-collision extension in the Anatolide Orogen, western Turkey*. Tectonics, 25, TC3005.

Withney D. L. and Evans B. W., 2010. *Abbreviations for names of rock-forming minerals*. American Mineralogist, 95(1), 185-187.

Withney D. L., Teyssier C., Rey P. & Buck W. R., 2013: *Continental and oceanic core complexes*. Geological Society of America Bulletin, 125 (3/4), 273-298.

Wernike, B., 1985. *Uniform-sense normal simple shear of the continental lithosphere*. Canadian Journal of Earth Sciences, 22(1), 108-125.

Wintsch, R.P., Aleinikoff, J.N., Yi, K., 2005. *Foliation development and reaction softening by dissolution and precipitation in the transformation of granodiorite to orthogneiss, Glastonbury Complex, Connecticut, U.S.A*. The Canadian Mineralogist, 43, 327-347.

CHAPTER 4

TECTONO-STRATIGRAPHIC EVOLUTION OF THE GEDIZ SUPRADETACHMENT BASIN (MENDERES MASSIF, W TURKEY)

Riccardo Asti, Claudio Faccenna, Federico Rossetti, Domenico Cosentino, Elsa Gliozzi, Costanza Faranda

Università degli Studi Roma Tre, Department of Sciences, Rome, Italy

Abstract: Unravelling the evolution of supradetachment basins developed at the hanging wall of low-angle detachment faults may be an invaluable tool in reconstructing the tectonic evolution of highly extended terrains. These basins may in fact record main regional tectonic events related to the exhumation of metamorphic core complexes and the reconstruction of their evolution may be helpful in quantifying the amount of extension accommodated in such processes. It this work we present stratigraphic and structural field evidences together with new micropaleontological constrains for the Neogene-to-Quaternary evolution of the supradetachment Gediz Graben, whose evolution is related to the exhumation of the Central Menderes Massif (SW Turkey). This basin displayed three different structural styles during its evolution: (i) it developed as a ramp-basin following the activation of the Gediz Detachment in the Middle Miocene; (ii) it evolved in an half graben during Late Miocene following the activation of high-angle brittle faults at its southern margin; (iii) it reached its final symmetric graben configuration in Late Pliocene (?) – Quaternary times with the activation of its northern margin. Our new micropaleontological data show that a short-lived upper Tortonian marine episode occurred at the end of the first phase of the basin evolution. The reconstruction of the amount of extension accommodated since the formation of the basin suggest that no large amount of extension might be required to exhume to the surface ductilely deformed metamorphic rocks and that the activation of high-angle brittle faults at the hanging wall of detachment faults might make the exhumation process much more efficient. Field evidences together with existing thermochronological data suggest that the exhumation related to the

Gediz Detachment and its associated structure was extremely localized and did not involve the whole Central Menderes Massif.

1. INTRODUCTION

Supradetachment basin constitutes subsiding regions developed on the hanging wall of highly extended terranes over low angle shear zones, or detachment. Several examples of supradetachment basin have been proposed during the last decades (e.g. Fillmore et al., 1994; Friedmann & Burbank, 1995; Fillmore & Walker, 1996; van Hinsbergen & Meulenkamp, 2006; Öner & DIlek, 2011; Vetti & Fossen, 2012; Bargnesi et al., 2013). They usually show high sedimentation rates (Friedmann & Burbank, 1995) and may thus easily record in their sedimentary fill major tectonic events. Unravelling of the evolution of supradetachment basins may represent a key tool in understanding the evolution of highly extended terrains, yielding important insights on the amount and rates of extension and exhumation.

Western Turkey is the eastern termination of the Aegean Extensional Province and is one of the best example of active continental extension. The ~N-S oriented extension led between the latest Paleogene and the Neogene to the exhumation of the Menderes Massif (e.g. Hetzel et al., 1995a; Gessner et al., 2001, 2013; Ring et al., 2003; Ring & Collins, 2005; Thomson & Ring, 2006) and to the formation in this region of a series of sedimentary basins oriented both parallel and perpendicular to the stretching direction (e.g. Şengör, 1987; Ersoy et al., 2011 and references therein). The Gediz Graben developed at the hanging wall of the ductile-to-brittle N-dipping Gediz Detachment (e.g. Cohen et al., 1995; Emre, 1996; Koçyiğit et al., 1999; Seyitoğlu et al., 2002; Purvis & Robertson, 2005; Çiftçi & Bozkurt, 2009; Öner & Dilek, 2011), displaying all the characteristics of a supradetachment basin.

Despite many studies have addressed this region in the last three decades, and in particular the Gediz Graben, there are still some major issues to be solved. In particular, the sedimentary history of the graben is not well constrained and also its structural evolution is debated. General agreement exists in the recognition of two distinct deformation styles related to the Neogene extensional phase, one represented by an early low-angle ductile-to-brittle detachment faulting and the other represented by a following high-angle brittle faulting

(e.g. Bozkurt and Oberhänsli, 2001 and references therein); the relationship between these two different styles is still debated and general agreement is also lacking on whether the two extensional phases where continuous (e.g. Seyitoğlu et al., 2000; Glodny & Hetzel, 2007) or if an interruption occurred between the two (possibly with a compressional phase in between) (e.g. Koçyiğit et al., 1999; Yilmaz et al., 2000; Purvis and Robertson, 2004, 2005; Çiftçi & Bozkurt, 2009a; Öner & Dilek, 2011).

In this study we present an evolutionary model for the Gediz Graben based on structural and stratigraphic field evidences and on new paleontological constrains for the Neogene-to-Quaternary sedimentary fill of the basin. Our reconstruction provides useful insights on the amount of extension accommodated by the basin and the related Gediz Graben and in general for the tectonic evolution of the Central Menderes Massif.

2. GEOLOGICAL SETTING

The Menderes Massif in Western Turkey is generally considered an outstanding example of Tertiary metamorphic core complex (Şengör & Yilmaz, 1981; Şengör et al., 1984; Bozkurt and Park, 1994; Gessner et al., 2001; Işık and Tekeli, 2001; Ring et al., 2003; Seyitoğlu et al., 2004; Van Hinsbergen et al., 2010). It is exposed along the southwestern Anatolian portion of the Alpine-Himalayan belt, which has undergone during the Cenozoic an orogenic contractional phase followed by post-orogenic extension, both related to the dynamics and evolution of the Aegean subduction (e.g. Şengör et al., 1984; Şengör, 1987; Jolivet & Brun, 2010). This portion of the chain is built up of continental fragments with African affinity accreted along the southern margin of Laurasia and separated by major suture zones (Şengör et al., 1984). The Menderes Massif is located in the southernmost among these continental blocks, namely the Tauride-Anatolide Platform, and is separated from the Sakarya zone to the North by the Izmir-Ankara Suture Zone (Şengör & Yilmaz, 1981). This region has recorded a complex and polyphasic Pan-African, Variscan and Alpine tectono-metamorphic history (e.g. Ring et al., 1999; Lips et al., 2001; Oberhänsli et al., 2010 and references therein) and has undergone extension and exhumation since the latest Oligocene (e.g. Gessner et al., 2001; Ring et al., 2003; Thomson & Ring, 2006).

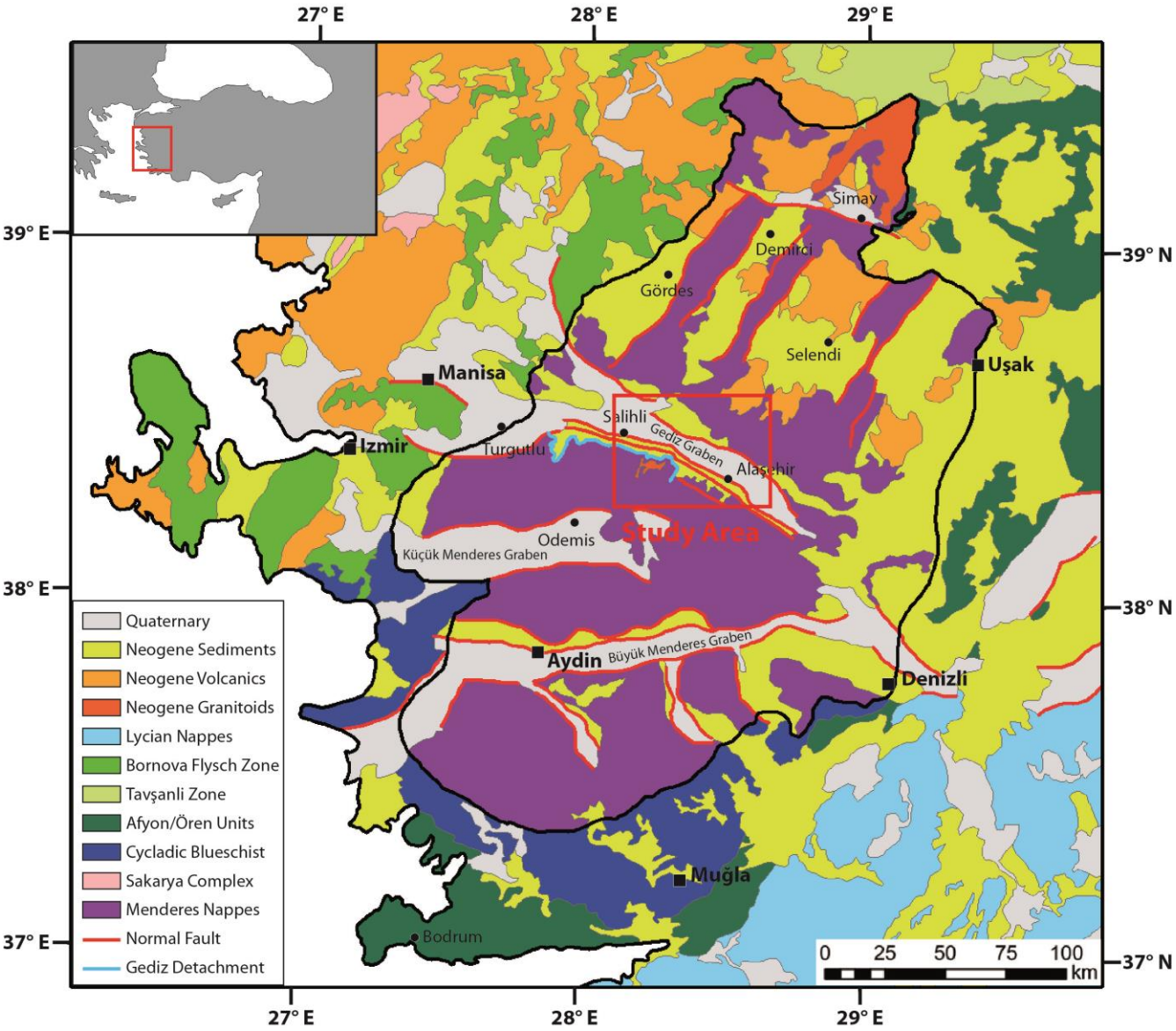

Figure 1: *Schematic tectonic map of SW Turkey. The black line delimitates the Menderes Massif; the red box show the location of the study area represented in Fig. 2.*

During the Neogene-to-Present extensional phase, a series of E-W trending sedimentary basins developed and dissected the Menderes Massif in three sub-massifs (Fig. 1). Apatite fission track show distinct cooling ages for those three sub-massifs; the Northern and the southern sub-massifs show ages between latest Oligocene and Middle Miocene (Gessner et al., 2001, 2013; Ring et al., 2003; Thomson & Ring, 2006), whereas the Central sub-massif show ages mostly spanning between Late Miocene and Early Pleistocene (even if some Early-Middle Miocene cooling ages are preserved in its central part) (Gessner et al., 2001;

Ring et al., 2003; Buscher et al., 2013). The distribution of this younger exhumation ages is concentrated along the footwall of the two major structures bounding the Central sub-massif, namely the Gediz Detachment (to the N; also named Kuzey, Alaşehir or Karadut Detachment) and the Büyük Menderes Detachment (to the S; also named Güney or Basçayir Detachment). Two granodioritic bodies intruded at the northern margin of the Central sub-massif in the latest Early Miocene, namely the Salihli and Turgutlu granodiorite, and are presently outcropping at the footwall of the ductile-to-brittle Gediz Detachment (Hetzel et al., 1995a; Glodny & Hetzel, 2007; Chapter 3, this work); this magmatic event triggered the extensional detachment tectonics in this sector (see Chapter 3, this work).

Proposed models for exhumation of the Menderes Massif can be divided into two main groups: (i) models claiming for symmetric bivergent exhumation through a southern and a northern detachment system (e.g. Bozkurt & Park, 1994; Hetzel et al., 1995b; Gessner et al., 2001; Ring et al., 2003) and (ii) models claiming for asymmetric north-verging exhumation via the northern Simav Detachment system (e.g. Seyitoğlu et al., 2004; Gessner et al., 2013). Nevertheless, all these models agree that the Central sub-massif was further symmetrically exhumed between latest Middle Miocene and Early Pleistocene.

The formation of the Neogene-to-Quaternary Gediz Graben is related to the activity of the Gediz Detachment and of the the other major normal faults bounding the northern margin of the Central Menderes Massif (e.g. Cohen et al., 1995; Emre, 1996; Koçyiğit et al., 1999; Seyitoğlu et al., 2002; Purvis & Robertson, 2005; Çiftçi & Bozkurt, 2009; Öner & Dilek, 2011; Chapter 2, this work); during its evolution this basin has recorded the major exhumation events involving only its southern margin (Chapter 2, this work).

Despite many studies have addressed the stratigraphy of the Gediz Graben, clear age constrains for the onset of the sedimentation and for the main sedimentary events are lacking. The age of the older sequence has been inferred to be Early-Middle Miocene in age, on the base of palynological data (e.g. Seyitoğlu and Scott, 1992; Ediger et al., 1996). More recently, well log data interpretation (Çiftçi & Bozkurt 2009a) and detrital apatite fission track data (Chapter 2, this work) showed that the basin is younger than Middle Miocene. In particular, Çiftçi & Bozkurt (2009a) suggested that the basin developed as an half-graben with an active southern margin during Miocene and changed its geometry during post-Miocene times with the activation of the northern margin.

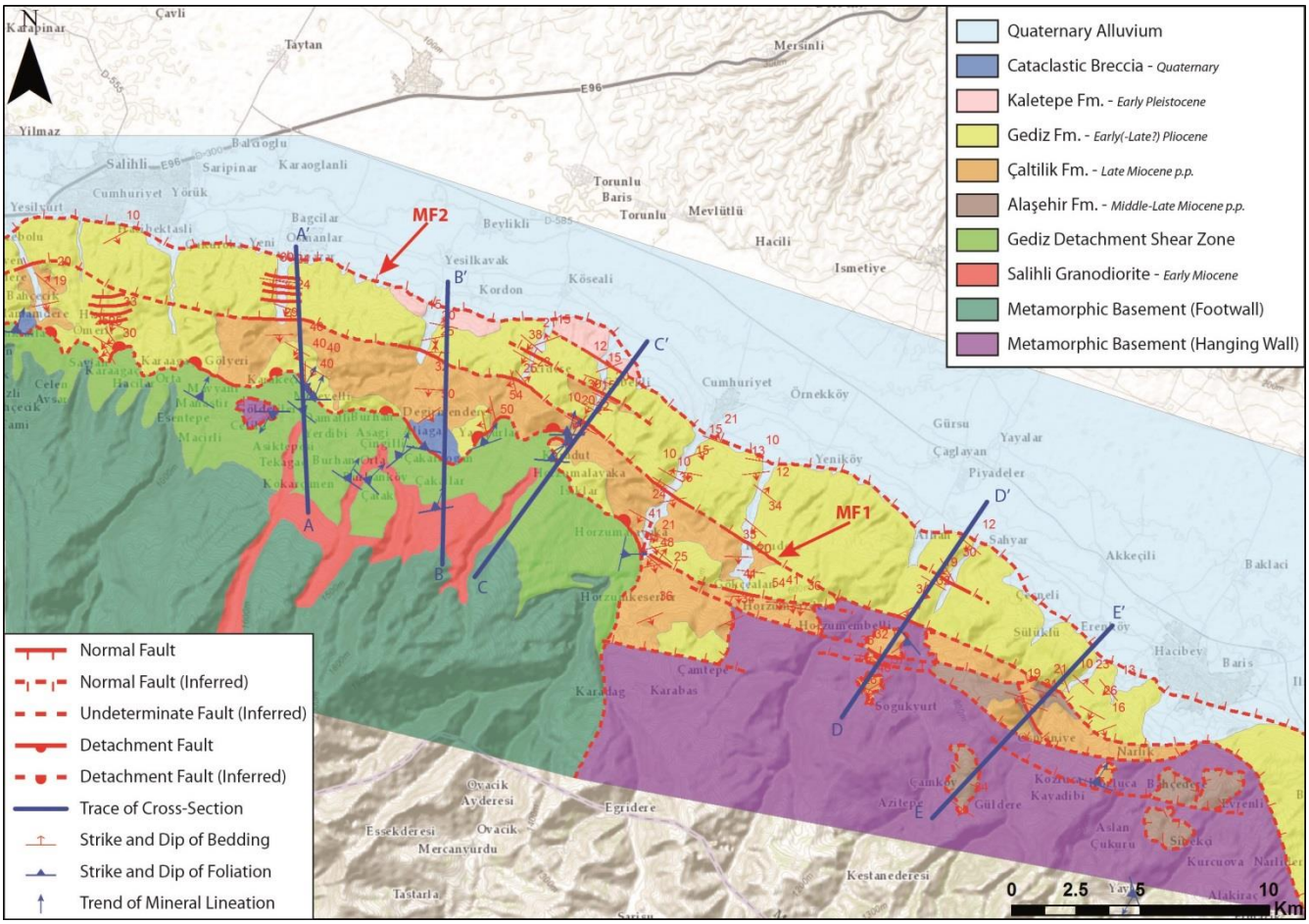

Figure 2: *Geological map of the southern margin of the Gediz Graben between Salihli (to the W) and Alaşehir (to the E). Thick blue lines show the locations of the geological cross-sections represented in Fig. 16.*

In this study, for the subdivision of the lithostratigraphic units of the Gediz Graben we use the nomenclature proposed by Çiftçi & Bozkurt (2009a), used the earliest proposed stratigraphic scheme (i.e. İztan and Yazman, 1991; Yazman et al., 1998), in order to try to resolve the complications derived by the introduction of different stratigraphic names in different studies on the area (İztan and Yazman, 1991; Cohen et al., 1995; Yazman et al., 1998; Koçyiğit et al., 1999; Sarıca 2000; Yılmaz et al., 2000; Seyitoğlu et al., 2002; Purvis and Robertson, 2005a; Çiftçi & Bozkurt, 2009a; Öner and Dilek, 2011), which also produced controversial age assignments for the same deposits. This subdivision consists in four different lithostratigraphic formations outcropping at the southern margin of the basin in unconformity with the metamorphic bedrock (from bottom to top): the concordant Alaşehir Fm., Çaltilik Fm. and Gediz Fm., and the unconformably overlaying Kaletepe Fm. We introduced some

modifications in order to integrate field observations and to take into account differences in the stratigraphic sequence in outcrop between western and the eastern sectors (Fig. 2 and 3).

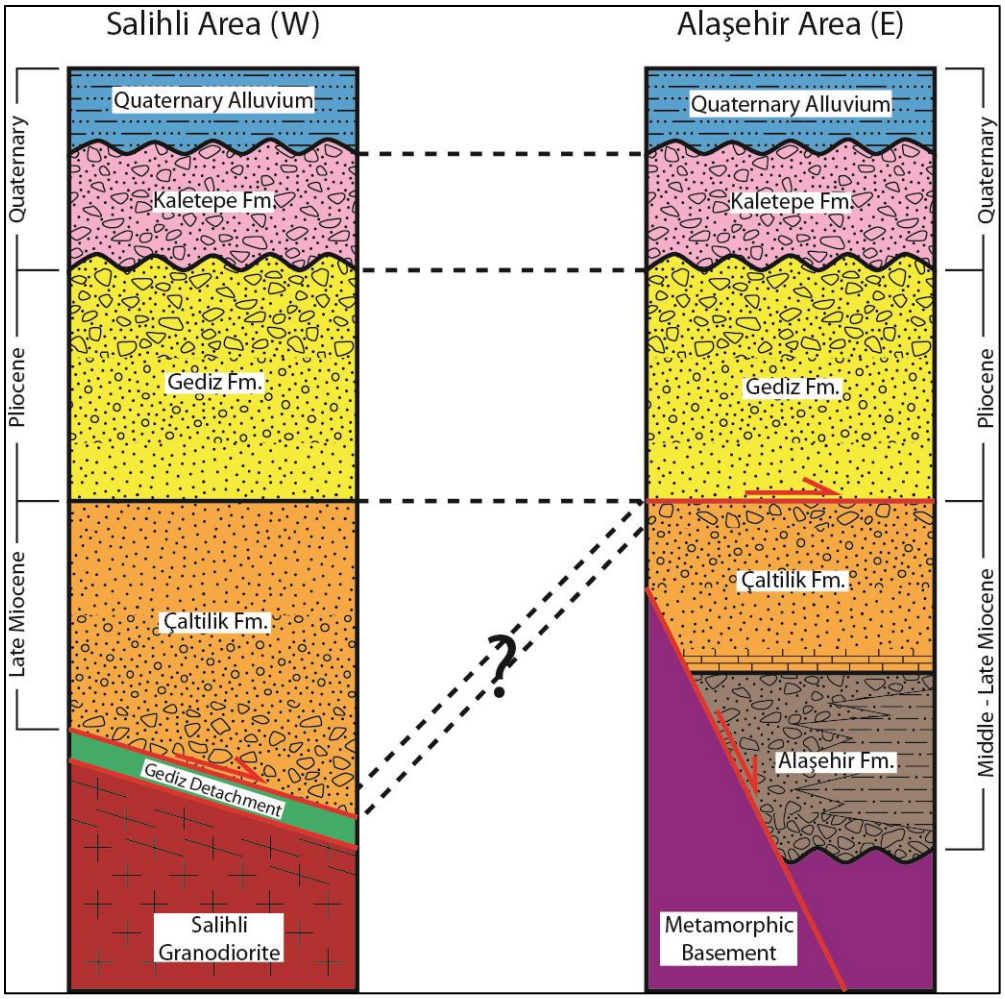

Figure 3: *Stratigraphy of the Neogene-to-Quaternary sedimentary fill of the Gediz Graben in the study area. On the left the stratigraphic pattern of the Salihli area (western sector) and on the right the one of the Alaşehir area (eastern sector); dashed black lines between the two columns show possible correlations between the two sectors. Undulated black horizontal lines between two formations indicate angular unconformity.*

3. METHODS

3.1. *Field data collection*

We carried out field mapping at 1:25.000 scale along the southern margin of the Gediz Graben, between Salihli (to the W) and Alaşehir (to the E) (Fig. 2). We carried out stratigraphic log and structural analysis to define the tectono-stratigraphic evolution of the

basin. these latter have been integrated by observations in thin section to reconstruct the fabric and the kinematics of the deformed rocks. In the following we will first present the stratigraphic results and then the results of structural analysis.

3.2. Sampling strategy and samples preparation for micropaleontological analyses

In order to obtain chronostratigraphic constrains for the evolution of the Gediz Graben sedimentary fill, many samples in the whole stratigraphic succession were collected for micropaleontological analysis, from the fine-grained levels (shales and silts) of the whole stratigraphic succession and from the limestone at the base of the Çaltilik Fm.

The poorly or not cemented fine-grained samples were washed and disaggregated in an hydrogen peroxide solution ($5\%_{vol}$) and then sieved under running water through 500µm, 125µm and 63µm mesh-sieves. The resulting sediment fractions were dried at 50°C and then analyzed under a stereomicroscope.

Limestone from the Çaltilik Fm. where first analyzed in thin section in order to preliminarily define the possible fossil content, then the samples retrieving positive results were selected for disaggregation. These rocks are very cohesive, so a disaggregation technique that is comparable with natural weathering that makes use of sodium thiosulfate pentahydrate ($Na_2S_2O_3 \cdot 5H_2O$, commonly and improperly called sodium hyposulphite) was used, as described in Tinn & Meidla (1999, and references therein). This salt melts at 48°C and crystallizes pretty easily below this temperature, if seed crystal are present.

About 300-400g of limestone for each sample were mechanically crushed into 1-2 cm diameter pieces; a comparable amount, in terms of volume, of thiosulfate was added, then the compound was heated on a stove to melt the salt and finally was cooled for few hours at room temperature to let the salt crystallize again. The cycle was repeated about 30 times for each sample/disaggregation cycle in order to obtain a suitable amount of fine crushed material. After this treatment, the samples were drown in Rewoquate® WE15 and then sieved under running water through 2cm, 500µm, 125µm and 63µm mesh-sieves. The resulting sediment fractions were dried at 50°C and then the two intermediate fractions were analyzed under a stereomicroscope.

4. RESULTS

4.1. Stratigraphic setting

In the following, we will present our result from the lower to the upper units, considering the differences between the western sector (Salihli area) and eastern sector (Alaşehir area) that mostly concern the lower deposits (Fig. 2 and 3). In general, the proposed thicknesses for the formations described below might be overestimated because of a large number of syn- and post-sedimentary minor faults that affected the sedimentary sequence (see section 4.3.3), thus making hard a precise estimation of thicknesses.

4.1.1. Alaşehir Formation

The Alaşehir Fm. is the lowermost Neogene lithostratigraphic formation outcropping at the southern margin of the Gediz Graben and represents the first and oldest sedimentary unit of the basin. This formation outcrops only in the eastern part of the study area, and particularly in proximity of the town of Alaşehir. According to Çiftçi & Bozkurt (2009a), this formation is composed by two interdigitating members, the coarser Evrenli Mbr. and the finer Zeytinçayi Mbr.

In the study area, the Evrenli Mbr. outcrops in the area around the Evrenli village (to the south of the town of Alaşehir); its base is represented by well-cemented, unsorted and reddish matrix-supported conglomerates (Fig. 4e). In this part the clasts are from millimetric to metric in dimension and range between angular to sub-rounded, with a sandy matrix. The upper part of this member is mainly composed of stratified sandstones, pebbly sandstones and minor siltstones with parallel and convolute laminations, locally associated with fluid expulsion structures (Fig. 4d). Pebbles are always derived from metamorphic rocks, mostly gneiss, schists, quartzite and marble. The general trend of this member seems to be fining-upward.

The finer Zeytinçayi Mbr. outcrops extensively to the north and to the south of the Osmaniye village, to the SW of the town of Alaşehir. This member is mainly represented by alternations of well-bedded, grayish-to-yellowish, finely laminated clayey siltstones (Fig. 4b), organic shales and silty sandstones. In the finer-grained layers, vegetal fragments and oxide nodules (Fig. 4c) are quite frequent. The coarser sandy layers generally show an internal normal gradation.

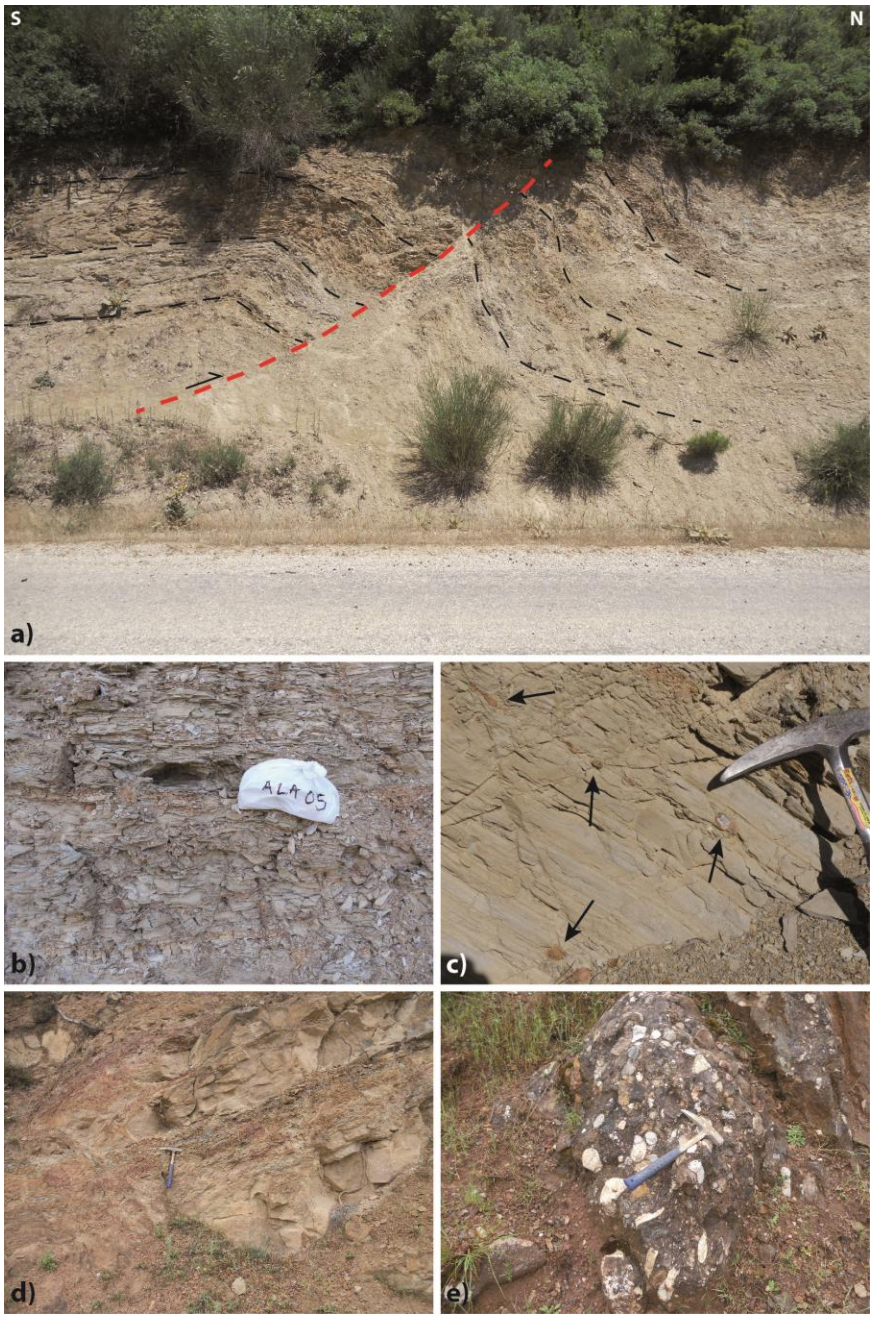

Figure 4: *Outcrop pictures showing some characteristic features of the Alaşehir Fm. a) Meso-scale folds and minor thrust fault in the Zeytinçayi Mbr.; these structural features are confined inside this member (see text for further explanations). b) Highly foliated paper-shales in the Zeytinçayi Mbr. c) Oxides nodules (indicated by black arrows) in laminated silts of the Zeytinçayi Mbr. d) Well stratified alternation of sandstones and siltstones layers in the Evrenli Mbr. e) Well cemented conglomerate in the Evrenli Mbr. (note that all the clasts are derived from metamorphic lithologies).*

The upper limit of the Alaşehir Fm. is always marked by alternations of layers of yellowish stratified cross-bedded sandstones and pebbly sandstones, with dimension of pebbles

ranging between centimetric and decimetric (Fig. 5a). Occasionally and only in this upper portion, imbrication of the coarser component is detectable, pointing to a mean NE direction of the paleo-currents (even though this indication is not very clear).

The thickness of the Alaşehir Fm. is hardly detectable due to internal syn- and post depositional faulting (Fig. 4a), but its maximum thickness in outcrop should not exceed 200m.

4.1.2. *Çaltilik Formation*

The Çaltilik Fm. conformably overlay the deposits of the Alaşehir Fm. and outcrops extensively along all the southern margin of the study area, with major differences between the Salihli and the Alaşehir areas.

The base of this formation outcrops only in the Alaşehir area, particularly near Soğukyurt, Osmaniye and Çaltilik villages, and is represented by an irregularly bedded, decametric thick, grayish-to-yellowish limestone interval (Fig. 5). The limestone sequence consists of micrtitic matrix wake-stones and minor pack-stones, rich in extraclasts and bioclastic fragments, with a minor presence of well-preserved bioclasts, such as foraminifera and ostracod shells. To the top, the limestone gradually pass to continental red sandstones layers, with an alternations of decimetric calcareous layers and metric red arenaceous layers with calcareous cement (Fig. 5d and 5e). The total thickness of this limestone interval does not exceed few tens of meters.

In the Alaşehir area, above the limestone interval, this formation follows with mainly sandy layers with muddy matrix and minor gravelly intervals, with sedimentary structures such as horizontal lamination and low-angle cross-lamination. These layers are generally poorly sorted and polymictic, concerning the nature of the clasts, with components derived from the Menderes Massif's metamorphic lithologies. Upward, in this sector, this formation show a coarsening-upward trend, passing from mainly arenaceous deposits to mainly matrix-supported conglomeratic red layers with sandy/silty matrix (Fig. 6a and 6b); in this upper part, outcropping extensively on the eastern flank of the Cumhuriyet/Dereköy valley, the clasts are generally sub-rounded (from rounded to sub-angular), range in dimension from gravel to boulder and are still derived exclusively from metamorphic lithologies. Clasts' imbrication suggest a NNE directed transport during the deposition of this formation. In this area, it is not

possible to estimate the total thickness of the Çaltilik Fm., but the exposed portion is around 400m at its maximum.

Figure 5: *Outcrop pictures showing some characteristic features of the limestone at the base of the Çaltilik Fm. a) Stratigraphic limit between stratified sandstones and conglomerates of the Alaşehir Fm. (below) and the irregularly stratified limestone at the base of the Çaltilik Fm. (above); the red circle show the location of sample 10a characterized by an upper Tortonian shallow marine faunal assemblage (Section10, between Soğukyurt and Kara Kirse villages; see text for further explanations). b) Regularly bedded facies. c) Irregularly bedded facies. d) and e) Uppermost part of the limestone interval with decimetric limestone strata (indicated by black arrows) alternating red sandstone layers.*

In the Salihli area the red clastic deposits of the Çaltilik Fm. lay directly on top of the Gediz Detachment's surface, but the calcareous layer at the base of this formation is not present in outcrop; contrastingly with what observed in the Alaşehir area, here these deposits show a fining-upward trend. The lower and coarser member is well exposed to the S of the Acidere village, right at the footwall of the MF1 fault (see below), and consists of poorly sorted, mainly conglomeratic, matrix supported, red layers with minor silty/sandy layers (Fig. 6c and 6d); the clasts, always related to the Menderes metamorphic basement, are angular or sub-angular, with dimensions from centimetric to decimetric. The upper part of the formation is characterized by a marked decrease in the mean grain-size and is represented by mainly arenaceous red layers, sometimes with gravel intercalations, and minor siltstone/mudstone layers (Fig. 6e and 6f); cross-laminations are characteristic of arenaceous layers, while fine-grained layers might preserve parallel laminations. When visible, imbrication of clasts suggest a NNE direction of sediment transport during deposition of this formation. Also this area it is not possible to estimate the whole thickness of the Çaltilik Fm., but the exposed section reaches a maximum value of about 800m.

Because clear reference levels (e.g. volcanic layers, biochronologically constrained levels, etc…) in the Çaltilik Fm. are lacking, there is not the possibility to make straight-forward correlations between the portions of this formation outcropping in the eastern and western sector of the study area. We suggest, dubitatively, that the higher and coarser deposits outcropping in the eastern sector might be correlated with the lower and coarser part outcropping in the western sector (see Fig. 3); this would mean that in the Alaşehir area mainly the older portion of the Çaltilik Fm. is exposed, whereas in the Salihli area only the upper part of the formation is outcropping.

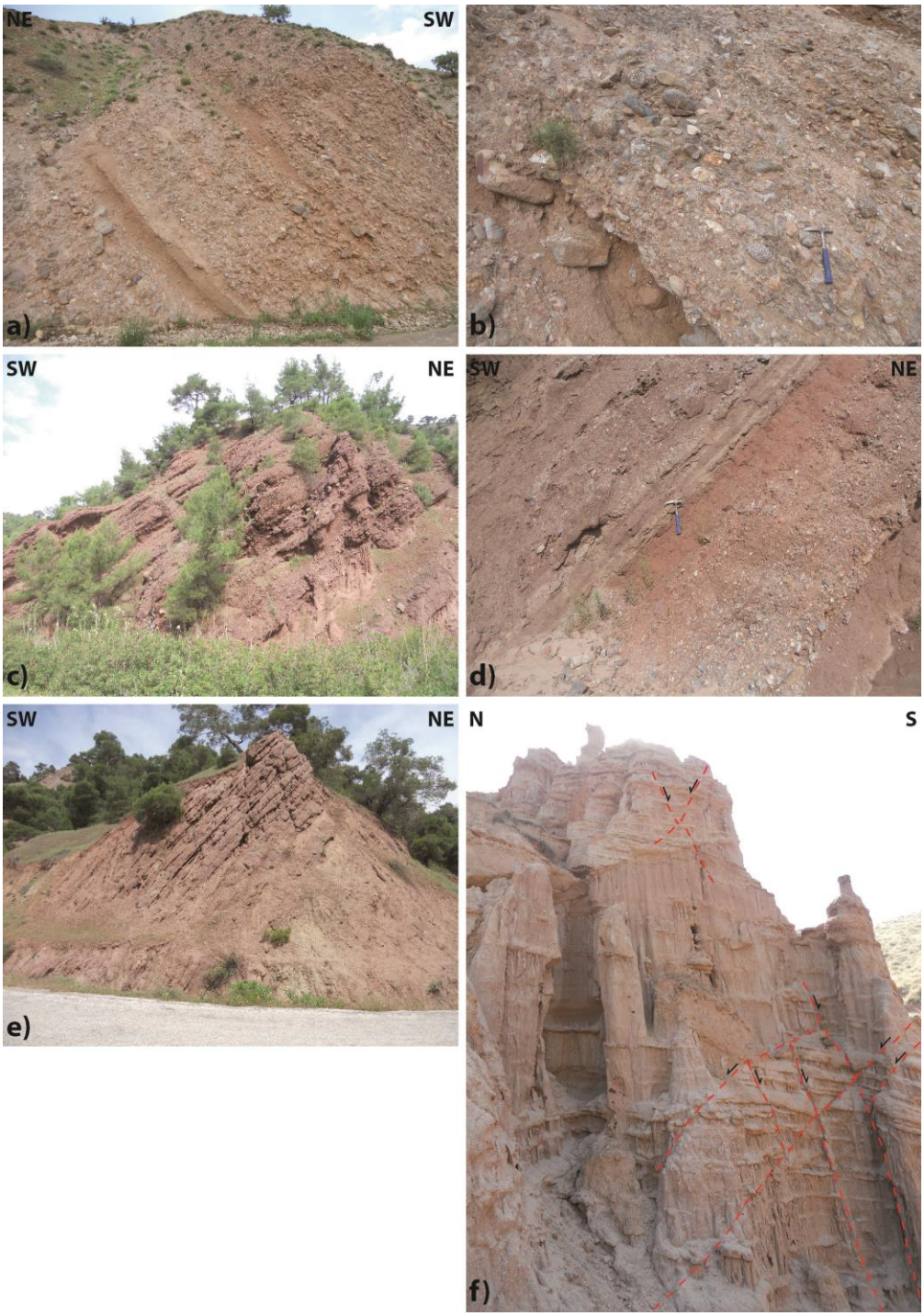

Figure 6: *Outcrop pictures showing some characteristic features of the Çaltilik Fm. a) and b) Conglomerate and sandstone layers of the lower part of the formation outcropping in the eastern part of the study area (Alaşehir area). c) and d) Conglomerate and sandstone layers of the lower part of the formation outcropping in the western part of the study area (Salihli area). e) Sandstone layers in the upper part of the formation. f) High-angle conjugated faults system in sandstone layers in the upper part of the formation (with typical spire-like erosional morphology).*

4.1.3. *Gediz Formation*

The transition to the overlaying Gediz Fm. is seldom visible in outcrop. It is not straight, but is represented by a gradual change in the color of the upper deposits of the Çaltilik Fm., that gradually pass from light red to grayish/yellowish moving up-section. This relationship between the two formations is clearly visible approaching to the Yagmurlar village, moving from N to S (Fig. 2).

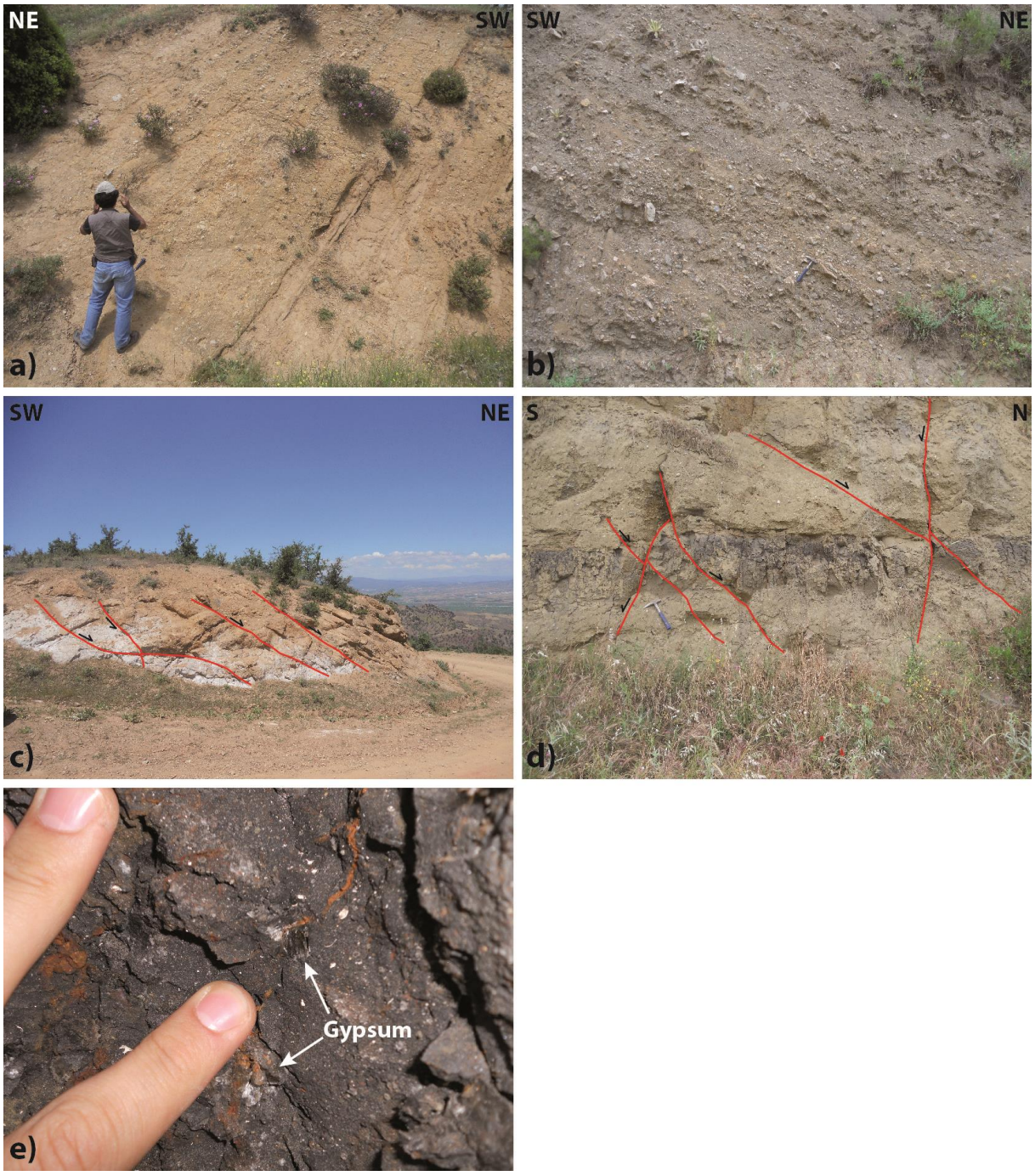

Figure 7: *(on the previous page) Outcrop pictures showing some characteristic features of the Gediz Fm. a) Finer-grained (sandstones and minor conglomerates) lower part of the formation. b) Higher-grained (conglomerates and minor sandstones) upper part of the formation. c) and d) High-angle conjugated faults system in the lower part of the formation. e) Gypsum crystals and shell fragments in an organic matter-rich shale layer in the lower part of the formation.*

In general, the Gediz Fm. shows an overall coarsening-upward trend. The lower part is more fine-grained and mainly represented by yellowish/brownish, cross-bedded, sandy and silty layers with gravel intercalations (Fig. 7a, 7c and 7d); pebbles are generally well sorted, centimetric to decimetric in dimension, rounded to sub-rounded and derive only from metamorphic lithologies of the Menderes bedrock. In the very lower part of this formation, also decimetric layers of organic matter-rich dark shale with ostracods and gastropods fragments are present (well exposed right to the S of the town of Salihli) (Fig. 7d and 7e). The upper part of this formation is dominated by yellowish/brownish matrix supported conglomerates, intercalated with minor sandy and silty layers. Clasts are sub-rounded to sub-angular and still derived exclusively from the metamorphic basement; imbrication of the clasts show a variable direction of the flow direction, ranging between NE and NW. No major differences in the Gediz Fm. where observed between the western and the eastern sector of the study area. The thickness of this formation is hardly detectable, but should exceed 400m.

4.1.4. *Kaletepe Formation*

The overlaying Kaletepe Fm. is the highest and youngest formation of the pre-modern Gediz Graben sedimentary fill. It outcrops to the S of the Yeşilkavak and Köseali villages, right at the footwall of the active fault presently bounding the alluvial plain (MF2) and unconformably overlay the older formations (Fig. 8a). It is represented by brownish, mainly conglomeratic, poorly-bedded deposits with a silty matrix. In this formation the sub-rounded to sub-angular clasts are derived not only from the Menderes metamorphic bedrock, but also from the underlying Çaltilik and Gediz Fm. (Fig. 8c and 8d), thus suggesting that at the time of the deposition of this formation the older basin fill was already exhumed and undergoing erosion. In this deposits it was not possible to recognize any imbrication of the coarser component.

In outcrop, we observed only a small portion of the Kaletepe Fm., which is less than 100m thick. Previous studies (e.g. Çiftçi & Bozkurt, 2009a; Oner & Dilek, 2011) suggested that this formation might be thicker.

Figure 8: *Outcrop pictures showing some characteristic features of the Kaletepe Fm. a) Stratigraphic erosional contact between the Gediz Fm. (below) and the Kaletepe Fm. (above). b) Gediz Detachment-derived pebble (indicated by black arrow). c) and d) Neogene sediments-derived pebbles (indicated by black arrows). e) Dextral strike-slip fault with associated negative flower structure separating Kaletepe Fm. deposits (to the NE) from Gediz Fm. deposits (to the SW) at the northern termination of the Göbekli valley.*

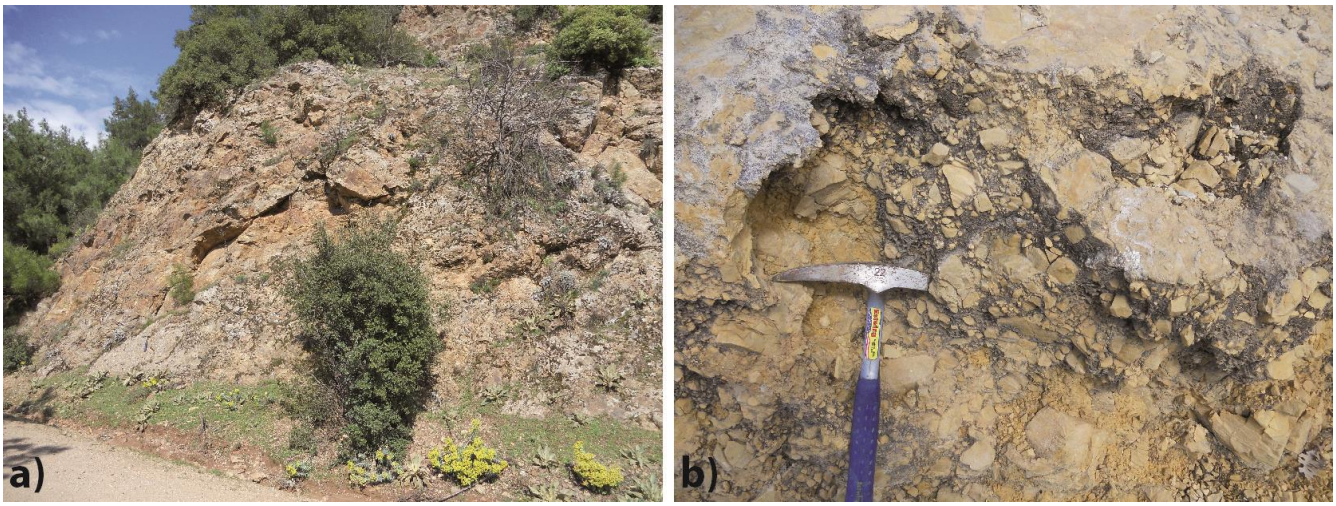

Figure 9: *Outcrop pictures showing some characteristic features of the Cataclastic Breccia associated to the Gediz Detachment at the large- (a) and meso-scale (b).*

4.2. *Micropaleontological analyses*

Among the 18 shale and silt samples collected in the Alaşehir Fm., Çaltilik Fm., Gediz Fm. and Kaletepe Fm., only sample GED_SAL, from the lower Gediz Fm., yielded some fossil remains, while all the others were sterile. Sample GED_SAL was collected in a ~30cm thick layer of organic matter-rich dark shale, with vegetal remains, shell fragments and gypsum crystals embedded in the matrix, in the lower part of the Gediz Fm., right at the S of the town of Salihli (N 38°28'15.5'', E 028°08'29.0'') (Fig. 7d and 7e). The outcrop is cut by a number of small-offset conjugate faults (Fig. 7d). The stratigraphic level of this layer should be, in our opinion, more or less the same of the one reported by Emre (1996) as bearing Dacian (Mio-Pliocene boundary) continental gastropods near the village of Yagmurlar (~20Km to the SE). In sample GED_SAL some ostracod shells, entire or in fragments, and some gastropod fragments have been found; unfortunately, all the well preserved ostracod shells represent only young specimens related to the genus *Candona*, only confirming the continental depositional setting.

We sampled the limestone at the base of the Çaltilik Fm between the villages of Soğukyurt and Kara Kirse (Section10) (Fig. 5a), where the limit with the lower Alaşehir Fm. is exposed, and many other outcrops along the eastern sector of the study area. After thin section analysis (Fig. 10), 3 samples from Section10 were disaggregated by sodium thiosulfate

pentahydrate, but only from one them (sample 10a) a small, but significant, number of ostracods and planktonic foraminifera was recovered (Fig. 11).

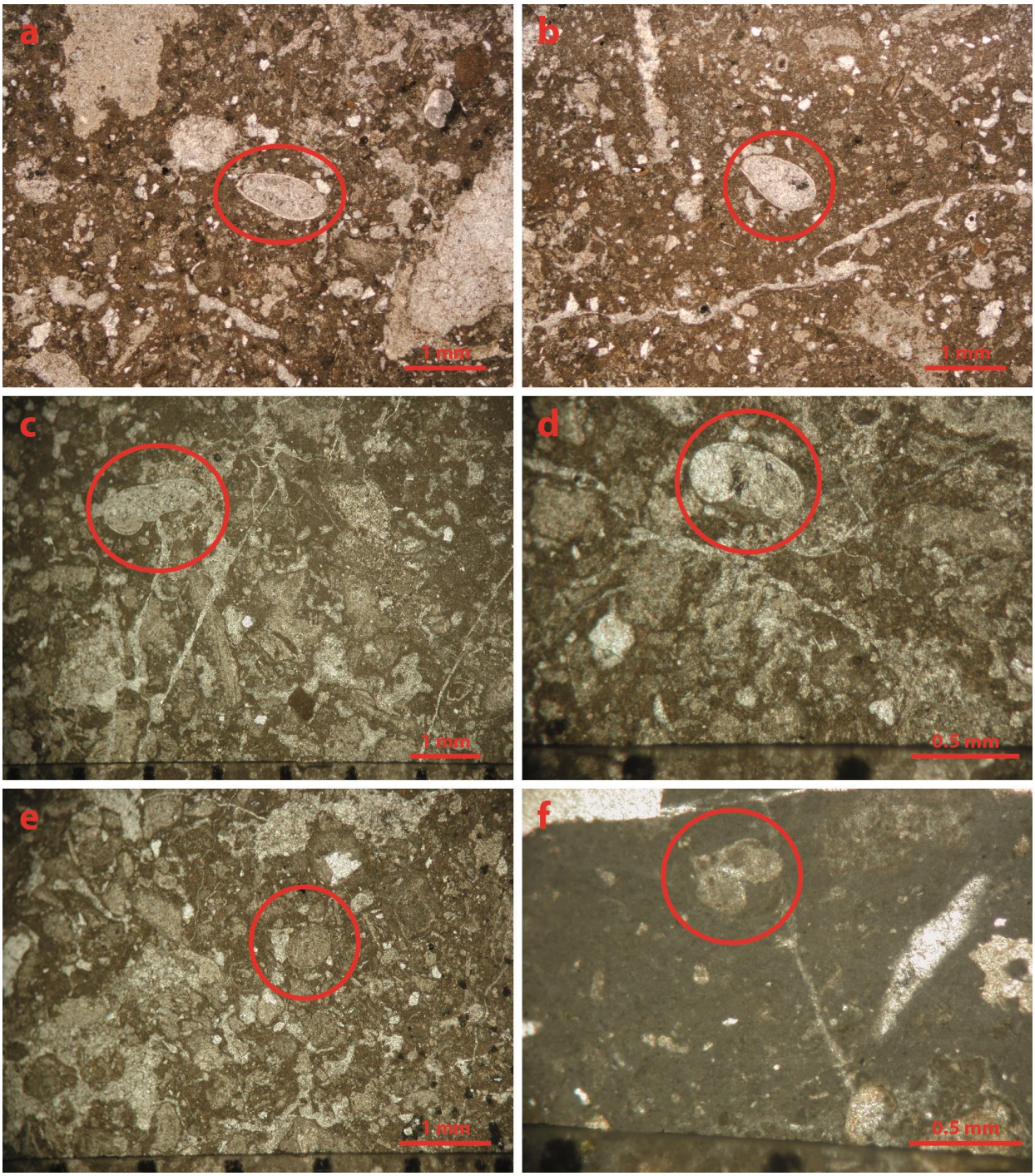

Figure 10: *Examples of thin sections of limestone at the base of Çaltilik Fm. from Section10 (between Soğukyurt and Kara Kirse villages) showing the evidences for microfossils' presence highlighted by red circles. In a) and b) ostracod shells; in c), d), e) and f) foraminifera.*

In sample 10a, 6 different species of surprisingly well-preserved marine planktonic Foraminifera have been recognised: *Orbulina universa* d'Orbigny (Fig. 11f), *Globigerinoides obliquus* Bolli (Fig. 11c and 11d), *Globigerinoides extremus* Bolli & Bermudez (Fig. 11b), *Globigerinoides quadrilobatus* (d'Orbigny) (Fig. 11e), *Globigerina bulloides* d'Orbigny (Fig. 11a) and *Globoturborotalia druryi* (Akers). In addition, also few ostracod remains have been found, among which a single right valve with preserved shell identified as *Pseudopsammocythere kollmanni* Carbonnel (Fig. 11g), and few internal mold of other undetermined ostracod species, dubitatively related to the genus *Cyprideis* (Fig. 11h).

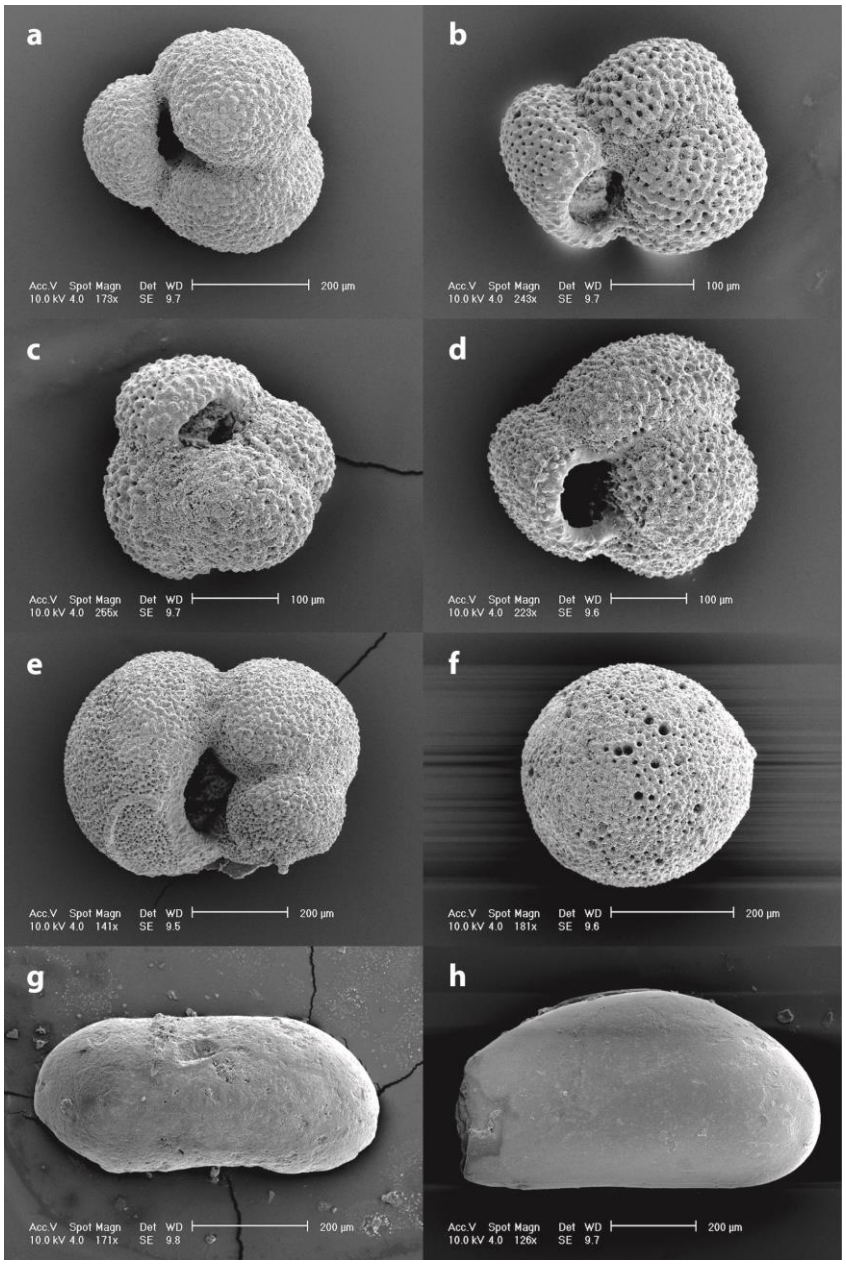

Figure 11: *SEM photographs of foraminifera and ostracods retrieved from sample 10a (Section10, Çaltilik Fm., between Soğukyurt and Kara Kirse villages) after sodium thiosulfate pentahydrate separation. a) Globigerina bulloides d'Orbigny, ventral view; b) Globigerinoides extremus Bolli & Bermudez, ventral view; c) and d) Globigerinoides obliquus Bolli, ventral view; e) Globigerinoides quadrilobatus (d'Orbigny), ventral view; f) Orbulina universa d'Orbigny, ventral view; g) Pseudopsammocythere kollmanni Carbonnel, right valve, external view; h) internal mold of ostracod, dubitatively related to the genus Cyprideis.*

Among all these species, only *G. extremus* and *P. kollmanni* seem to be biostratigraphically useful, with the latter also retrieving information on the possible bathymetry of the depositional setting of the limestone at the base of the Çaltilik Fm. *G. extremus* is distributed from the uppermost Tortonian (base of the MMi 12a biozone) and the lowermost Pleistocene (top of the MPl 5a biozone) (Iaccarino et al., 2007). *P. kollmanni* is an extinct Mediterranean marine species found in France, Austria, Italy and Crete. It has been arised by Carbonnel (1966) who firstly found it in Tortonian marine infra-littoral deposits of the Rhone Basin (France). Ascoli (1968) found this species in the Tortonian type-section of Rio Mazzapiedi (Italy) in association with other circa-littoral species. Sissingh (1972) found *P. kollmanni* in the Apostoli Section (Crete), in deposits attributed to an infra-littoral to circa-littoral environment and suggested this species to be confined in the *Cytherella vandenboldi* Zone, corresponding to the "Middle Tortonian" chronostratigraphic interval. Dall'Antonia & Bossio (2001) reported its occurrence in marine shelf deposits from the uppermost Langhian to the Serravallian in the Salentine Peninsula (Italy). Finally, Gebhardt et al. (2009) found this species in association with other circa-littoral species in deposits of the Austrian Molasse Basin, attributed to the lower Badenian (corresponding to the upper Langhian). In general, *P. kollmanni* seems to be distributed from the upper Langhian to the Tortonian in marine shelf deposits, from circa-littoral to external infra-littoral environments. The co-existence of *G. extremus* and *P. kollmanni* in the faunal assemblage point to a possible upper Tortonian age (MMi 12 biozone, i.e. 8.35-7.246 Ma) for the deposition of the limestone at the base of the Çaltilik Fm. (Fig. 12), possibly in a 50-150m deep marine shelf environment.

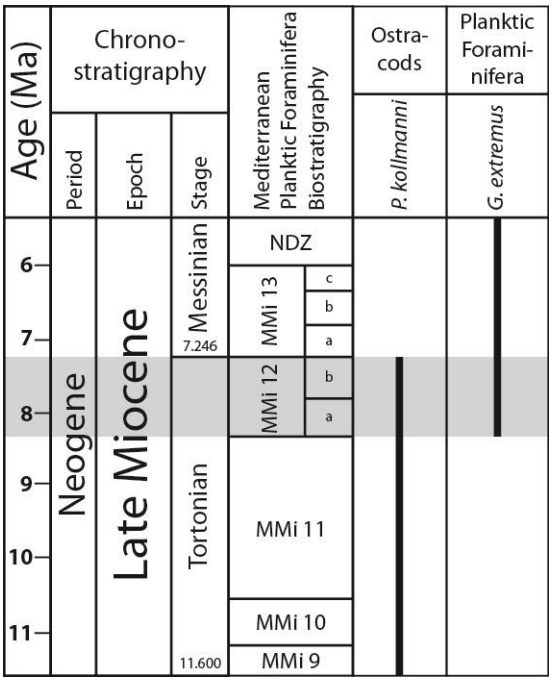

Figure 12: *Mediterranean biostratigraphic scheme for the Late Miocene with the distribution of biostratigraphically useful species recovered in sample 10a from Section10 (Çaltilik Fm., between Soğukyurt and Kara Kirse villages). The light-gray horizontal band show the proposed age interval for sample 10a (i.e. overlapping period for the distribution of G. extremus and P. kollmanni). Mediterranean planktic foraminifera biostratigraphy from Iaccarino et al. (2007). NDZ – nondistinctive zone.*

4.3. *Structural analysis*

Major differences exist in the structural pattern of the southern margin of the basin between the western (Salihli area) and eastern (Alaşehir area) sector of the study area, especially for what concerns the most external structures (Fig. 2 and Fig. 15).

4.3.1. *Structure of the basin margin in the Salihli area – The Gediz Detachment*

The Salihli area is morphologically dominated by the N-to-NE gently dipping Gediz Detachment Fault, that represents the southern margin of the basin in this sector (Fig. 2 and 13). This structure has been extensively described (e.g. Hetzel et al., 1995a; Seyitoğlu et al., 2000, 2015; Işik et al., 2003; Sarikaya, 2004; Çemen et al., 2005). It consists in a ductile-to-brittle shear zone with variable thickness that generally doesn't exceed ~100m; it can be defined as a mylonite with cataclastic overprint and ductile-brittle transition that gradually turns upward into a very fine grained ultra-cataclasite. Mineral composition is dominated by

quartz and feldspar, formed at the expense of a metaluminous/peraluminous granodioritic protolith (i.e. the Salihli Granodiorite).

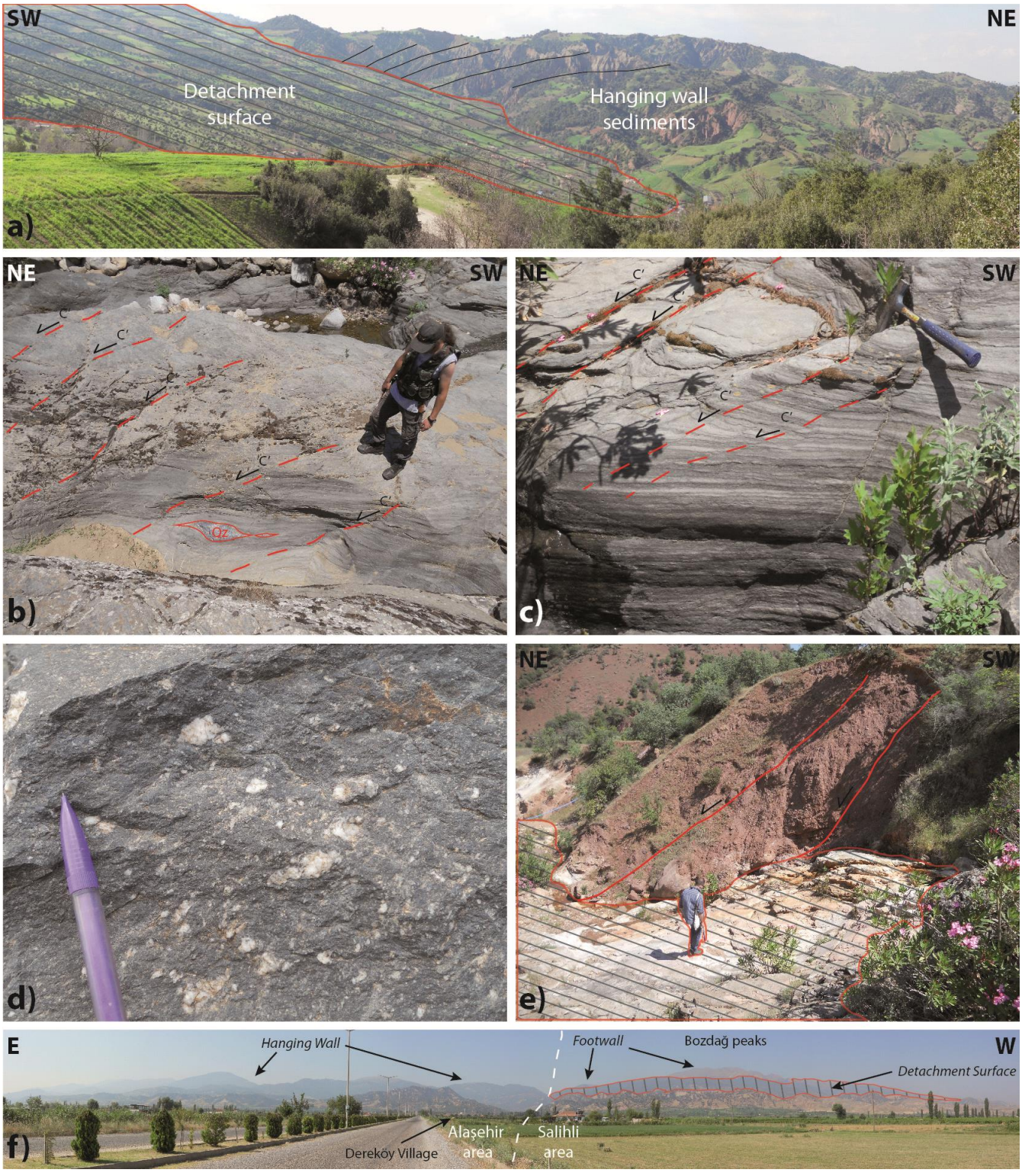

Figure 13: *(on the previous page) Outcrop pictures showing some characteristic features of the Gediz Detachment. a) Landscape view of the gently NE-dipping Gediz Detachment surface (to the left) with Neogene sediments at the hanging wall (to the right) tilted towards the SW. b) Large quartz porphyroclasts and C' planes cutting the mylonitic foliation in the upper ductile layer. c) C' planes cutting the mylonitic foliation in the upper ductile layer. d) detail of the ultracataclastic layer with macroscopic quarts fragments. e) High-angle brittle faults cutting the Neogene sediments rooting on the detachment surface. f) Landscape view of the southern margin of the Gediz Graben; on the right (W) the NE-dipping Gediz Detachment and its footwall (with the Bozdağ peaks), on the left (E) the Menderes metamorphic bedrock at the hanging wall of the detachment. The dashed white line in correspondence of the Dereköy valley marks the limit between the Alaşehir area (to the E) and the Salihli area (to the W).*

The Gediz Detachment shear zone is constituted by (from top to bottom): 1) an extremely fine-grained ultracataclastic dark layer with quartz and chlorite veins and, occasionally, macroscopic quartz fragments in its lower part with evidences for cataclastic flow (Fig. 13d); 2) a dark-grey strongly foliated (phyllonite-looking) mylonitic rock, with quartz porphyroclasts and foliation defined by micaceous minerals (Fig. 13b and c); 3) a brittle deformation dominated layer represented by a fractured granitoid (previously mylonitized) with quartz and chlorite veins and minor oxide and calcite mineralizations (namely, Chlorite Breccia); 4) a mylonitized granodioritic rock (gneiss) with brittly deformed feldspar porphyroclasts and foliation defined by stretched quartz, with microstructures like deformation bands and kink bands, with generally a top-to-the-NE/NNE sense of shear; 5) the undeformed Salihli Granodiorite (outcropping only between the Yeşilkavak and Göbekli valleys).

The dip of the detachment surface is gentle, between 10° and 30° (green box in Fig. 15). The stretching lineation mostly trend NNE, varying generally between N20° and N40°, with a sense of shear always top-to-the-NNE; an exception is represented by the easternmost outcropping area of the detachment surface (western side of the Cumhuriyet/Dereköy valley), where the direction of the stretching lineation turns abruptly to the E, with a mean direction around N90° (Fig. 15, station 15). The foliation of the mylonitic layers and the detachment surface itself dip on average to the NNE, but is folded by a gentle antiform and sinform folds with axis parallel to the stretching direction on an overall convex-up detachment surface, thus defining a corrugated turtleback structure.

When visible, high angle normal faults on the hanging wall cutting the Neogene-to-Quaternary basin fill root into the detachment surface (Fig. 13e). Main syncline and anticline on the

hanging wall with axis almost parallel to the detachment's strike, possibly reflect the ramp-flat geometry of the detachment surface at depth (e.g. Gibbs, 1984) (Fig. 16 A-A', B-B' and C-C' cross-sections).

4.3.2. Structure of the basin margin in the Alaşehir area

Figure 14: *(on the previous page) Outcrop pictures showing some characteristic features of the gently NE-dipping brittle fault surfaces representing the most external structures bounding the southern margin of the basin in the Alaşehir area (eastern sector of the study area). a) and b) Outcrop evidence low-angle brittle fault surfaces at the Soğukyurt and Kozluca villages respectively. c) Minor low-angle brittle fault separating Menderes metamorphic rocks (at the footwall) from Çaltilik Fm. deposits (at the hanging wall). d) Landscape view of remnants of low-angle brittle fault surface (indicated by black arrows). e) and f) Details of brittle features associated to these low-angle surfaces.*

In the Alaşehir area the morphology of the southern margin of the basin is defined by NE-dipping normal faults with a step-like pattern (Fig. 2). The most external structure is represented by isolated remnants of a gently dipping (between 15° and 30°) fault surface (brown box in Fig. 15), with NE trending lineation, that separate the metamorphic rocks of the Menderes Massif at the footwall from the older formations of the Gediz Graben sedimentary fill (i.e. Alaşehir Fm. and Çaltilik Fm.); contrastingly with what observed at the footwall of the Gediz Detachment, here no ductile fabric related to a top-to-the-NE extensional shear can be observed but only brittle features (such as fractures, slicken lines and cataclasite; Fig. 14e and f). Here the surface is cut and dislocated by high-angle normal faults, which is not the case for the Gediz Detachment. Moreover, for the determination of the sense of shear, no kinematic indicators were find in outcrop in the field, nor in thin sections oriented parallel to the X-Z plane of the strain ellipsoid.

In the Menderes metamorphic units at the southern margin of the graben, foliation always dips between S and SW (purple box in Fig. 15), with a stretching lineation parallel to the one observed on the mylonitic detachment shear zone, but with sense of shear on both directions.

4.3.3. *High-angle brittle faulting and syn-sedimentary faults*

To the N of the Gediz detachment a series of parallel high angle normal faults are clearly visible in outcrop, with dipping angles generally decreasing from N to S and ranging from ~45° for the more external to ~70° for the more internal structures (yellow box in Fig. 15). Among all these structures it is possible to identify two major normal faults that affect the whole length of the study area (Fig. 2): 1) the southernmost (hereafter MF1) separates an area where mainly outcrops the Gediz Fm., to the N (at the hanging wall), from an area where almost only the older deposits outcrop, to the S (named Master Graben Bounding Fault in Çiftçi & Bozkurt, 2009a,b, or Acidere Fault in Öner & Dilek, 2011) and has a direction between

NNE and NE, a medium dip of ~45° and a normal kinematics; 2) the northernmost (hereafter MF2) is the active normal fault bounding the present-day alluvial plain, separating the Quaternary deposits to the N (hanging wall) from the outcrop area of the ancient basin fill to the S (footwall).

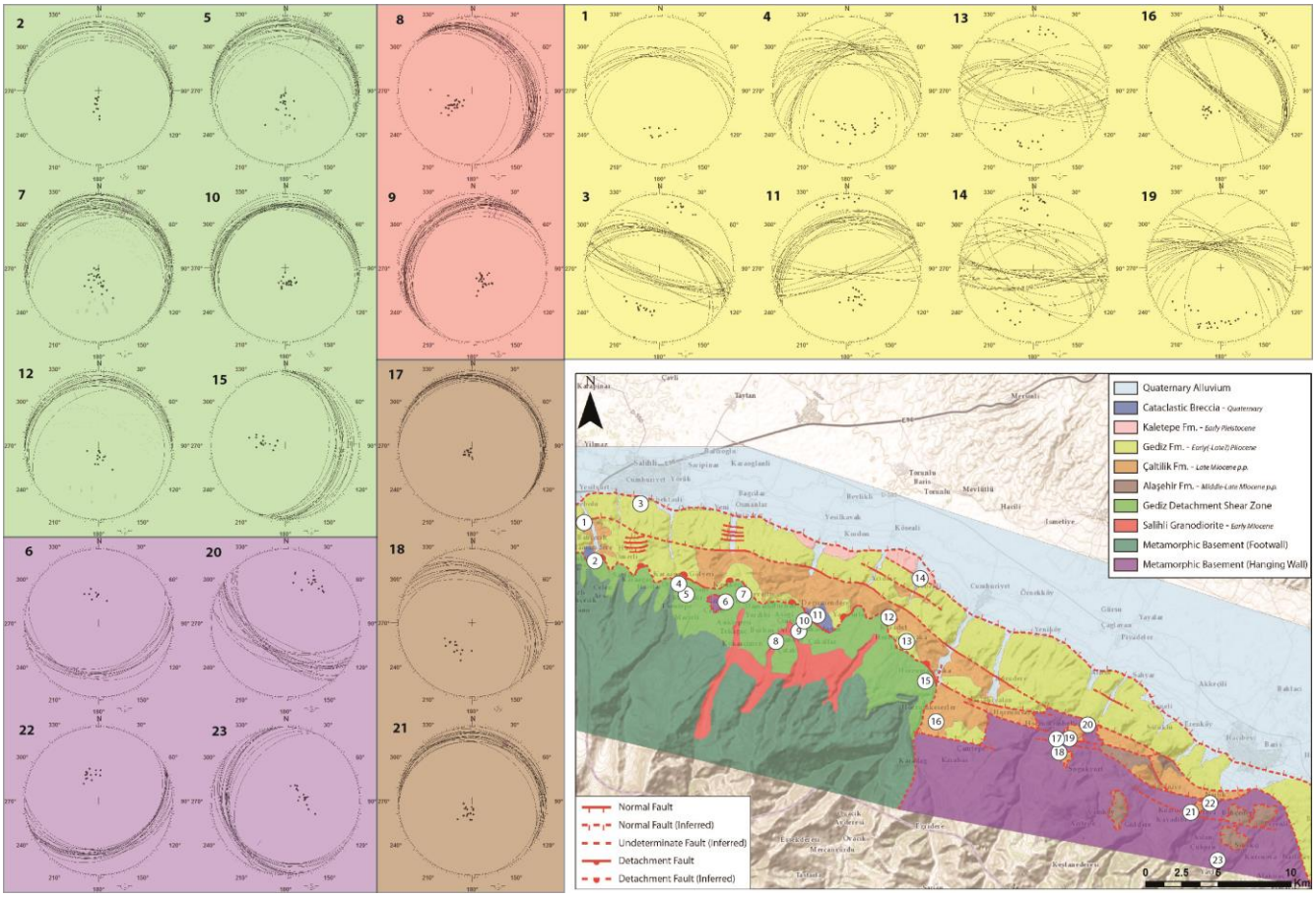

Figure 15: *Lower hemisphere stereoplots of measured faults and other structural features in the study area. Numbers of the stereoplots refer to the number of the measure station indicated in the map. Stereoplots in the green box are related to measurements on the Gediz Detachment fault surface; stereoplots in the purple box are related to measurements of foliation in the Menderes metamorphic bedrock; stereoplots in the red box are related to measurements of foliation in the Salihli Granodiorite; stereoplots in the brown box are related to measurements of low-angle brittle normal fault surfaces in the eastern part of the study area; stereoplots in the yellow box are related to measurements of high angle brittle faults cutting both the basin sedimentary fill and the metamorphic bedrock. See text for further explanations.*

In between these two major faults and to the S of the first-one in the Alaşehir area, a large number of minor and segmented normal faults exists; all these structures define a step-like morphology for the southern margin of the graben already described in previous studies

(Koçyiğit et al.,1999; Seyitoğlu et al., 2002; Bozkurt and Sözbilir, 2004; Ciftci & Bozkurt, 2009b).

In the western part of the study area, to the S of the town of Salihli and of the Yenipazar village, it is possible to observe post-sedimentary E-W trending domino faulting involving deposits of the Gediz Fm. at the hanging wall of the Gediz Detachment. The spacing between the faults bounding the tilted blocks is in the order of few hundreds of meters.

Evidences for syn-sedimentary fault activity are widespread. In the area close to the Evrenli village, right to the south of the town of Alaşehir, it is possible to observe syn-sedimentary faults confined in the coarser member of the Alaşehir Fm. (Evrenli Mbr.), that show a variable offset that decrease up-section.

In the finer member of the Alaşehir Fm. (Zeytinçayi Mbr.), especially in the area between Güldere and Osmaniye villages, many deformation structures trending parallel to the basin's margin can be observed, such as anticline and syncline folds (from sub-metric to decametric in amplitude), normal faults and north-verging thrust faults (Fig. 4a).

Syn-sedimentary fault activity involved all the units, as shown by growth strata (e.g., Çaltilik Fm. and in the Gediz Fm.) and from synthetic faults sealed by the same unit. Conjugate normal fault systems in the Çaltilik Fm. and in the Gediz Fm. are generally rotated (Fig. 6f, 7c and d). At places, it is possible to observe an slight increase in thickness of strata the Gediz Fm. close to MF1.

Rare evidences for recent strike-slip fault activity are present on the southern margin of the alluvial plain. At the northern end of the Göbekli valley, ~1 Km to the N of the Göbekli village, an almost vertical E-W trending fault plane is visible in outcrop, separating deposits of the Kaletepe Fm. to the N from deposits of the Gediz Fm. to the S (Fig. 8e); almost horizontal direction of slicken-lines and kinematic indicators point to a dextral strike-slip movement for this fault plane. Moreover, a series of high-angle fault planes dipping toward the strike-slip fault plane from both sides, with kinematic indicators pointing to an oblique-slip to dip-slip normal movement, defines a few-meters wide negative flower structure associated to the main strike-slip fault.

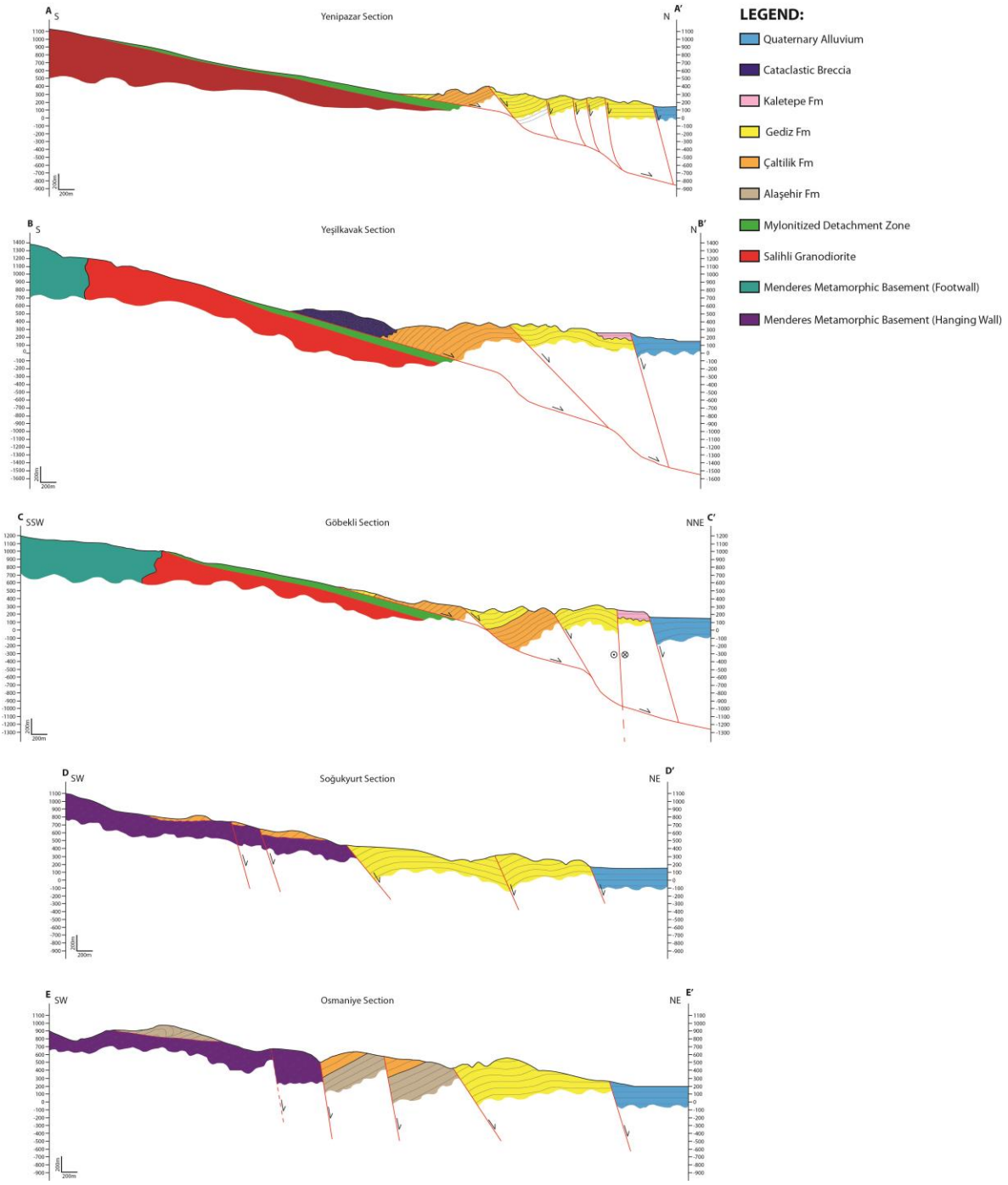

Figure 16: *Geological cross-sections across the southern margin of the Gediz Graben (see Fig. XXX for the location of each cross-section). High-angle brittle faults cutting the basin sedimentary fill root on the detachment, rather than cross-cutting it. High-angle brittle faults in the eastern part of the study area cut and displace low-angle brittle fault surfaces. Major sinforms and antiforms in sediments at the hanging wall of the detachment, with axis almost parallel to the detachment's strike, are interpreted as reflecting the ramp-flat geometry of the detachment surface at depth.*

5. DISCUSSION

5.1. *Insights from micropaleontological data*

Our micropaleontological data represent a new constrain on the age and the paleogeographic evolution of the Neogene extensional basins in SW Anatolia, and especially for the Gediz Graben. Our findings represent the first report of Neogene marine deposits in the Gediz Graben (and, in general, in the whole Menderes Massif area). Moreover, our biostratigraphic data gives a younger Middle-Late Miocene age for the formation of the Gediz Graben, with respect to the previosuly proposed Early-Middle Miocene ages (Cohen et al., 1995; Emre, 1996; Yazman et al., 1998; Koçyiğit et al., 1999; Yılmaz et al., 2000; Seyitoğlu et al., 2002; Purvis & Robertson, 2005a,b; Öner & Dilek, 2011). This new age is in agreement with borehole data interpretation (Çiftçi & Bozkurt; 2009a), and with detrital apatite fission track data (see Chapter 2, this work). The pluri-decametric thick limestone at the base of the Çaltilik Fm. are, as far as we could observe in the field, preceded and followed exclusively by continental deposits, thus representing the record of a short-lived marine episode in the evolution of the Gediz Graben; the end of this marine episode probably marks the limit between a first phase of the evolution of the basin, which was dominated by subsidence and increase of the accommodation space, and a second phase dominated by a pronounced uplift of the southern margin of the basin, producing a large sedimentary flux that filled the marine environment and led to “continentalization”, as suggested also by detrital apatite fission track data (Chapter 2, this work).

Considering a thickness of ~1000m for the Çaltilik Fm., and integrating our micropaleontological results with paleontological data by Emre (1996), who assigned a Dacian age (Mio-Pliocene boundary) to the Göbekli Fm. (that, in our interpretation based on field observation, can be correlated to the lower part of the Gediz Fm.) we obtain a Messinian sedimentation rate of ~500m/Ma. This is in agreement with what obtained from detrital apatite fission track studies (Chapter 2, this work).

The sampled limestone deposit is presently located at an altitude of ~760 m a.s.l.; considering a bathymetry of -100 ± 50 m for the depositional environment of these deposits, we could estimate a mean topographic uplift of 860 ± 50 m for the southern margin of the

basin in the Alaşehir area since the upper Tortonian, with a mean uplift rate of 107.5 ± 6 m/Ma. Since after the deposition of these limestone the basin underwent major subsidence and sedimentation, it is likely that the larger part of the topographic uplift occurred with/after the major quaternary tectonic reorganization of the basin margin with a much higher uplift rate.

5.2. Considerations on the Neogene-to-Quaternary basin fill

The distribution of the Neogene-to-Quaternary basin fill in outcrop, as described above, show then major differences between the Alaşehir and the Salihli areas. The older deposits (i.e. the Alaşehir Fm. and the lower part of the Çaltilik Fm.) outcrop only in the eastern sector, while in the western sector the older outcropping sediments are represented by the middle part of the Çaltilik Fm. This setting might be explained in two different ways. In the first model, the depositional setting was not homogeneous and therefore some sediments deposed only on the eastern side of the basin (e.g. Yilmaz et al., 2000; Çiftçi & Bozkurt, 2009a, 2010). For the other possible model the older deposits were deposited in the whole Gediz Graben area but are now buried below the younger sediments in the Salihli area; in this scenario, the Alaşehir Fm. and the limestone at the base of the Çaltilik Fm. might also have been exposed in outcrop in the southernmost part of the western sector in the past (as nowadays in the eastern sector), but have been eroded earlier because of a larger uplift of the basement in this sector with respect to the Alaşehir area. In our opinion this second scenario is more likely, because there are different indications pointing in this direction, like the structural relationship between the two sectors, with the ductile-to-brittle Gediz Detachment shear zone that has been exhumed (and probably uplifted) only in the Salihli area. The same indication is furnished by detrital apatite fission-track data (Chapter 2, this work), that revealed a younger exhumation event of the basement in the western sector (less than 5 Ma) than did not affect the eastern sector.

The lithological differences between the Çaltilik Fm. and the Gediz Fm., with the notable exception of the basal limestone, are not relevant; both formations deposed mostly in a continental alluvial environment (Çiftçi & Bozkurt, 2009a; Öner & Dilek, 2011; this study), and the main difference for their division is based on color, with the older one showing a very distinctive red color and the younger one yielding a predominantly yellowish/brownish/greyish

coloration. The reddish color is probably due to syn-diagenetic oxygenated groundwater circulation (e.g. Walker, 1967; Van Houten, 1973; Mücke, 1994) and this may be not uniform and the transition between the two units is indeed a gradual transition. The boundary between these two formations is then variable and possibly not representing an isochronous surface.

5.3. Considerations on the structural pattern

The low-angle fault surface at the southern margin of the basin in the Alaşehir area has been previously interpreted as the eastern prosecution of Gediz Detachment (e.g. Çiftçi & Bozkurt, 2009a; Seyitoğlu et al., 2015). In our interpretation this is unlikely, because this sector of the basin's margin (and all the outcropping structures therein) belongs to the hanging wall of the Gediz Detachment, as suggested by direction of the detachment's surface and of the stretching lineation at the eastern termination of its outcropping area (i.e. western side of the Cumhuriyet/Dereköy valley), thus representing an higher crustal level with respect to the mylonitic detachment. This may explain the lack of a top-to-the-NE extensional ductile mylonitic fabric. The structure observed may be also related to older deformational phase, possibly reactivated in extension, rather than being purely related to the Miocene extensional phase.

The contractional structures observed in the Alaşehir Fm., confined in these deposits, were already described and were interpreted as related to a N-S oriented compressional phase (Çiftçi & Bozkurt, 2008), or as being extension-related (Şengör & Bozkurt, 2013). In our opinion, it is likely that those apparently compressive structure in the Alaşehir Fm. have formed in an extensional setting, possibly due to large-scale slumps in unconsolidated deposits. This hypothesis is supported by the fact that those structures are spatially and stratigraphically confined.

For what concerns the activity of MF1, field evidences point to a syn-sedimentary phase of activity for this structure during the deposition of the Çaltilik Fm. and Gediz Fm., but it is likely that it has been active also after the sedimentation of this formations, because the slight increase of thickness of the strata does not fit with the large displacement accommodated by this structure (more than 1000 m).

5.4. Evolution of Neogene-to-Present extensional process revealed by schematic 2D across-strike reconstruction of the activity of the Gediz Detachment

In order to try to quantify the amount of extension accommodated by the Gediz Detachment, we produced a schematic 2D across-strike reconstruction through the western sector of the Gediz Graben (Fig. 17). In agreement with previous interpretation (e.g. Öner & Dilek, 2011; Buscher et al., 2013), we consider that the Gediz Detachment originate with a dip similar to the present day one. For the sediment thicknesses used in this reconstruction we integrated our field observations with subsurface data interpretation by Çiftçi & Bozkurt (2009a, 2010); in this way we obviously introduced some minor approximations, but these don't affect the order of magnitude of the results.

For the explanation of the general geologic evolution represented in Fig. 17 we invite the reader to refer to section 5.5 (Evolutionary model).

In our reconstruction the dip of the Gediz Detachment is constant through-time, hence all the rotations are confined at the hanging wall of the detachment. The brittle faults at the southern margin of the basin controlling most of the sedimentation root on the ductile detachment; these developed at high angle (60-70°) and then progressively rotated during their activity bordering titled blocks above the detachment surface.

In this reconstruction a considerable amount of material is removed below the base of the basin at the base of the fault-bounded blocks on top of the detachment during their rotation and the progressive exhumation of the detachment surface (shaded areas above the detachment in Fig. 17b, c, and d show the amount of material removed with respect to the following step in the reconstruction); it is likely that this material have been involved in the deformation process, in both the ductile and cataclastic processes, leading to hanging wall thinning in proximity of the detachment surface. Part of the material might have been removed downward in a ductile or ultracataclastic flow favored by the high thermal anomaly and intense fluid circulation, whereas some other might have been displaced toward the surface by the cataclastic process and eventually involved in the sedimentary process, as suggested by the Cataclastic Breccia deposits found in proximity of the presently outcropping detachment surface.

Between the last two steps of our reconstruction blocks 1 and 2 at the hanging wall of the detachment are much more uplifted than the rest of the basin margin and are thus removed by erosional processes (the area with horizontal lines overlay to the left in Fig. 17b show the amount of material uplifted above the detachment and eroded between these last two steps).

After the restoration to the pre-stretching conditions in this model we ended up with an intrusion depth for the Salihli Granodiorite between ~3.5 and ~7 Km; this result is in agreement with the thermobaric modeling of the emplacement conditions of this intrusion, which have occurred at very shallow crustal depths at pressure lower than 2 kbar (Erkül et al., 2013; Chapter 3, this work), causing a relevant upward migration of the ductile-to-brittle transition.

Our reconstruction show that the total amount of stretching accommodated by the Gediz Detachment and the faults at its hanging wall during their activity, producing the ~3 Km deep and ~20 Km wide Gediz Graben and exhuming the detachment itself, has been relatively small (~7.2 Km) during the last ~15 Ma. Moreover, it is quite evident that the exhumation process is much more efficacious by high-angle normal faulting, rather than by low-angle detachment faulting. In fact, the exhumation has been much more pronounced since the activation and the rotation of the high-angle normal faults at the hanging wall of the Gediz Detachment.

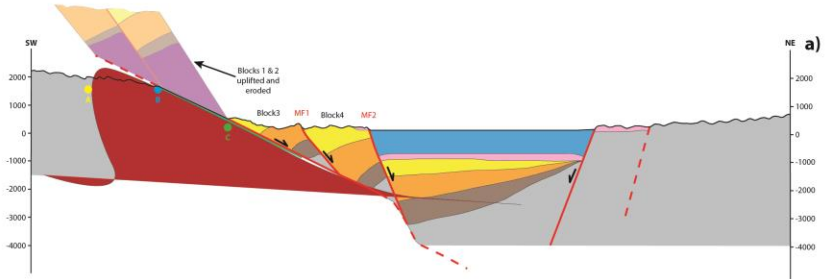

Symmetric graben (Pleist.-Present)

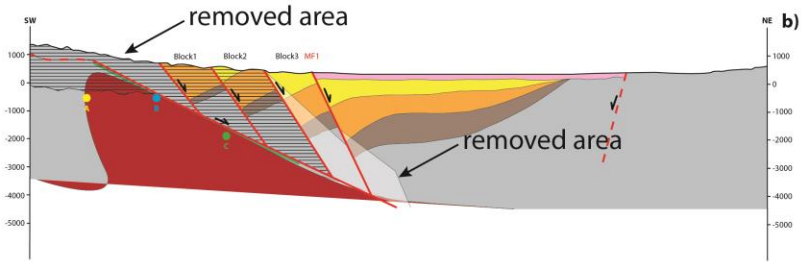

Fast exhumation phase (Late Pliocene-Early Pleist.)

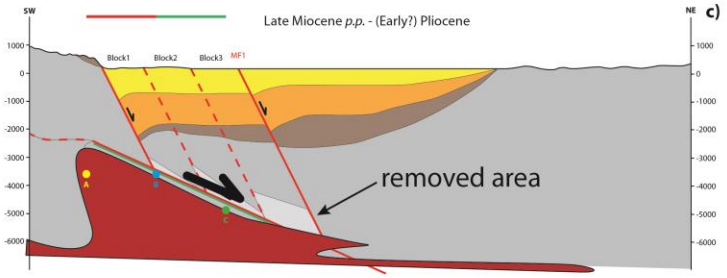

High-angle normal faults activation (Late Miocene-Early Pliocene)

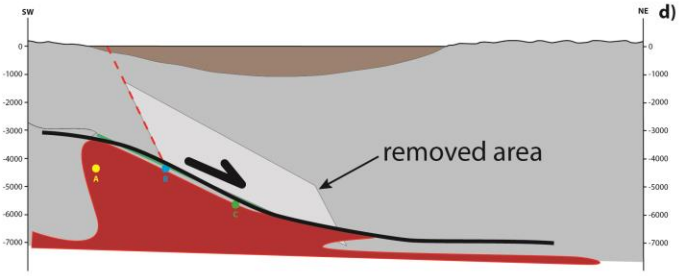

Localization of detachment along the BDT and subsidence of ramp basin (Middle Miocene)

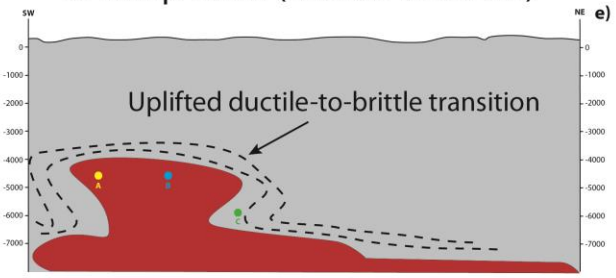

Upwarping of the regional BDT by magmatic emplacement (Early Miocene)

Figure 17: *2D across-strike reconstruction of the western part (Salihli area) of the study area, showing the Neogene-to-present evolution of this sector of the basin. Orange line on the left of each step-section represents the amount of extension accommodated since the previous step represented in the underlying section; points A, B and C (yellow, blue and green respectively) are reference point with fixed relative position at the footwall of the Gediz Detachment used to show the amount of horizontal displacement after each step; shaded areas above the detachment in b), c) and d) represents the amount of material removed during the following stage by possible by the ductile and/or cataclastic process (hanging wall thinning); the area with horizontal lines overlay in b) (blocks 1 and 2) show the amount of material uplifted above the detachment surface and eroded before the following stage (a); blocks 1 and 2 are represented shaded in a) to show their possible position if not eroded.See text for further explanations.*

5.5. *Evolutionary model*

By integrating our field observation and paleontological data with the very large amount of published data on the Gediz Graben and on the Gediz Detachment, we could elaborate the Neogene-to-Present schematic evolutionary model reported in Fig. 18.

Stage 1) The ductile deformation on the Gediz Detachment at shallow depths started around 14.6 Ma, following the intrusion of the Salihli Granodiorite at ~17 Ma (see Chapter 3, this work). It is likely that the formation of the basin at the surface and the deposition of the Alaşehir Fm. started contemporaneously with the ductile activity of the detachment at depth (i.e. Middle Miocene; Fig. 18a), as suggested by volcanoclastic borehole evidences (Çiftçi & Bozkurt, 2009a) and by detrital apatite fission track data (Chapter 2, this work), rather than in the Early-Middle Miocene as previously thought on the base of palynological evidences (İztan and Yazman, 1991; Seyitoğlu and Scott, 1992; Ediger et al., 1996; Seyitoğlu et al., 2002). Since the original relationship between the first deposits of the basin and its margin are no more visible in outcrop, it is not easy to reconstruct the geometry of the basin at the time of its formation. The lack of growing strata towards the south, seems to suggest that no major extensional faults was controlling the formation of the basin and the sedimentation of the Alaşehir Fm.; this might suggest that the sedimentation started in a sag-like depression that might have reflected the flat-ramp geometry of the Gediz Detachment at depth (e.g. Gibbs, 1984). This hypothesis is supported by the evidence that no major exhumation event was ongoing during this phase, according to detrital apatite fission track data (Chapter 2, this work).

Stage 2) The subsidence-dominated phase terminates with the upper Tortonian short-lived marine episode represented by the limestone at the base of the Çaltilik Fm. (Fig. 18b). In this phase the onset of a relatively shallow (50-150 m) marine environment is witnessed by the faunal assemblage identified in this study.

Stage 3) Starting from Messinian time, a major tectono-sedimentary reorganization occurs in the Gediz Graben (Fig. 18c). During this phase, at the southern margin of the basin an high-angle brittle normal faults system is clearly activated, controlling the sedimentation of the Çaltilik Fm. during Messinian and of the Gediz Fm. during (Early?) Pliocene, and definitely turning the basin in to a pronounced half-graben; this intense phase of tectonic activity is attested by a large number of syn-sedimentary faults cutting these formations. This fault system likely controlled also the relevant episode of exhumation and influx of sediments at the southern margin of the basin recorded by detrital apatite fission track (Chapter 2, this work), leading to the “continentalization” of the basin.

Stage 4) During (Late?) Pliocene-(Early?) Pleistocene the normal fault-bounded tectonic wedges placed between the Gediz Detachment and the MF1 started being exhumed at the footwall of this latter structure, leading to the exhumation of the previously deposited portion of the sedimentary sequence during the deposition of the Kaletepe Fm. (Fig. 18d); the stronger evidence for this mechanism is the fact that in the conglomeratic levels of the Kaletepe Fm. also sedimentary rocks-derived pebbles are present, contrastingly with respect to the older formation that were feed exclusively by metamorphic source rocks. Seismic reflection profile interpretation suggests that in this period the northern margin of the basin was activated, definitively transforming the geometry of the basin from half-graben into symmetric graben (Çiftçi & Bozkurt, 2009a, 2010).

Stage 5) The last exhumation event that involved only the southwestern sector of the study area led to the surface in this sector the Gediz Detachment and its footwall, including the Salihli Granodiorite (Fig. 18e). This event is clearly registered by fission track data (Gessner et al., 2001; Ring et al., 2003; Buscher et al., 2013; Chapter 2, this work) that revealed at the southern margin of the graben along-strike variation in the most recent cooling pattern and in the short term erosion pattern. This latter and localized exhumation event likely generated a recent uplift of the southwestern portion of the margin, thus uplifting the older portion of the

sedimentary fill exposed in this sector and facilitating their erosional removal. In this period was likely activated the MF2 that, together with the northern margin bounding fault, controlled the formation of the present-day alluvial plane.

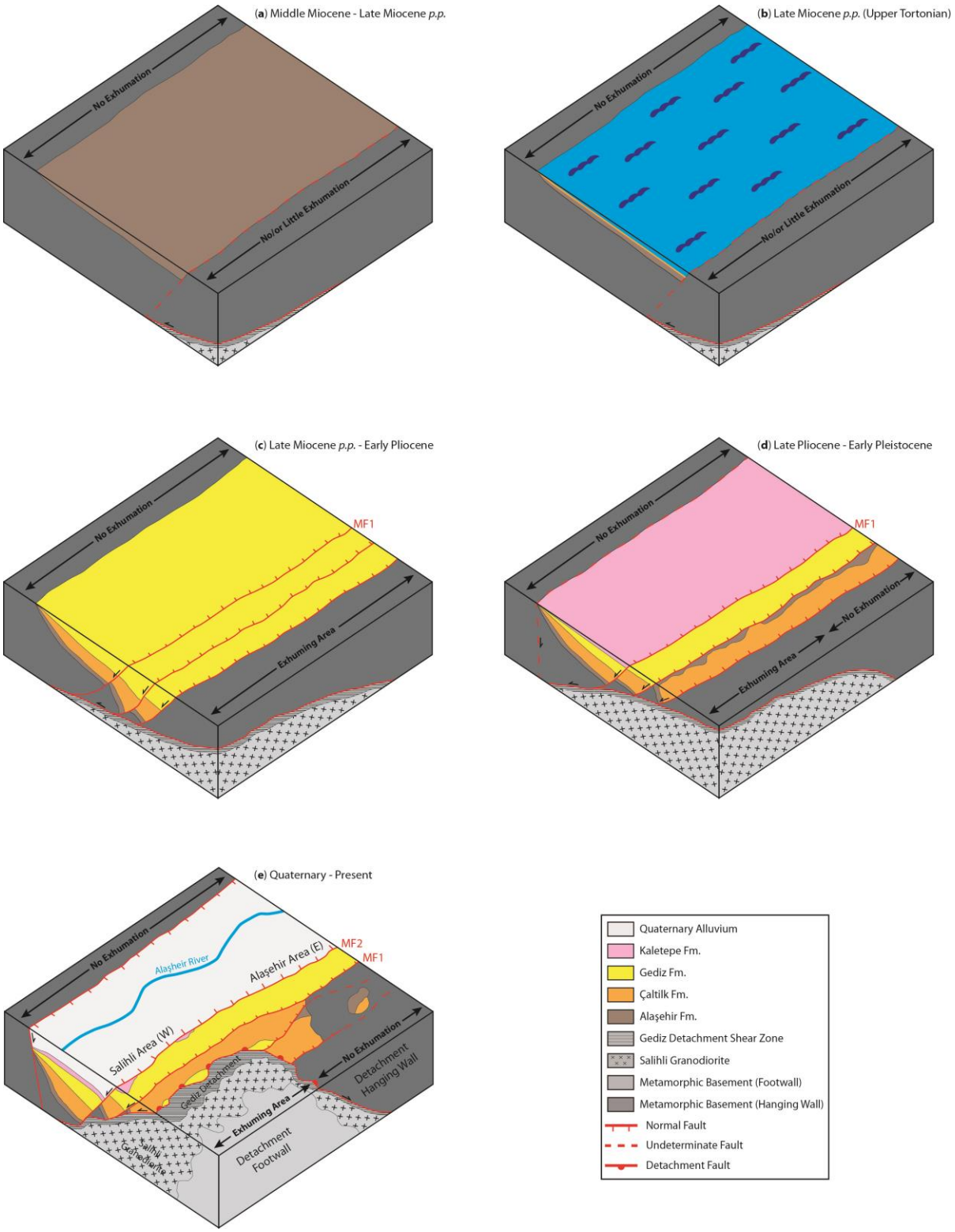

Figure 18: *Block-diagrams schematically showing the main sedimentary and tectonic events in the evolution of the Gediz Graben. a) Middle Miocene – Late Miocene p.p.: deposition of the Alaşehir Fm. in a no-major-fault-bounded basin contemporaneously with the activation of the ductile deformation on the Gediz Detachment at depth; no major exhumation of the basin margins occurs during this period. b) Late Miocene p.p. (upper Tortonian): marine transgression in the Gediz Graben and deposition of the limestone at the base of the Çaltilik Fm. c) Late Miocene p.p. – Early Pliocene: activation of major brittle faults bounding the southern margin of the basin and controlling the sedimentation of the Çaltilik Fm. and Gediz Fm. in an half-graben setting; in this phase all the southern margin of the basin underwent relevant exhumation. d) Late Pliocene (?) – Early Quaternary: deposition of the unconform Kaletepe Fm. and activation of the norther margin of the basin; during this phase the oldest portions of the sedimentary fill are tilted and exposed at the surface and the Salihli Granodiorite and the Gediz Detachment are moving towards the surface in the western part of the graben. e) Quaternary – Present: activation of the MF2 fault and formation of the present-day Gediz Graben alluvial plain; during this phase the oldest sedimentary units previously exposed along the southern margin are more uplifted in the western part than in the eastern part and then eroded in the former sector, thus leading to the present-day pattern of the distribution of the ancient sedimentary fill in outcrop.*

5.6. *Implications for the exhumation of the Central Menderes Massif*

The proposed tectonic reconstruction has major implications on the evolution and exhumation of the Central Menderes Massif.

The Late Miocene or younger exhumation events are localized at the southern margin of the Gediz Graben. The same seems to be also for the northern margin of the Büyük Menderes Graben (see contour map of the bedrock apatite fission track ages of the Menderes Massif in Gessner et al., 2013). Moreover, some older bedrock apatite fission track ages are preserved in the inner part of the Central sub-massif (Gessner et al., 2001; Ring et al., 2003). All this evidences suggest that the Central Menderes Massif was already exhumed at the surface more or less at the same time of the rest of the Menderes Massif by the same major cooling event (i.e. latest Oligocene – Middle Miocene), and only its northern and southern margins have undergone major and along-strike localized exhumation since latest Middle Miocene. In this light, all the previously proposed models (e.g. Hetzel et al., 1995b; Gessner et al., 2001; Ring et al., 2003; Seyitoğlu et al., 2004; Gessner et al., 2013) claiming for a younger exhumation phase of the whole Central sub-massif with respect to the rest of the Menderes Massif are unlikely.

Moreover, the most recent exhumation event recorded at the northern margin of the Central Menderes Massif did not involve the whole margin along its strike, but was extremely localized at the area where the pre-kinematic Salihli and Turgutlu Granodiorites intruded, thus suggesting that these intrusion might have had a major role not only in triggering the ductile-to-brittle detachment tectonics in this area (Chapter 3, this work), but also in controlling the exhumation process.

6. CONCLUSION

The main conclusions of this work can be summarized as follows:

- An upper Tortonian marine episode has been identified in the Neogene stratigraphic succession of the Gediz Graben: in the limestone at the base of the Çaltilik Fm. a shallow marine faunal assemblage has been dated between 8.35 Ma and 7.246 Ma. Our finding represent the first report ever for a Neogene marine episode in the whole Menderes Massif area and constrains the onset of the basin at the Middle Miocene as well as it subsequent mean uplift rate.
- The lower part of the stratigraphic succession (i.e. the Alaşehir Fm. and the lower part of the Çaltilik Fm.) has been deposited in the whole Gediz Graben, rather than only in the eastern sector, in a ~E-W trending basin; in the western part of the study area these deposits are now buried below the younger formations in the more internal part of the basin, whereas have been probably uplifted and eroded in the more external part.
- The stratigraphic limit between the Çaltilik Fm. and the overlying concordant Gediz Fm. is represented mainly by a chromatic change, is not straight and might be due to post depositional alterations, thus not representing an isochronous surface.
- Many evidences of syn-sedimentary fault activity have been found in the whole stratigraphic succession.
- It is unlikely that the contractional structures observed in the finer Zeytinçayi Mbr. of the Alaşehir Fm. are related to a regional compressional tectonic event, but might rather be extension-related structures, as suggested by Şengör & Bozkurt (2013), or

large-scale slumps in pre-diagenized sediments. In general, no evidences for a Neogene compressional event have been observed in the study area.

- The Gediz Graben displayed many different structural styles during its extensional evolution, starting in the Middle Miocene as a sag-like basin (where the sedimentation was not controlled by major basin bounding faults), passing to an half-graben geometry with a southern active margin during the Late Miocene and ending in as a symmetric graben since the (Late Pliocene? -) Quaternary activation of the northern margin. Since no major interruption of the sedimentation have been identified in the Neogene-to-Quaternary stratigraphic sequence, it is likely that this evolution developped as a continuous process without major interruptions.
- Field evidences have confirmed the structural relationship between the western and the eastern sector of the southern margin of the basin: the former is represented by the Gediz Detachment and its footwall (including the Salihli Granodiorite), whereas the latter is represented by the metamorphic bedrock at the hanging wall of the detachment, thus representing an higher and less exhumed crustal level. This implies that the Gediz Detachment does not bound all the southern margin of the Gediz Graben along its strike, but is rather exhumed only in the western sector of the basin, where the pre-kinematic Salihli and Turgutlu Granodiorites intruded its footwall.
- No major rotation of the gently dipping Gediz Detachment occurred since the beginning of its activity in the Middle Miocene. The amount of exhumation accommodated by this structure and by the high-angle brittle faults since the early formation of the Gediz Graben is relatively small (i.e. less than 10 Km since the Middle Miocene). This implies that relatively small amounts of extension might be required on a low-angle detachment system to exhume shallow (i.e. less than 7 Km of depth) pre-kinematic magmatic intrusions.
- The tectonic exhumation of the southern margin of the basin has been much more effective since the activation of high-angle brittle faults at the hanging wall of the Gediz Detachment, rather than via low-angle extensional activity of the detachment fault itself.
- It is likely that the Central Menderes Massif was already exhumed during the Main Menderes Cooling Event in the latest Oligocene – Middle Miocene, so the younger

exhumation events where localized to and involved only its northern and southern margins at the footwall of the structures bounding the Gediz Graben and the Büyük Menderes Graben.

- The youngest Late Pliocene – Early Pleistocene exhumation event that led the ductile-to-brittle Gediz Detachment to the surface was extremely localized at the exposure area of the Salihli and Turgutlu Granodiorites, thus suggesting that the presence of these intrusion might have controlled the exhumation process.

REFERENCES

Ascoli, P (1968) – *Preliminary report on the Ostracoda of the Type-Tortonian*. G. Geol., 35 (2), 31-51.

Bargnesi, E.A., Stockli, D.F., Mancktelow, N., Soukis, K., 2013. *Miocene core complex development and coeval supradetachment basin evolution of Paros, Greece, insights from (U–Th)/He thermochronometry*. Tectonophysics, 595-596, 165-182.

Bozkurt, E., Park, G.R., 1994*. Southern Menderes massif: an incipient metamorphic core complex in western Anatolia, Turkey.* Journal of the Geological Society of London, 151, 213–216.

Bozkurt, E., Oberhänsli, R., 2001. *Menderes Massif (Western Turkey): structural, metamorphic and magmatic evolution — a synthesis*. International Journal of Earth Sciences (Geologische Rundschau) 89, 679–708.

Bozkurt, E., Sözbilir, H., 2004. *Tectonic evolution of the Gediz Graben: field evidence for an episodic, two-stage extension in western Turkey*. Geological Magazine 141, 63–79.

Buscher J.T., Hampel A., Hetzel R., Dunkl I., Glotzbach C., Struffert A., Akal C., Ratz M., (2013). *Quantifying rates of detachment faulting and erosion in the central Menderes massif (western Turkey) by thermochronology and cosmogenic 10Be*. J. Geol. Soc. London, 170, 669–683.

Carbonnel, G., 1966. *Essai d'étude statistique à propos d'un nouveau genre d'Ostracode Pseudopsammocythere*. Rev. Micropaléont., 9 (1), 50-54, 4 text-figs., 1 pl., Paris.

Çemen İ., Tekeli O., Seyitoğlu G., Işık V., 2005. *Are turtleback fault surfaces common structural elements of highly extended terranes?* Earth-Sci. Rev., 73, 139–148.

Çiftçi, N.B., Bozkurt, E., 2008. *Folding of the Gediz Graben fill, SW Turkey: extensional and/or contractional origin?* Geodinamica Acta 21, 145–167.

Çiftçi, N.B., Bozkurt, E., 2009a. *Evolution of the Miocene sedimentary fill of the Gediz Graben, SW Turkey*. Sedimentary Geology 216, 49–79.

Çiftçi, N.B., Bozkurt, E., 2009b. *Pattern of normal faulting in the Gediz Graben, SW Turkey*. Tectonophysics 473, 234–260.

Çiftçi, N.B., Bozkurt, E., 2010. *Structural evolution of the Gediz Graben, SW Turkey: temporal and spatial variation of the graben basin*. Basin Research 22, 846–873.

Cohen, H.A., Dart, C.J., Akyüz, H.S., Barka, A.A., 1995. *Syn-rift sedimentation and structural development of Gediz and Büyük Menderes graben, western Turkey*. Journal of the Geological Society, London 152, 629–638.

Dall'Antonia, B., Bossio, A., 2001. *Middle Miocene ostracods from the Salentine peninsula*. Rivista Italiana di Paleontologia e Stratigrafia, 107 (3), 395-424.

Ediger V. Ş., Batı Z., Yazman M., 1996. *Paleopalynology of possible hydrocarbon source rocks of the Alaşehir-Turgutlu area in the Gediz Graben (western Anatolia)*. Turkish Association of Petroleum Geologists, 8, 94–112.

Emre T., 1996. *Geology and tectonics of Gediz Graben*. Turkish Journal of Earth Sciences, 5, 171–185.

Erkül F., Erkül S.T., Ersoy Y., Uysal I., Krötzli U., 2013. *Petrology, mineral chemistry and Sr–Nd–Pb isotopic compositions of granitoids in the central Menderes metamorphic core complex: Constraints on the evolution of Aegean lithosphere slab*. Lithos, 180-181, 74-91.

Ersoy, E.Y., Helvacı, C., Palmer, M.R., 2011 - *Stratigraphic, structural and geochemical features of the NE–SW-trending Neogene volcano-sedimentary basins in western Anatolia: implications for associations of supradetachment and transtensional strike-slip basin formation in extensional tectonic setting*. J. Asian Earth Sci., 41, 159–183.

Fillmore, R.P., Walker, J.D., Bartley, J.M., and Glazner, A.F., 1994. *Development of three genetically related basins associated with detachment-style faulting: Predicted characteristics and an example from the central Mojave Desert, California*. Geology, 22, 1087–1090, doi:10.1130/0091- 7613(1994)0222.3.CO;2.

Fillmore, R.P., Walker, J.D., 1996. *Evolution of a supradetachment extensional basin: The Lower Miocene Pickhandle basin, central Mojave Desert, California*. In: Beralan, K.K., ed., Reconstruction the History of Basin and Range Extension using Sedimentology and Stratigraphy. Boulder, Colorado, Geological Society of America Special Paper, 303, 107-126.

Friedmann S. J. & Burbank D. W., 1995. *Rift basins and supradetachment basins: intracontinental extensional end-members*. Basin Research, 7, 109-127.

Gebhardt H., Zorn I., Roetzel R., 2009. *The initial phase of the Early Sarmatian (Middle Miocene) transgression. Foraminiferal and ostracod assemblages from an incised valley fill in the Molasse Basin of Lower Austria*. Australian Journal of Earth Sciences, 102 (2), 100-119.

Gessner K., Ring U., Johnson C., Hetzel R., Passchier C.W. & Gungor, T., 2001. *An active bivergent rolling-hinge detachment system: Central Menderes metamorphic core complex in western Turkey*. Geology, 29, 611–614.

Gessner K., Gallardo L. A., Markwitz V., Ring U. & Thomson S. N., 2013. *What caused the denudation of the Menderes Massif: Review of crustal evolution, lithosphere structure, and dynamic topography in southwest Turkey*. Gondwana Research, 24(1), 243–274.

Gibbs A.D., 1984. *Structural evolution of extensional basin margins*. Journal of the Geological Society of London, 141, 609-620.

Glodny, J., Hetzel, R., 2007. *Precise U-Pb ages of syn-extensional Miocene intrusions in the central Menderes Massif, western Turkey*. Geological Magazine, 144, 235-246.

Hetzel, R., Ring, U., Akal, C., Troesch, M., 1995a. *Miocene NNE-directed extensional unroofing in the Menderes Massif, southwestern Turkey*. Journal of the Geological Society of London, 152, 639-654.

Hetzel, R., Passchier, C.W., Ring, U., Dora, O.Ö, 1995b. *Bivergent extension in orogenic belts; the Menderes Massif (southwestern Turkey)*. Geology, 23, 455-458.

Iaccarino, S.M., Premoli, S.I., Biolz, M., Foresi, L.M., Lirer, F., Urco, E., and Petrizzo, M.R., 2007. *Practical Manual of Neogene Planktonic Foraminifera*. VI Course (February 19–23): Neogene: Perugia, Italy, International School on Planktonic Foraminifera, 181 p.

Isik, V., Tekeli, O., 2001. *Structure of lower plate rocks in metamorphic core complex: Northern Menderes Massif, Western Turkey*. International Journal of Earth Sciences (Geologische Rundschau) 89, 757–765.

Işik, V., Seyitoğlu, G., Çemen, I., 2003. *Ductile-brittle transition along the Alaşehir detachment fault and its structural relationship with the Simav detachment fault, Menderes massif, western Turkey*. Tectonophysics, 374, 1-18.

İztan H. & Yazman M., 1991. *Geology and hydrocarbon potential of the Alaşehir (Manisa) area, western Turkey*. Proceedings of the International Earth Sciences Congress on Aegean Regions, Izmir, 327–338.

Jolivet, L., Brun, J.P., 2010. *Cenozoic geodynamic evolution of the Aegean*. International Journal of Earth Sciences, 99, 109–138.

Koçyiğit A., Yusufoğlu H. & Bozkurt, E., 1999. *Evidence from the Gediz Graben for episodic two-stage extension in western Turkey*. Journal of the Geological Society, London 156, 605–616.

Lips, A.L.W., Cassard, D., Sözbilir, H., Yilmaz, H., Wijbrans, J.R., 2001. *Multistage exhumation of the Menderes Massif, western Anatolia (Turkey)*. International Journal of Earth Sciences (Geologische Rundschau), 89, 781–792.

Mücke, A., 1994. *Postdiagenetic ferruginization of sedimentary rocks (sandstones, oolitic ironstones, kaolins and bauxites) - including a comparative study of the reddening of red*

beds. [in] Wolf, K. H. and Chilingarian, G V. (eds.) pp 361-395 Diagenesis, IV. Developments in Sedimentology 5 1, Elsevier, Amsterdam.

Oberhänsli, R., Candan, O., Wilke, F., 2010. *Geochronological evidence of Pan-African eclogites from the central Menderes Massif, Turkey*. Turkish Journal of Earth Sciences, 19, 431–447.

Öner Z. & Dilek Y., 2011. *Supradetachment basin evolution during continental extension: the Aegean province of western Anatolia, Turkey*. Geological Society of America Bulletin, 123, 2115–2141.

Purvis, M., Robertson, A.H.F., 2004. *A pulsed extension model for the Neogene–Recent E–W-trending Alaşehir Graben and the NE–SW-trending Selendi and Gördes basins, western Turkey*. Tectonophysics 391, 171–201.

Purvis, M., Robertson, A.H.F., 2005a. *Sedimentation of the Neogene–Recent Alaşehir (Gediz) continental graben system used to test alternative tectonic models for western (Aegean) Turkey*. Sedimentary Geology 173, 373–408.

Purvis, M., Robertson, A.H.F., 2005b. *Miocene sedimentary evolution of the NE–SWtrending Selendi and Gördes basins, W Turkey: implications for extensional processes*. Sedimentary Geology 174, 31–62.

Ring, U., Gessner, K., Gungor, T., Passchier, C.W., 1999. *The Menderes Massif of western Turkey and the Cycladic Massif in the Aegean - do they really correlate?* Journal of the Geological Society, 156, 3–6.

Ring, U., Johnson, C., Hetzel, R., Gessner, K., 2003. *Tectonic denudation of a Late Cretaceous– Tertiary collisional belt: regionally symmetric cooling patterns and their relation to extensional faults in the Anatolide belt of western Turkey*. Geological Magazine, 140, 421–441.

Ring, U., Collins, A.S., 2005. *U–Pb SIMS dating of synkinematic granites: timing of core–complex formation in the northern Anatolide belt of western Turkey*. Journal of the Geological Society, 162, 289–298.

Sarıca N., 2000. *The Plio–Pleistocene age of Büyük Menderes and Gediz grabens and their tectonic significance on N–S extensional tectonics in West Anatolia: mammalian evidence from the continental deposits*. Geological Journal 35, 1–24.

Sarikaya M.A., 2004. *Gediz ayrılma zonu: Fay kayacı stratigrafisi ve tektonik önemi (Gediz detachment zone: Fault rock stratigraphy and tectonic significance)*. Hacettepe Üniversitesi Yerbilimleri Uygulama ve Arafltırma Merkezi Bülteni, 30, 63-79.

Şengör A.M.C., 1987. *Cross faults and differential stretching of hangingwalls in regions of low-angle normal faulting: examples from Western Turkey*. In: Coward, M.P.,Dewey, J.F., Hancock, P.L. (Eds.), Continental Extensional Tectonics, 575–589.

Şengör A. M. C. & Yilmaz Y., 1981. *Tethyan evolution of Turkey: a plate tectonic approach*. Tectonophysics, 75, 181–241.

Sengör, A.M.C., Satir, M., Akkök, R., 1984. *Timing of the tectonic events in the Menderes massif, western Turkey: implications for tectonic evolution and evidence for Pan- African basement in Turkey*. Tectonics, 3, 693–707.

Şengör, A.M.C., Bozkurt, E., 2013. Layer-parallel shortening and related structures in zones undergoing active regional horizontal extension. International Journal of Earth Sciences 102, 101–119.

Seyitoğlu G. and Scott B. C., 1992. *The age of the Büyük Menderes graben (west Turkey) and its tectonic implications*. Geological Magazine, 129, 239–242.

Seyitoğlu, G., Çemen, İ., Tekeli, O., 2000. *Extensional folding in the Alaşehir Gediz graben, western Turkey*. Journal of the Geological Society, London 157, 1097–1100.

Seyitoğlu G., Tekeli O., Çemen İ., Şen Ş. & Işık V., 2002. *The role of flexural rotation/rolling hinge model in the tectonic evolution of the Alaşehir Graben, western Turkey*. Geology Magazine, 139, 15–26.

Seyitoğlu, G., Işık, V., Çemen, İ., 2004. *Complete Tertiary exhumation history of the Menderes Massif, western Turkey: an alternative working hypothesis*. Terra Nova 16, 358–363.

Seyitoğlu, G., Işık, V., Esat, K., 2015. *A 3D model for the formation of turtleback surfaces: the Horzum Turtleback of western Turkey as a case study*. Turkish Journal of Earth Sciences, 23, 479-494.

Sissingh W., 1972. *Late Cenozoic Ostracoda of the South Aegean island arc*. Utrecht Micropaleontological Bulletins, 6, 188 p.

Tinn, O., Meidla, T., 1999. *Ordovician ostracodes from the Komstad Limestone*. Bulletin of the Geological Society of Denmark, 46, 25–30.

Thomson S. N. & Ring U., 2006. *Thermochronologic evaluation of post-collision extension in the Anatolide Orogen, western Turkey*. Tectonics, 25, TC3005.

van Hinsbergen, D.J.J., and Meulenkamp, J.E., 2006. *Neogene supradetachment basin development on Crete (Greece) during exhumation of the South Aegean core complex*. Basin Research, 18, 103–124, doi:10.1111/j.1365 -2117.2005.00282.x.

van Hinsbergen, D.J.J., Dekkers, M.J., Bozkurt, E., Koopman, M., 2010. *Exhumation with a twist: paleomagnetic constraints on the evolution of the Menderes metamorphic core complex, western Turkey*. Tectonics, 29, TC3009, doi:10.1029/2009TC002596.

Van Houten, F. B., 1973. *Origin of red beds. A review -1961-1972*. Annual Review Earth Planetary Science, 1, 39-61.

Vetti, V.V., Fossen, H., 2012. *Origin of contrasting Devonian supradetachment basin types in the Scandinavian Caledonides*. Geology, 40 (6), 571-574.

Walker, T.R., 1967. *Formation of redbeds in ancient and modern deserts*. Geol. Soc. Am. Bull., 78, 353- 368.

Yazman, M.K., Güven, A., Ermiş, Y., Yılmaz, M., Özdemir, İ., Akçay, Y., Gönülalan, U., Tekeli, Ö., Aydemir, V., Sayılı, A., Batı, Z., İztan, H., Korucu, Ö., 1998. *Alaşehir Grabeni'nin ve Alaşehir-1 Prospektinin Değerlendirme Raporu*. TPAO Exploration Group, unpublished technical report, 142 p.

Yılmaz Y., Genç S. C., Gürer Ö. F., Bozcu M., Yılmaz K., Karacık Z., Altunkaynak Ş. & Elmas A., 2000. *When didwesternAnatolian grabens begin to develop*. In: Bozkurt, E.,Winchester,

J.A., Piper, J.D.A. (Eds.), Tectonics and Magmatism in Turkey and the Surrounding Area. Geological Society, London, Special Publications, 173, p. 353-384.